# DEVELOPMENT OF GEOPOLYMER BONDED WOOD COMPOSITES

By

**Hamed Olafiku Olayiwola**

Dissertation presented for the degree of

**DOCTOR OF PHILOSOPHY**

**(Wood Product Science)**

at

**Stellenbosch University**

Dept. of Forest and Wood Science, Faculty of AgriSciences

Supervisor: Dr. Luvuyo Tyhoda

Co-supervisor: Prof Martina Meincken

March 2021

## Declaration

By submitting this thesis electronically, I declare that the entirety of the work contained therein is my own, original work, that I am the sole author thereof (save to the extent explicitly otherwise stated), that reproduction and thereof by Stellenbosch University will not infringe any third-party rights and that I have not previously in its entirety or in part submitted it for obtaining any qualification.

March 2021

## Abstract

In the wake of finding alternative sustainable and environmentally friendly products to conventional construction materials, geopolymers offer large potential as a low carbon footprint material. Their excellent properties and the ability to be synthesized from industrial waste make them promising alternative binders in wood-based composites where durability, environmental sustainability, structural integrity, and low cost of final products are of utmost importance. This study investigated the application of unary and binary precursor based geopolymers in the development of composite products for use in outdoor conditions. The unary geopolymer is based on 100% ground granulated blast slag, while the binary precursor is composed of 75% class F fly ash and 25% metakaolin. The precursors were activated with a combination of sodium hydroxide and sodium silicate solutions formulated at a weight ratio of 1:2.5. The lignocellulosic materials used include sugarcane bagasse (*Saccharum officinarum*) and forest biomass waste from the clearing of locally occurring invasive alien species including Long-leaved wattle (*A. longifolia*), Black wattle (*A. mearnsii*) and Port Jackson (*A. saligna*).

The production process involved using a mixed factorial experimental design. The variables considered included precursor-activator ratio (PA), curing pattern (CP), amount of lignocellulosic material (LM) and alkali concentration (MCon). For the unary system, the variables were CP, LM and MCon. PA and CP were considered at 2 levels, while LM and MCon were considered at 3 levels. The effects of the main factors and their interactions on the observed composite properties were evaluated using analysis of variance (ANOVA). The boards have comparable physical properties to cement-bonded particleboard according to the EN 632-2: 2007 standard. However, for the unary system only *A. saligna* boards produced with 6M NaOH and cured at 40°C for 24 h met the mechanical strength requirements, while in the binary system, only *A. longifolia* boards produced with 12M NaOH, PA ratio of 2:1 and cured at 100°C for 6h met the mechanical strength requirements. The boards were also thermally stable as the residues retained at the end of thermal analysis was above 70%.

There was a concern about the durability of the LM in the alkaline matrix. Scanning electron microscopy (SEM) micrographs indicated mineralization of the particles and a partial degradation of hemicellulose was confirmed by Fourier transform infrared (FTIR) spectroscopy and thermogravimetry analysis (TGA). Although the degraded products did not prevent geopolymer

setting, the degree of geopolymeric reaction was impeded. The lignocellulosic materials were subjected to alkalization, acetylation, and hot water extraction to remove the lower molecular components, which could impede geopolymerization kinetics and enhance their surface characteristics. This was aimed at improving the durability of LM in the matrix and the overall properties of the boards. The influence of each treatment on the lignocellulosic materials was evaluated using HPLC, SEM and FTIR, while the resulting boards were tested to specification and characterized using SEM and FTIR. The treatments improved the surface characteristics of the fibres and the fibre yield was not impacted significantly. FTIR indicated formation of more geopolymer products after fibre treatment, which was confirmed by SEM micrographs. The treated samples exhibited a compact and densely populated gel-like amorphous microstructure with fewer unreacted precursor particles. In the unary system, the mean modulus of rupture (MOR) increased by 3.25% for hot water extracted, 23.61% for acetylated and 23.94 % for alkalized AM boards. In the binary system, the mean MOR increased by 18.31% for hot water extracted, 6.03% for acetylated and 18.22% for alkalized AM boards. The study concluded that South African woody invasive plants (IPs) and sugarcane bagasse are suitable to produce both unary- and binary precursor-based geopolymer wood composites of comparable properties to cement-bonded particleboards.

# Opsomming

In die nasleep van alternatiewe volhoubare en omgewingsvriendelike produkte as konvensionele konstruksiemateriaal, bied geopolimere 'n groot potensiaal as 'n lae koolstofvoetspoor. Die uitstekende eienskappe en die vermoë om deur industriële afval gesintetiseer te word, maak dit belowende alternatiewe bindmiddels in houtsaamgestelde produkte waar duursaamheid, volhoubaarheid in die omgewing, strukturele integriteit en lae koste van finale produkte van die uiterste belang is. Hierdie studie ondersoek die toepassing van eenvormige en binêre voorgangergebaseerde geopolimere in die ontwikkeling van saamgestelde produkte vir gebruik in buitelugtoestande. Die eenvormige geopolymeer is gebaseer op 100% gemaalde ontploffingslak, terwyl die binêre voorloper bestaan uit 75% klas F-vliegas en 25% metakaolien. Die voorlopers is geaktiveer met 'n kombinasie van natriumhidroksied- en natriumsilikaatoplossings wat met 'n gewigsverhouding van 1:2.5 geformuleer is. Die gebruikte lignocellulosemateriale sluit in suikerriet bagasse (*Saccharum officinarum*) en bosbiomassa-afval van die skoonmaak van plaaslik voorkomende uitheemse spesies, waaronder langblaarwattel *(A. longifolia*), swartwattel (*A. mearnsii*) en Port Jackson (*A. saligna*) deel was.

Die produksieproses is met behulp van 'n gemengde faktorale eksperimentele ontwerp saamgestel. Die veranderlikes wat in ag geneem is, het die voorgang-aktivator-verhouding (PA), drogingspatroon (CP), die hoeveelheid lignocellulose materiaal (LM) en die alkalikonsentrasie (Mcon) ingesluit. Vir die eenvormige stelsel was die veranderlikes CP, LM en MCon. PA en CP is op 2 vlakke oorweeg, terwyl LM en MCon op 3 vlakke beskou is. Die effekte van die belangrikste faktore en hul interaksies op die waargenome saamgestelde eienskappe is geëvalueer met behulp van variansieanalise (ANOVA). Die borde het vergelykbare fisiese eienskappe met sementsaamgestelde veselbord volgens die EN 632-2: 2007-standaard. Vir die eenvormige stelsel het slegs A. saligna-borde wat met 6M NaOH geproduseer is en 24 uur lank by 40 ° C gedroog is, aan die meganiese sterktevereistes voldoen, terwyl slegs A. longifolia-borde met 12M NaOH, PA-verhouding van 2:1 in die binêre stelsel en gedurende 100 uur by 100 ° C gedroog, het aan die meganiese sterktevereistes voldoen. Die planke was ook termies stabiel, aangesien die afval wat aan die einde van die termiese analise behou is, bo 70% was.

Daar was kommer oor die duursaamheid van die LM in die alkaliese matriks. Skandering-elektronmikroskopie (SEM) mikrografieke het aangedui op mineralisering van die deeltjies en 'n

gedeeltelike agteruitgang van hemisellulose is bevestig deur Fourier transvorm infrarooi (FTIR) spektroskopie en termogravimetrie-analise (TGA). Alhoewel die afgebreekte produkte nie die verharding van geopolymeer verhinder het nie, is die mate van geopolymeriese reaksie belemmer. Die lignocellulosemateriale is onderwerp aan alkalisering, asetilering en ekstraksie van warm water om die laer molekulêre komponente te verwyder, wat geopolymerisasie-kinetika kan belemmer en die oppervlakkenmerke daarvan kan verbeter. Dit was gerig op die verbetering van die duursaamheid van LM in die matriks en die algehele eienskappe van die borde.

Die invloed van elke behandeling op die lignocellulosemateriaal is geëvalueer deur gebruik te maak van HPLC, SEM en FTIR, terwyl die saamgestelde borde volgens spesifikasie getoets is en gekarakteriseer is met behulp van SEM en FTIR. Die behandelings het die oppervlakkenmerke van die vesels verbeter en die veselopbrengs is nie beduidend beïnvloed nie. FTIR dui op die vorming van meer geopolymeerprodukte na veselbehandeling, wat deur SEM-mikrografieke bevestig is. Die behandelde monsters vertoon 'n kompakte en dig bevolkte gel-agtige amorfe mikrostruktuur met minder ongereageerde voorgangdeeltjies. In die eenvormige stelsel het die gemiddelde breukkrag (MOR) met 3,25% toegeneem vir warm water wat onttrek is, 23,61% vir geasetileerde en 23,94% vir alkaliseerde AM-borde. In die binêre stelsel het die gemiddelde MOR met 18,31% toegeneem vir warm water wat onttrek is, 6,03% vir geasetileerde en 18,22% vir alkaliseerde AM-borde. Die studie het tot die gevolgtrekking gekom dat Suid-Afrikaanse houtagtige IP's en suikerriet-bagasse geskik is om sowel eenvormige as binêre voorlopergebaseerde geopolymeer-houtsaamgestelde produkte te produseer, wat vergelykbaar is met sementvesel saamgestelde borde.

# Dedication

To my beloved father of blessed memory, Imam. Sulaiman Olafiku Salahudeen and my grandparents, Imam. Salahudeen Olayiwola Olafiku and Mrs. Shifahu Aarinade Olafiku. May Allah (SWT) be pleased with their souls and make Jannat Firdaus their final abode (Aamin).

## Acknowledgements

Praise be unto Allah (SWT), The Lord of the worlds, for all the things He has done in my life and for blessing me with wonderful people who made the completion of this thesis possible.

I am indebted to my supervisor, Dr. Luvuyo Tyhoda, and co-supervisor, Prof. Martina Meincken for the support and contributions towards the completion of my study.

I would also like to thank the German Academic Exchange (DAAD) and DLR for funding my research under the BioHome Project. I also appreciate the Department of Forest and Wood Science for the award of departmental bursary. Also, my profound appreciation goes to the Stellenbosch University Postgraduate office for the award of Overseas Conference Grant (OCG) to attend the 62nd International Convention of the Society of Wood Science and Technology in Fresno, California, United States.

My sincere gratitude goes to the staff and postgraduate students in the department for their assistance and supports. Notable among them are Mr Solomon Henry, Mr Wilmour Hendrikse, Dr Brand Wessels, Mrs Mavis Mangala, Paul Mwansa, Gloria Buregengwa, Siviwe Soludongwe, Lehlohonolo Mngomezulu, Alade Adefemi (Friendship Mi), Charles Malunga, Sadiq Muhammad and Drs. Francis Munalula, Stephen Amiandamhen, Philip Crafford and Justin Erasmus. I appreciate your contributions and the wonderful moments we shared. You all made the programme worthwhile and memorable.

This section would be incomplete without a note of thanks to my colleagues in the BioHome Research group: Bright Asante, Hanzhou Ye, Marco De Angelis, Gebrewold Teklay, Keresa Defa, Fikru Bedada, Emilin Joma Da Silva, Xhelona Haveriku, Victor Ovri and Drs. Goran Schmidt, Esayas and Bernard Effah. Special appreciation also goes to Prof. Andreas Krause.

I also appreciate the unflinching support of Adeyinka Adesope (Iwarere), Baba Kenny, Adewale Adesope, Tafara Gwanongodza and Fatimatu Bello (Obaa). My deepest appreciation goes to my uncle Dr. Isiaka Salawu Olafiku, my mum, Iya Hamed (smiles), Opeyemi (Ajiun mi), my darling daughters, Maymunah and Mahmoodah, and to my siblings. Your prayers, love and continual encouragement saw me through the darkest moments.

To everyone who has directly or indirectly contributed to my success, I say thank you and God bless.

# List of publications

The following is a list of publications, on, which this dissertation is based. They are presented in the results and discussion chapters of this dissertation.

## 1. Publication I

Investigating the suitability of fly ash/metakaolin-based geopolymers reinforced with South African alien invasive wood and sugarcane bagasse residues for use in outdoor conditions

Olayiwola H.O, Amiandamhen S.O, Meincken M, Tyhoda L.

*European Journal of Wood and Wood Products*

*Accepted November, 2020. DOI:10.1007/s00107-020-01636-4*

## *2.* Publication II

Characterization of unary precursor-based geopolymer bonded composite developed from ground granulated blast slag and forest biomass residues

Olayiwola H.O, Amiandamhen S.O, Meincken M, Tyhoda L.

## 3. Publication III

The influence of chemical pre-treatment of fibres on the properties and durability of binary precursor-based geopolymer bonded wood and fibre composites

Olayiwola H.O, Amiandamhen S.O, Meincken M, Tyhoda L.

# List of conference presentations

1. **62nd International Convention of the Society of Wood Science and Technology, USA. 20th – 25th October 2019 at Tenaya Lodge, Yosemite National Park, Fresno, CA**.
   Presentation:
   Investigating the thermal and mechanical properties of fly ash/metakaolin-based geopolymer reinforced with alien invasive wood species.

2. **International Conference on Composites, Biocomposites and Nanocomposites, Port Elizabeth, South Africa. 7th – 9th November 2018 at Nelson Mandela Bay Stadium, Port Elizabeth, South Africa.**
   Presentation:
   Investigating the thermal and mechanical properties of fly ash/metakaolin-based geopolymer reinforced with alien invasive wood species.

## Table of contents

## List of figures

## List of tables

## List of acronyms and abbreviations

| | |
|---|---|
| ACE | Acetylated |
| AIWS | Alien Invasive Wood Species |
| AL | *A. longifolia* |
| ALK | Alkalized |
| AM | *A. mearnsii* |
| AS | *A. saligna* |
| ASTM | American Standard Test Methods |
| ATR | Attenuated Total Reflectance |
| BS | British Standard |
| C2S | Di-Calcium Silicate |
| C3S | Tri-Calcium Silicate |
| CBFB | Cement Bonded Fibre Board |
| CBOSB | Cement Bonded Oriented Strand Board |
| CBPB | Cement Bonded Particle Board |
| CBWC | Cement Bonded Wood Composites |
| CP | Curing Pattern |
| DAAD | German Academic Exchange |
| DLR | German Aerospace Centre |

| | |
|---|---|
| DSC | Differential Scanning Calorimetry |
| DTG | Derivative thermographs |
| EN | English Standard |
| FA | Fly Ash |
| FTIR | Fourier Transform Infra-Red Spectroscopy |
| GBWC | Geopolymer Bonded Wood Composites |
| GGBFS | Ground granulated blast furnace slag |
| GHG | Greenhouse gases |
| HDB | High Density Boards |
| HT | High Tenacity |
| IARC | International Agency for Research on Cancer |
| ICC | Isothermal Conduction Calorimetry |
| IR | Infra-Red |
| LCA | Life Cycle Assessment |
| MC | Moisture Content |
| MCon | Molar concentration |
| MK | Metakaolin |
| MOE | Modulus of Elasticity |
| MOR | Modulus of Rupture |

| | |
|---|---|
| NH | Sodium Hydroxide |
| NMR | Nuclear Magnetic Resonance |
| NREL | National Renewable Energy Laboratory |
| NS | Sodium Silicate |
| OD | Oven Dry |
| OPC | Ordinary Portland Cement |
| PA | Precursor- Activator Ratio |
| PVA | Poly Vinyl Alcohol |
| PVAc | Poly Vinyl Acetate |
| SANS | South African National Standards |
| SCB | Sugarcane bagasse |
| SEM | Scanning Electron Microscopy |
| SFA | Class S Fly Ash |
| SL | Slag |
| TAPPI | Technical Association of Pulp and Paper Industry |
| TGA | Thermogravimetric Analysis |
| TS | Thickness Swelling |
| UNT | Untreated |
| VS | Volumetric Swelling |

| | |
|---|---|
| W/B | Water-Binder ratio |
| WA | Water Absorption |
| WWCBC | Wood Wool Cement Bonded Composites |
| XPS | X-Ray Photoelectron Spectroscopy |
| XRD | X-Ray Diffraction |
| XRF | X-Ray Fluorescence |

# Chapter 1

# General introduction

## 1.1 Background and motivation

Application of synthetic polymeric resins has dominated wood-based panel industries for more than eight decades (Sarmin et al. 2014). They are used for reconstituting particle boards, oriented strand boards, chipboards, plywoods and fibreboards (Irle 2010), while Portland cement is the major inorganic binder used in cement-bonded boards (Semple and Evans 2004). These composite products possess excellent properties, which make them suitable for different indoor and outdoor applications. However, recent studies have provided sufficient proof that volatile substances such as formaldehydes from formaldehyde-based polymeric resins are highly carcinogenic- causing leukemia, nasopharynx and sinonasal cancers in human (IARC 2012). Production of Portland cement, on the other hand, also contributes about 5% to 7% of the total greenhouse gas emission globally (Duan et al. 2016; Najimi et al. 2016; Sun et al. 2015). Production of 1 ton of cement releases about 1 ton of $CO_2$ into the atmosphere. The emissions add to the global carbon emissions, which are responsible for increasing temperatures that lead to adverse climate changes (Hardjito and Rangan 2005). The frequent cases of fire in recent times have been attributed to the multiplier effects of the global warming (Archibald et al. 2010; FPASA 2017). The fire incidents in Knysna, South Africa and Grenfell Tower, London in 2017 claimed many lives and loss of invaluable properties. Therefore, the continued growing global awareness of these pressing challenges has stimulated renewed interest in finding alternative low-cost materials that exhibit excellent properties and zero to low impact on man and the environment.

Geopolymer is an emerging alternative inorganic binder with an excellent potential to substitute conventional materials such as Portland cement in several applications. It is produced by geo-synthesis of materials rich in aluminosilicate materials with an alkaline metal solution at ambient or slightly elevated temperatures (Alomayri et al., 2013). It does not only provide performance comparable to ordinary Portland cement (OPC) in many applications, but has many additional advantages, such as rapid curing, high acid and fire resistance, excellent adherence to aggregates, immobilization of toxic and hazardous materials and significantly reduced energy usage and greenhouse gas emissions (Alomayri et al., 2013; Chen, 2014; Duan et al., 2016). Durability, environmental sustainability, structural integrity and cost effectiveness of materials are important requirements in building construction and wood-based manufacturing. The excellent properties of

geopolymer and its ability to be synthesized from industrial waste an overall low impact on the environment make it a promising alternative binder in these sectors.

However, it also exhibits brittle behaviour with low tensile strength, ductility, and fracture toughness common to most inorganic cementitious materials. Different synthetic materials have been used to reinforce geopolymer concrete to contain these weaknesses. These include polypropylene (Korniejenko et al. 2015), polyvinyl alcohol (PVA) (Yunsheng et al. 2008), steel and carbon fibres (Natali et al. 2011). Synthetic fibres are non-biodegradable and difficult to dispose of at the end of service life of the products (Herrmann et al. 1998; Pacheco-Torgal and Jalali 2011). High energy usage, cost, and serious concern about their disposal at the end-of-life cycle inarguably hinder the overall objective of developing sustainable eco-friendly and low-cost materials. Lignocellulosic fibres, such as cotton, bagasse, hemp, wood, bamboo, rattan, coir, jute, sisal, and others offer excellent properties, which make them promising alternatives to synthetic fibres. They are biodegradable with low density and adequate mechanical properties (Sarmin 2016). They have been successfully incorporated into different polymeric and inorganic matrices to produce lignocellulosic fibre composites (Evan 2000; Sudin et al. 2000; Jorge et al. 2004; Semple et al. 2004; Del Menezzi et al. 2007; Sales et al. 2011; Omoniyi 2012; LIMA 2015; Onuaguluchi et al. 2016). Previous investigations have shown that lignocellulosic fibres can be incorporated into a geopolymeric binder to produce composite products, but their development and utilization have not yet been extensively studied.

Sarmin et al. (2014) studied the properties of fly ash/metakaolin based geopolymer with 10% wood particles to make a lightweight composite. Addition of wood particles increased the magnitude of water absorption in the composite. Alomayri et al. (2014) studied the mechanical properties of a fly ash geopolymer reinforced with cotton fabric at elevated temperatures. The fly ash was activated with a combination of sodium silicate and sodium hydroxide at a ratio of 2.5:1. The molar concentration of sodium hydroxide was not indicated. Chen et al. (2014) reinforced fly ash-based geopolymers with sorghum fibres and concluded that the addition of fibres decreased the workability and unit weight of geopolymer pastes. It was reported that a fibre content up to 2% increased both tensile and flexural strength of the geopolymer composites. Duan et al. (2016) encapsulated a mixture of wood particles into a geopolymer matrix made of class F fly ash activated with sodium silicate and 10M NaOH at a ratio of 8:1. Addition of sawdusts up to 20 % improved the mechanical properties of the composites. The targeted application areas for the composite products were not mentioned in these previous investigations. Sarmin (2016), Sarmin and Welling (2016) and Sarmin and Welling (2015) added wood particles to a binary precursor made from FA and MK to produce a lightweight material.

Addition of wood particles improved the strength, but no mention was made about how the inherent wood properties influenced the performance of the geopolymer product.

Biomass residues from the clearing of alien invasive wood species (AIWS) and the bulk of industrial waste generated in South Africa could serve as a huge deposit of raw materials to produce low-cost geopolymer bonded wood composites (GBWC). South Africa has a high proportion of invasive plants (IPs) in the world (Le Maitre et al. 2000; Moyo and Fatunbi 2010). The IPs have serious socio-economic impact as about 30% of the South African grassland biome has been permanently modified (Mucina et al. 2006), posing a threat to the sustainable biodiversity of natural ecosystems; affecting both livestock and wildlife production (Shackleton et al. 2019). However, the prevailing approach to reduce the density of established, terrestrial, invasive alien plants is based on total clearing by mechanical and chemical means (DEA 2019). The removal generates excessive waste and impacts the environment negatively (Amiandamhen et al. 2017). In a bid to add value to the cleared AIWS, previous studies have incorporated them into calcium and magnesium phosphate matrices to produce phosphate-bonded composite products for use in building applications (Amiandamhen et al. 2016; Amiandamhen et al. 2017). These composite products showed promising properties, but recent studies have revealed that the high cost of this particular binder could prohibit its eventual use in the production of board products (Chimphango 2020).

Biomass waste, paper, slag and ash constitute about 80 million tonnes of waste annually in South Africa, out of which 74 million tonnes (or 93%) is landfilled (DEA, 2012). The development of geopolymer bonded composites is a promising alternative, which has a great potential to cause diversion of huge quantity of the generated waste from landfills. The current study investigated the properties of unary (slag) and binary (fly ash/metakaolin) precursor based geopolymers reinforced with wood particles from AIWS and sugarcane bagasse (SCB) targeted for use in outdoor conditions, such as wall cladding, roof and floor tiles. By reducing landfills, the innovation in this study will create opportunities for more effective and sustainable utilization of industrial waste in the development of eco-friendly building materials.

## 1.2 Research aim and objectives

The project was aimed at developing alternative eco-friendly, low-cost, and fire-resistant building components using AIWS and agricultural crop residues bonded with geopolymers derived from industrial waste, such as fly ash and blast furnace slag.

### 1.2.1 *The specific objectives addressed in this study are as follows:*

***Objective 1***

*Investigate and characterize binary precursor-based geopolymer bonded wood and fibre composites from alien invasive wood species and bagasse*

To address this objective, crushed sugarcane bagasse (*Saccharum officinarum*) and wood particles from two alien invasive acacia species, namely Black wattle (*Acacia mearnsii*) and Long-leafed wattle (*A. longifolia*) were incorporated into a geopolymer matrix developed from a binary precursor system made up of fly ash and metakaolin at a fixed ratio of 3:1. The production parameters included curing temperature, molar concentration of the activator and precursor-to-activator ratio. The production process was established using a mixed factorial design based on 2 factors at 2 levels (precursor-activator ratio and curing pattern) and 2 factors at 3-level (lignocellulose type and alkali concentration). The physical, mechanical, and thermal properties of the geopolymer composites were evaluated and the results are presented in Chapter 5.

***Objective 2***

*Investigate and characterize slag-based geopolymer bonded wood and fibre composites from alien invasive wood species and bagasse*

The geopolymer matrix was formulated using ground granulated blast slag activated with a mixture of sodium silicate and sodium hydroxide at a fixed ratio of 2.5:1. The precursor-to-activator ratio and lignocellulose content were kept constant at 2:1 and 25% respectively. The lignocellulosic materials used included *A. mearnsii*, Port Jackson (*A. saligna*) and crushed sugarcane bagasse. A factorial design based on one factor at two levels (curing pattern) and two factors at three levels (lignocellulose type and alkali concentration) was established for the production process. The properties of the resulting geopolymer bonded composites are presented in Chapter 6.

***Objective 3***

*Evaluate the influence of lignocellulose pre-treatment and surface modification on the properties of both fly ash/metakaolin-based and slag-based geopolymer bonded composites.*

To accomplish this objective, the pre-treatment methods included acetylation, hot water and mild alkalization with 1% sodium hydroxide. *A. mearnsii,* and crushed sugarcane bagasse fibres were used in this study. The fibres were characterized before and after treatment using FTIR, HPLC and SEM. A full factorial design based on two factors (treatment method and lignocellulose) at three levels with three replications was established for the fibre yield experiment. In order to evaluate the influence of fibre treatment on the properties of the boards, the experiment was established based on a completely randomized design with three replications. The boards were produced according to the best conditions derived from Objectives 1 and 2. The treatment methods are designated independent variables and the lignocellulose types investigated independently. The results were analysed using the one-way ANOVA in Statistica software (version 13). Separation of means for comparison was performed using Duncan's multi-stage range test. The results are presented and discussed in Chapter 7.

## 1.3 Structure of the dissertation

This dissertation consists of an introduction, a chapter detailing the materials and experimental methods, followed by three chapters discussing the chemical characterization of lignocellulose and precursor materials, lignocellulose pre-treatments, fly ash/metakaolin-based geopolymer bonded wood composites and slag-based geopolymer bonded wood composites.

Chapter 2 discusses the challenges associated with traditional inorganic wood binders and the development of geopolymer as an innovative alternative.

Chapter 3 is about the materials, methods and the experimental designs

Chapters 4 discusses the characterization of the materials

Chapters 5 discussed the development of fly ash/metakaolin based geopolymer reinforced with invasive species and sugarcane bagasse. It has been published and available online (Publication I)

Chapter 6 discussed development and characterization of slag-based geopolymer wood composites using untreated invasive wood species and sugarcane bagasse.

Chapter 7 discussed the influence of fibre pre-treatment methods on the properties of the geopolymer composites, including the durability of fibres in the matrices

Chapter 8 summarised the overall conclusions and recommendations for the study.

# Chapter 2

# Literature review

# Geopolymer binders: innovative alternatives to the traditional inorganic wood binders

## 2.1 Introduction

Wood and wood fibres have been incorporated into polymeric resins and inorganic matrices to make composite materials for use in different applications. Wood composite panels were introduced to find use for wood waste and develop low cost building materials (Irle 2010). The application of synthetic polymeric resins has dominated wood-based panel industries for more than eight decades (Sarmin et al. 2014). They are used for reconstituted particle boards, oriented strand boards, chipboards, plywoods and fibreboard (Irle 2010), while Portland cement is the major inorganic binder used in wood-cement boards. Polymeric resins and cement possess excellent properties, which make them suitable for different indoor and outdoor applications, such as partitioning, roofing, sheathing, floor tiles and outdoor furniture. However, due to the growing concern about the effect of their manufacture and utilization on man and the environment, different alternative binders with similar or superior properties are being developed. Geopolymer binders are an emerging alternative inorganic binding system developed by dissolution and polycondensation of aluminosilicate materials in alkali solution. This section reviews the challenges associated with the traditional inorganic wood binders, the development of geopolymers and previous studies on geopolymer-bonded wood composite products.

## 2.2 Challenges of early inorganic binders reinforced with lignocellulosic materials

Magnesia, gypsum, and Portland cement are the traditional inorganic binders used for reconstituting comminuted wood and other lignocellulosic materials. Inorganic bonded composites are made with 10–70% wood particles or fibres and 90–30% binder in reverse order (Youngquist 1999). The products exhibit excellent or superior properties when the individual fibres are fully encapsulated in the matrix (Simatupang and Geimer 1990). Consequently, to ensure full-encapsulation, more inorganic binder is usually required per unit volume of composite products than that of polymeric-bonded composites. The leading challenges associated with their applications in recent times are factors related to their impacts on man and the environment. Calcination of starting materials is involved in their respective manufacturing process, which makes them highly energy-intensive and

environmentally unfriendly. Relatively high cost and disposal at the end of their service life are also important factors being considered in construction industries.

### 2.2.1 *Magnesia-bonded wood composites*

The first commercial inorganic-bonded composite board was made with magnesite binder and wood shavings in the early 1900s in Austria (Van Elten 1999). Magnesite is a ternary-system binder made up of caustic magnesia (MgO), magnesium salt ($MgCl_2$ or $MgSO_4$) and water (Walling and Provis 2016). The reaction yield both 5–phase and 3–phase crystals of $5Mg(OH)_2–MgCl_2–8H_2O$ and $3Mg(OH)_2—MgCl_2–8H_2O$ at room temperature, respectively (Na et al. 2014; Tan et al 2014). Unreacted MgO may be present in varying quantity based on the thermal history and particle size of the starting caustic magnesia (Zhou and Li 2012). Several theories and propositions have been made on the hydration reactions. These include linkages between $[Mg(H_2O)_n]^{2+}$ and $[Cl•(–O–Mg–OH)_m]^-$ ions (Ved et al. 1976), interactions between magnesium, hydroxide and chloride ions (Bilinski et al. 1984) and the reaction between $MgCl_2$ and caustic magnesia (MgO) (Zhang et al. 1991). In the 1970s Ved et al (1976) proposed linkages between $[Mg(H2O)_n]^{2+}$ and $[Cl•(–O–Mg–OH)_m]^-$ ions as the major factor responsible. This position was cross-examined by Bilinski et al (1984). The authors assessed the similarities between $MgO–MgCl_2–H_2O$ and $NaOH–MgCl_2–H_2O$ systems and concluded that hydration reaction was based on the interactions between magnesium, hydroxide and chloride ions. Further thermodynamic studies of the reactions by Zhang et al (1991) revealed that the hydration reaction of magnesite binder is due to the reaction between $MgCl_2$ and caustic magnesia (MgO).

These 5–phase and 3–phase crystals represent the matrix that binds the wood fibres. Although the hydration reactions responsible for their formation are not yet fully understood, it has been reported that the process is impaired by wood species and extractive content. Na et al. (2014) studied the hydration process of a magnesia-bonded wood wool panel using DSC, SEM, XRD and XPS analyses. The authors discovered that addition of poplar sawdust caused a drop in exothermic peak during DSC analysis, inhibiting the hydration reaction. This is in line with the findings of Simatupang and Geimer (1990) that the relative hydration time of magnesia cement is affected by wood species and certain extractives. The effect is however not as pronounced as with cement (Simatupang and Geimer 1990; Youngquist 1999). Zhou and Li (2012) produced lightweight magnesia-bonded wood products using perlite as a partial substitute for wood content and a mixture of polyvinyl acetate (PVA) and glass fibres as filler. Sawdust was incorporated as aggregate resulting in a product with a specific gravity

of approximately 1 and nailabillity similar to solid wood. The composites were, however, thermally unstable as the flexural strength decreased considerably at elevated temperatures. Substitution of wood content with 50% perlite improved the thermal resistance.

Magnesia cement are highly hygroscopic in nature and hence exhibit prominent dimensional instability and loss of strength over prolonged exposure to water and moisture (Beaudoin and Ramachandran 1975; Misra and Mathur 2007; Plekhanova et al. 2007). This is why utilization of magnesia-bonded wood composite is restricted to indoor applications (Walling and Provis 2016).

### 2.2.2 *Gypsum-bonded wood composites*

Utilization of gypsum binder in wood composites dated back to the early 1900s (Aro 2008). α- and β- gypsums are the two major types of gypsum. α- gypsum is made through a wet process (autoclaving) while β- gypsum is produced by a dry process (calcination) (Abidoye and Bello 2010). α- gypsum forms a superstructure of excellent strength when mixed with water due to its prismatic crystals (Abidoye and Bello 2010). However, β-gypsum is preferable in composite production because of its low cost, ease of manufacturing (Simatupang and Geimer 1990) and rapid setting (Singh and Garg 1994). It is made up of gypsum hemihydrate ($CaSO_4 \cdot {}_{1/2}H_2O$) usually formed by heat treatment (at elevated temperature) of natural gypsum ($CaSO_4 \cdot 2H_2O$) or waste chemical by-products (phosphogypsum) (Mortensen 2007; Singh and Garg 1994).

Gypsum boards, also known as drywall, wallboard, plasterboard or sheetrock (Jang and Townsend 2001; Ndukwe and Yuan 2016) are made from gypsum mixed with water and lignocellulosic fibres (Youngquist 1999). Gypsum boards exhibit non-brittle behaviour with good working and fire resistance properties (Singh and Garg 1994) suitable for interior applications in both residential and commercial establishments (Jang and Townsend 2001). They are usually produced with about 93% gypsum (with 1% impurities and additives) and 7% paper fibre (Marvin 2000; Turley 1998). The formed composites cure readily as gypsum is less sensitive to wood species, water-soluble extractives and hydrolysable compounds in wood (Felton and DeGroot 1996). Araújo et al (2011) made gypsum-bonded panels with bamboo fibres and reported that the addition of bamboo fibres did not affect the hydration process of gypsum. The inhibitory index was very low, about 1.2%, compared to 10.1% recorded for those made with Portland cement following cold water extraction of soluble extractives. According to Simatupang et al (1991), wood extractives retard the hydration of the inorganic binders and alter their crystalline structures. The effects of wood extractives on the formation and geometry of gypsum crystals depend on the wood source. Birch veneer-gypsum boards exhibited three different

crystals layers with no form of interlocking. On the contact layer, the gypsum crystals were considerably smaller than those found at the transition layers. Only two crystal layers were found in spruce-gypsum and interlocking crystals were observed in the contact layer.

Gypsum board is an important interior component for building construction and remodelling in North America (Ndukwe and Yuan 2016). Apart from the fact that prolonged exposure to moisture and water can impair its performance and limit its use to interior applications, there is also a growing concern about its waste disposal. Economic and population growth in North America has caused an exponential increase in the generation of gypsum waste in recent years (Ndukwe and Yuan 2016). According to U.S Census Bureau (2017), privately-owned housing completions in September 2017 were at a seasonally adjusted annual rate of 1,109,000, which is 1.1 percent above the revised August 2017 estimate of 1,097,000 and 10.3 percent above the September 2016 rate of 1,005,000. Single-family housing completions also increased by about 4.6 %. Being the principal interior construction material in the United States, gypsum boards are used in virtually all newly built homes (Marvin 2000). Construction of a single-family home of about 2000ft$^2$ and office building of about 50,000ft$^2$ generate about 1 metric tonnes and 16 metric tonnes of gypsum waste respectively (Jang and Townsend 2001; Ndukwe and Yuan 2016; Turley 1998). It has been estimated that gypsum waste constitutes between 12 –27% of construction and demolition (C&D) debris in the United States and about 9% in Canada (Ndukwe and Yuan 2016). The bulk of these materials are usually landfilled or incinerated while only a fraction is recycled. These methods of disposal pose a serious challenge to human health and the environment. Apart from consuming a significant volume of landfill areas, the favourable anaerobic condition of landfills enables leaching of inorganic ions, most importantly sulphates and gases, such as $H_2S$ and $CO_2$.

### 2.2.3 *Cement-bonded wood composites*

A more water-resistant form of inorganic bonded wood composites was made with Portland cement in the 1920s (Van Elten 2006). Cement is a mixture of different inorganic minerals, such as calcium silicates and aluminates (Ridi et al. 2010). Tri-calcium silicate ($Ca_3SiO_5$, $C_3S$) and di-calcium silicate ($Ca_2SiO_5$, $C_2S$) are the most important components as they constitute about 80% of the clinker composition (Van Oss and Padovani 2003). On contact with water, $C_3S$ and $C_2S$ form hydrates, which are responsible for initial and long-term strength development, respectively (Van Oss and Padovani 2003; Ridi et al. 2010). The inclusion of wood fibres and other non-woody lignocellulosic materials

in cement matrix retard the formation of these hydrates- resulting in products of low structural integrity (Jorge et al. 2004).

The global understanding of health risks of asbestos products following the World War II made cement-bonded wood composite products generally acceptable alternatives. Since then, different cement bonded products have been produced and named with respect to the geometry and source of the wood fibres or particles. These include wood wool cement bonded composite, cement bonded particle board, cement bonded oriented strand board, cement bonded fibre boards, etc.

Unlike magnesia and gypsum bonded wood composites, the problems of cement-bonded composites are not based on structural integrity, but hydration reactions of cement are impaired due to the presence of extractives and hemicellulose components of wood. In order to deal with the compatibility issue, different approaches have been thoroughly studied. These included uses of chemical accelerators, such calcium chloride and magnesium chloride, hot water treatment of wood to remove the extractives as well as mild alkali treatment with sodium hydroxide to remove hemicelluloses.

## 2.3 Innovative geopolymeric binders

Due to the understanding of the challenges and setbacks associated with utilization of traditional inorganic binders in wood composite applications, hybrids and different innovative binders are being researched. Geopolymers have been touted to be a possible innovative alternative to traditional inorganic binders in different applications. They are described as a group of mineral binders with amorphous microstructure, but similar chemical composition to zeolites by Joseph Davidovits in 1978 (Wallah and Rangan 2006). He introduced the concept of poly(sialate) units as a representation of the chemical classification of geopolymers. Sialate stands for silicon-oxo-aluminate (Komnitsas 2011), which has a 3-D aluminosilicate network structure. The empirical formula is given as follows:

$$M_n = [-(SiO_2)_z - AlO_2]_n . wH_2O \quad (1)$$

Where z = Si/Al molar ratio (1, 2, 3 or more); M = Alkali cation ($Na^+$ or $K^+$); n = Degree of polymerization; and *w* = water content (Palomo et al. 1999).

The network is composed of $SiO_4$ and $AlO_4$ tetrahedrons bonded by oxygen bridges. Chains or rings united by Si – O – Al bridges are formed (Komnitsas 2011; Škvára 2007).

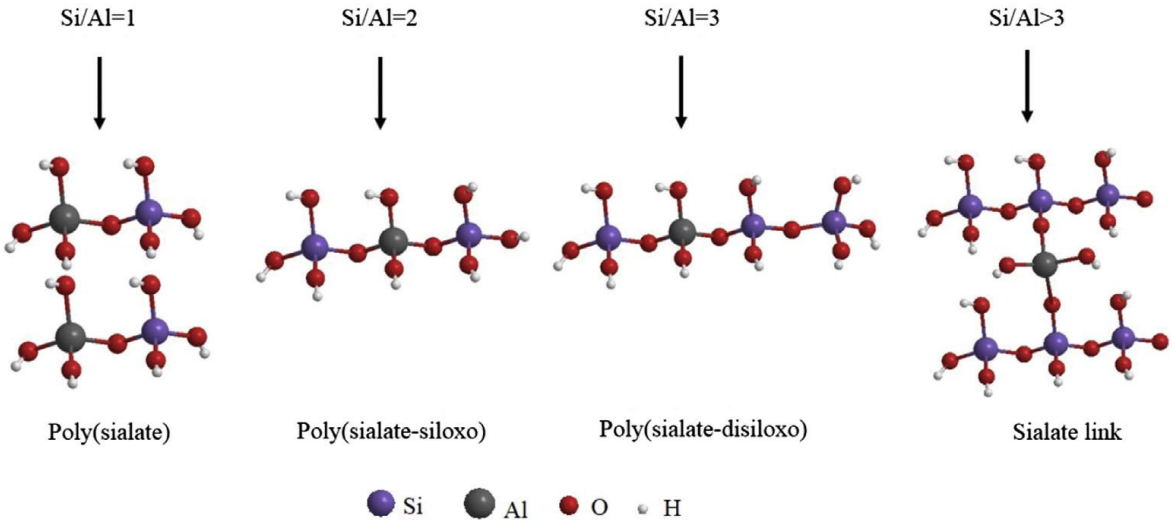


**Fig. 2-1** Chemical designation of geopolymer units by Davidovits (Source: Zhuang et al, 2016)

## 2.4 Development of geopolymers

Geopolymer is an inorganic polymer developed by alkali activation of amorphous aluminosilicate materials at room or slightly elevated temperatures (Alomayri et al. 2013). The structure of geopolymer is amorphous to semi-crystalline in nature (Mellado et al. 2014). Source materials for geopolymer include naturally occurring materials like Taftan pozzolan (pumice) and kaolinite (Duan et al. 2016). They can also be synthesized from industrial waste, such as fly ash (Najimi et al. 2016), blast furnace slags (Van Deventer et al. 2007) and silica fumes (Doan et al. 2010). The ability to synthesize them from industrial waste provides an alternative beneficial means of disposal. The common alkaline activators include sodium and potassium hydroxides (Hardjito and Rangan 2014; Petermann and Saeed 2012; Sedira et al. 2017), alkali silicates and carbonates (Provis and Van Deventer 2014). The processes involved in the development of geopolymer include the dissolution of source material into aluminosilicate species by alkali metal solutions, formation of oligomeric species, precipitation or polycondensation of the species to form an inorganic polymeric products, final hardening of the matrix and the growth of crystalline structures (Dimas et al. 2009; Petermann and Saeed 2012). The final strength of geopolymer concrete depends on many factors dependent on the source of starting materials, activator type, curing technique and production variables (Petermann and Saeed 2012).

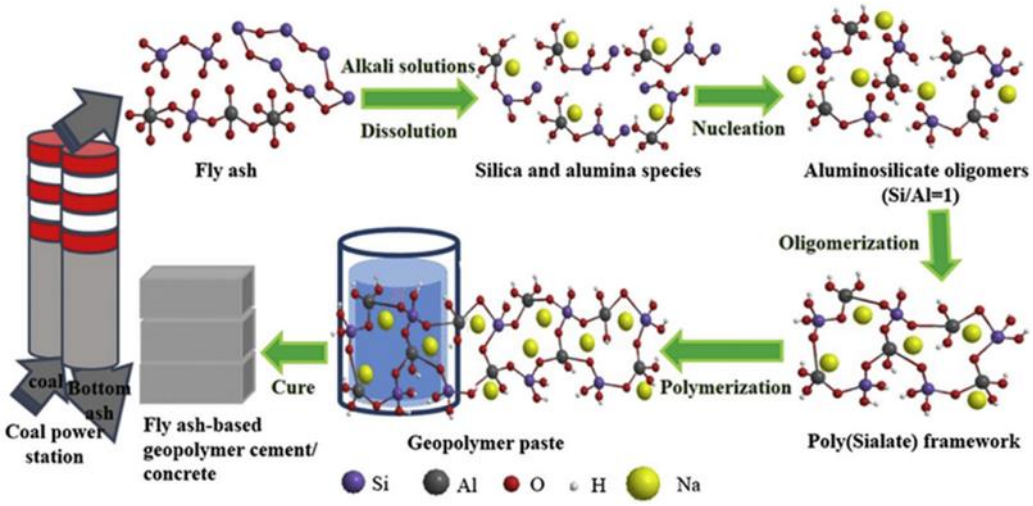


**Fig. 2-2** Development of fly ash-based geopolymer cement (Source: Zhuang et al. (2016)

### 2.4.1 *Dissolution of precursor in alkali solution*

On contact with the precursor material, the alkali metal solution causes the breakdown of Si–O–Si bonds to start a new phase with a mechanism of formation through synthesis via solution (Škvára 2007). According to Petermann and Saeed (2012), the breakdown of covalent bonds between silicon, aluminium and oxygen generates rapid and intense heat similar to Portland cement hydration. The Al atoms penetrate the original Si–O–Si structure with the formation of alumino-silicate gels known as zeolite precursors. The rate of dissolution depends on pH of the activating medium (Hanzlíček and Steinerová-Vondráková 2002), solid to liquid ratio (Glid et al. 2017) and composition of the source material. Ogundiran and Kumar (2016) conducted isothermal conduction calorimetry of fly ash and calcined clay as geopolymer precursors. The authors discovered that at the dissolution stage, calcined clay had higher early reactivity.

### 2.4.2 *Polycondensation and hardening of dissolved species and minerals*

Following the hydrolysis and dissolution stage, dissociation of the –Si–O–Si– or –Si–O–Al– bond leads to the release of free $Al^{3+}$ and $Si^{4+}$ tetrahedral species into the solution (Arioz et al. 2013). The active species combine to form nuclei and aluminosilicate oligomers in form of polysialate –Al–O–Si– chain, polysialate-siloxo –Al–O–Si–O–Si– and/or polysialate-disiloxo –Al–O–Si–O–Si–O–Si– chain based on the Si/Al ratio (Zhuang et al. 2016). The formed product contains cations from the activating medium (e.g. $Na^+$ or $K^+$), which compensate for the resultant negative charge due to partial

substitution of $Si^{4+}$ by $Al^{3+}$ (Palomo et al.1999; Petermann and Saeed 2012; Zhuang et al. 2016; Cui et al. 2017).

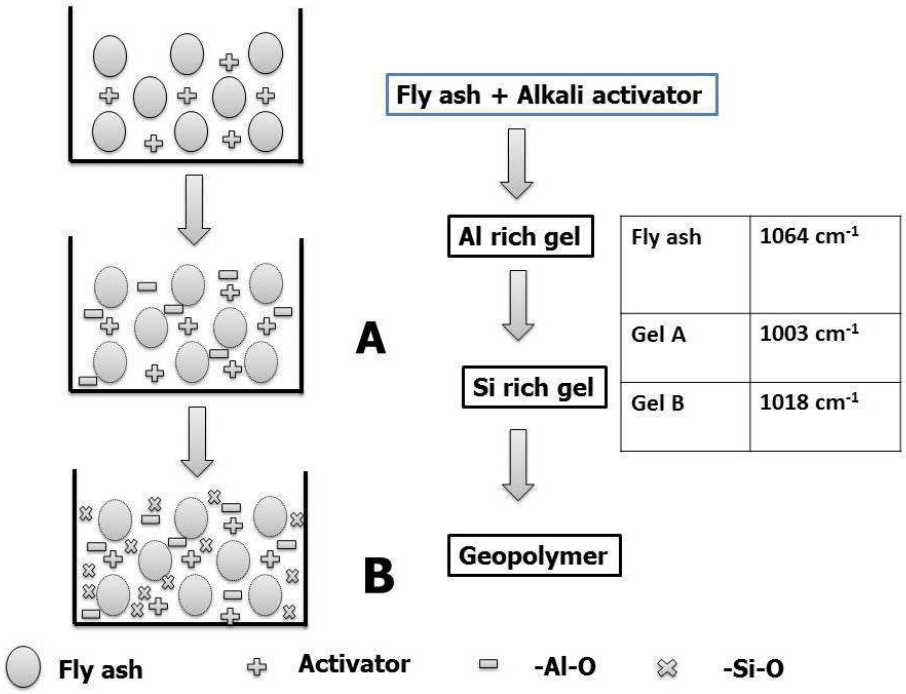


**Fig. 2-3** Geopolymerization mechanism and variation in FTIR bands

(Source: Fernández-Jimenez et al. 2005)

During polycondensation of the oligomers, an Al-rich phase precedes the formation of a more stable Si-rich 3–dimensional gel product designated by Q4(nAl) (Fernández-Jimenez et al. 2005). Formation of these phases, and most especially Si–rich gel product depends on the type of activator and the curing pattern. Palomo et al. (1999) studied the reaction mechanisms of Class F fly ash with four different alkaline activators (NaOH, KOH, NaOH + $Na_2SiO_5$ and KOH + $K_2SiO_5$) cured at elevated temperature of 65°C and 85°C. The reaction produced an amorphous aluminosilicate gel with a structure similar to that of zeolitic precursors. Similar reaction products have been reported in different independent studies (Natali et al. 2011). The authors concluded that temperature and activator type are significant factors affecting the strength properties. An increase in temperature accelerated the reaction, such that geopolymerization stages overlapped and could not be detected separately by calorimetry. Also, geopolymers made with NaOH and sodium silicate had better performance. Irrespective of the starting material, an increase in curing temperature seems to greatly

influence the rate of reaction. Mustafa Al Bakri et al (2012) investigated the possibility of making foam concrete using Class C fly ash based geopolymer. The author used a system of NaOH and sodium silicate as the activating medium and two different curing conditions (room temperature and 60°C). Samples cured at 60°C had maximum compressive strength which was supported by SEM analysis which indicated compact microstructures. It was concluded that increase in curing temperature accelerated the geopolymerization process, which led to a denser matrix. According to Petermann and Saeed (2012) the fast rate of reaction between the alkali activator and the precursor does not provide sufficient timeframe for the growth of a well-structured product.

## 2.5 Application areas of geopolymers

The chemical structures in terms of the atomic Si:Al ratio of geopolymeric materials determine their application areas (Hardjito and Rangan 2014). The classification of application areas based on the Si:Al ratio is given by Davidovits (1994) and shown in Table 2-1. Geopolymer products synthesized from waste materials are desired in the construction industry because they are more durable and highly fire resistant. They also offer many advantages over conventional materials like OPC and gypsum cement (Van Deventer et al. 2007). Geopolymers offer comparable or superior performance to ordinary Portland cement in many different applications, such as fire protection (Zhang et al. 2014) and immobilization of heavy metals from industrial and residential wastes, (Chen 2014; Van Deventer et al. 2007). Geopolymers are also applied in other sectors e.g., metallurgy, automobile, plastic, and civil engineering sectors. A low Si:Al ratio is suitable for many civil engineering applications (Davidovits, 1994 cited in: Hardjito and Rangan, 2014).

**Table 2-1** Applications of geopolymeric materials based on Si:Al atomic ratio (Davidovits, 1994 cited in: Hardjito and Rangan, 2014)

| Si:Al ratio | Applications |
|---|---|
| 1 | • Bricks<br>• Ceramics<br>• Fire protection |
| 2 | • Low $CO_2$ cements and concretes<br>• Radioactive and toxic waste encapsulation |
| 3 | • Fire Protection fibre glass composite<br>• Foundry equipment<br>• Heat resistant composites 200$^{o}$C to 1000$^{o}$C<br>• Tooling for aeronautics titanium process |
| >3 | • Sealants for industry, 200$^{o}$C to 600$^{o}$C<br>• Tooling for aeronautics SPF aluminium |
| 20 – 35 | • Fire resistant and heat resistant fibre composites |

## 2.6 Geopolymer starting materials

Materials rich in aluminosilicate oxides in amorphous phase are potential precursors for geopolymer synthesis (Yang et al. 2012; Petermann and Saeed, 2012; Alomayri et al., 2013). These include naturally occurring materials, such as natural zeolite (clinoptilolite) (Nikolov et al. 2017), kaolinite, feldspar, albite, stilbite (Arioz et al. 2013), and industrial waste, such as fly ash, GGBS (Nikolov et al. 2017), mine tailings , waste glass, and rice husk-bark ash (Hardjito and Rangan 2014; Sedira et al. 2017).

### 2.6.1 *Natural material*

#### *2.6.1.1 Kaolinite*

Kaolinite clays are directly mined from natural deposits, but they can also be found in the mine tailings or as a constituent of paper industry waste. Their reactivity in alkaline medium can be affected by properties such as particle size and degree of crystallinity, which are dependent on their source. However, the source does not inherently control its value in alkali-activated binder (Provis and Van Deventer 2014)

#### *2.6.1.2 Fly Ash*

Fly ash material can be categorized as either a low-calcium (Class F) or high-calcium fly ash (Class C). Fly ash is derived as a by-product from the burning of coal for power generation. It is regarded as one of the most desired precursor for geopolymer cement (Hardjito and Rangan 2005; Khale and Chaudhary 2007). Fly ash is composed majorly of acidic oxides such as alumina, silica and ferrite which provide potential for alkali activation (Williams et al. 2002). It is composed inhomogeneous mixture of amorphous aluminosilicates, silica glasses and crystalline materials like hematite, magnetite, mullite, and quartz in small quantities (Song et al. 2000). The inhomogeneity nature of the material should be considered in the mix design to ensure to ensure that the final product has a consistent property (Hardjito and Rangan 2005).

#### *2.6.1.3 Granulated blast furnace slag*

GGBFS is an industrial residue derived when molten steel is subjected to rapid water cooling. GGBFS is relatively inexpensive and has desirable properties such high resistance to chemical and thermal stability (Petermann and Saeed 2012). It is used as a supplementary material in cement industry due its advantageous pozzolanic properties. According to Pacheco-Torgal et al. (2008), a low-basic amorphous calcium silicate hydrate (C-S-H) gel with high aluminium content is produced when GGBFS is activated with alkali solution.

### 2.6.2 *Alkaline activators*

#### *2.6.2.1 Sodium hydroxide (NaOH)*

Sodium hydroxide is the mostly preferred hydroxide activator for producing alkali-activated materials due to its high alkalinity (Nematollahi and Sanjayan 2014; Provis and Van Deventer 2009; Somna et

al. 2011). An 8.0 molar concentration of NaOH gives a pH value of 13.32 at 23°C (Nematollahi and Sanjayan 2014). According to Palomo et al. (1999), the activation of precursor materials such as fly ash with NaOH solution produces some hydroxysodalite and other minerals based on the composition of the fly ash. Higher concentrations of NaOH improve the compressive strength of alkali-activated materials due to their positive influence on the dissolution of silica and alumina from the starting material (Chindaprasirt et al. 2009; Somna et al. 2011; Chindaprasirt and Chalee 2014). According to the study of Chindaprasirt and Chalee (2014), high concentrations of NaOH also improved the degree of polycondensation, which enhanced the development of long-term compressive strength of alkali-activated concrete. It was concluded that increasing the concentration of NaOH improved the resistance of the steel reinforcement to corrosion. Somna et al. (2011) also reported that the molar concentration of NaOH affected the compressive strength and microstructural development of alkali-activated materials.

*2.6.2.2 Potassium hydroxide (KOH)*

Like NaOH, KOH is commercially available in pellets with purity in the range of 97% - 100%. The two hydroxides are usually used in solution form to activate the precursor materials. At the same molarity KOH is more alkaline than NaOH, and thus causes greater dissolution of the precursor materials (Khale and Chaudhary 2007; Raijiwala et al. 2012). However, NaOH offers a greater capacity to liberate silica and alumina species (Hardjito and Rangan 2005).

*2.6.2.3 Calcium hydroxide ($Ca(OH)_2$)*

Calcium hydroxide is usually used to activate precursor materials through pozzolanic reaction. The activation of materials that do not exhibit pozzolanic properties with $Ca(OH)_2$ results in poor strength development (Sedira et al. 2017). It is less expensive, and it has lower pH values compared to other hydroxides (Jeong et al., 2016). It therefore presents itself as a safer alternative to other hydroxides from practical application point of view. Similar to NaOH and KOH, increasing the concentration leads to greater dissolution of the reactants species which enhances the formation of reactant products (Alonso and Palomo 2001).

*2.6.2.4 Sodium silicate ($Na_2SiO_3$)*

Sodium silicates are available as colourless glassy solids or white powders, which are readily soluble in water. They are the mostly used water-soluble silicates in alkali-activated materials (Davidovits

2008). They are produced in larger quantities and less expensive than potassium silicates (Davidovits 2008). Waterglass ($Na_2O{\cdot}nSiO_3$) contains dissolved glass that has water-like properties. They have excellent properties which make them applicable as sealants and binders (Christensen et al. 1982). Their suitability for geopolymer synthesis depends on its mass ratio of $SiO_2$ and $Na_2O$ which is usually in the range of 1.5 to 3.2. According to Fernández et al. (2005), a ratio of 3.2 is offers the best synthesis for geopolymer reactions. Different researchers have used a combination of sodium silicate with the hydroxides of sodium or potassium (Alomayri et al. 2013; Chuah et al. 2016; Duan et al. 2016; Hardjito and Rangan 2014). It has been reported that activating medium which contains high doses of soluble silicates produced mortars and concrete of superior strengths than a medium with little or no silicates (Feng et al. 2004). They also impart properties such as high resistance to acid and fire in the materials (Sedira et al. 2017). However, it has been observed that the utilization of sodium silicate to synthesise geopolymer has an impact on the environment apart from global warming (Habert et al. 2011; Habert and Ouellet-Plamondon 2016). The means of containing this has been highlighted by Habert and Ouellet-Plamondon (2016). These are (1) utilization of industrial wastes that have no allocation (2) reduction in the use of sodium silicate.

### 2.6.3 *Curing methods*

Geopolymers can be cured both at ambient conditions and slightly elevated temperatures. The curing conditions, such as temperature and duration of curing can significantly affect evolution of strength development of the final product (Hardjito and Rangan 2014). Geopolymers cured at elevated temperature have been reported to exhibit better strength properties. Arioz et al. (2013) investigated the effects of curing conditions on fly ash-based geopolymer. The samples were cured at 80$^o$C for 6h, 15h and 24 h and tested for compressive strength after 7days, 28days and 90days of aging. The compressive strength for all the samples increased with aging. The effect was more pronounced in samples cured for 6h. The strength increased by 1.6 times and 59% when tested at 28 and 90 days respectively. For samples cured for 15h and 24h, the increase in strength ranged between 16 - 28%. However, the curing conditions did not affect the microstructure of the samples as FTIR and XRD spectra were similar. FTIR spectra indicated that Al – O and Si – O asymmetric stretching vibrations increased with curing and the XRD diffractograms showed no significant difference in crystalline parts for curing durations. Wallah and Rangan (2006) also developed fly ash-based geopolymer concrete cured both at ambient and elevated temperature of 60$^o$C. Although geopolymer cured at room temperature had lower initial strength, which later increased with age. Extended curing times increases the strength of alkali-activated materials. However, the strength gain occurs at slower rate

due to alkaline saturation and product densification (Petermann and Saeed 2012). Curing at elevated temperature substantially enhances the reaction kinetics during geopolymerization (Hardjito and Rangan 2014).Those cured at 60$^{o}$C had better strength and lower creep behaviour.

## 2.7 Enhancement of geopolymer with fibre reinforcement

### 2.7.1 *Reinforcement with synthetic fibres*

Like other inorganic binders, geopolymer also exhibits brittle behaviour with low tensile strength, ductility, and fracture toughness. In a bid to improve these structural deficiencies, different synthetic fibres, such as polypropylene (PPE), polyvinyl acetate (PVAc), steel and carbon fibres have been incorporated into the matrix. Korniejenko et al. (2015) used polypropylene fibres to improve the mechanical properties of fly ash based geopolymer composites. The addition of polypropylene to geopolymer matrix improves the flexural strength of these materials. Composites made with the addition of 15 % vol. of reinforcing fibres had the best flexural strength. Also, in a different study by Yunsheng et al. (2008), short polyvinyl alcohol (PVA) fibres with an optimum volume fraction of 2.0% decreased the brittle tendency of fly ash- based geopolymer (Yunsheng et al. 2008). The addition of PVA fibres changed the impact failure mode of the composite product from brittle pattern to ductile, resulting in a great increase in impact toughness. Natali et al. ( 2011) embedded high tenacity (HT) carbon, E-glass, polyvinyl alcohol (PVA) and polyvinyl chloride (PVC) into metakaolin based geopolymer matrix. The resulting composite materials exhibited increased pore radii, which led to reduction in intruded volume, except for those reinforced with PVC fibres. It was reported that the fibres generally enhanced the mechanical properties of the composites despite an increase in the pore radii. The flexural strength increased by 30 – 70% compared to unreinforced geopolymers. An increase in strength was attributed to the bridging effect induced by the dispersed fibres. In another study, Zhang et al. (2014) reinforced metakaolin based geopolymer with carbon fibre. The addition of carbon fibres prevented crack formation and propagation, and enhanced bending strength under high temperature. It was also observed that substitution of metakaolin with fly ash reduced water demand for geopolymerization, which ultimately enhanced the properties after exposure to elevated temperature.

Although these synthetic fibres greatly improved the structural integrity of geopolymer, they are very expensive, highly energy-intensive and disposal at the end of their life cycle impact the environment negatively (Herrmann et al. 1998; Pacheco-Torgal and Jalali 2011). This has necessitated the need

for reinforcement with natural fibres from lignocellulose and industrial waste to improve its strength properties and make it ecologically sustainable.

### 2.7.2 *Reinforcement with lignocellulosic fibres*

Lignocellulosic fibres, both virgin and industrial residues, offer excellent properties, which make them better alternative to synthetic fibres. They are biodegradable with low density and adequate mechanical properties (Sarmin 2016). They have been extensively incorporated into different inorganic binders to improve the strength properties. However, their inclusion into geopolymer matrix is still being researched. Preliminary investigations have proven that they can be successfully incorporated into the matrix. The first wood-geopolymer product was a fire-resistant chipboard panel manufactured in a one-step process. It was prepared by sandwiching between two geopolymer nanocomposite coatings (Davidovits, 2008 cited in Sarmin et al., 2014). Alomayri et al. (2014) studied the mechanical properties of fly ash geopolymer reinforced with cotton fabric at elevated temperature. The addition of fibres prevented the matrix from cracking after exposure to a high temperature range of 200 – 1000$^{o}$C. This was attributed to the induced additional porosity and formation of small channels as the cotton fibres degrade. The formed pores and channels provided beneficial pathways for water vapour to escape thereby preventing the build-up of pore pressures. The composite also exhibited a significant reduction in mechanical strength after exposure to a temperature beyond 800 - 1000$^{o}$C, due to the formation of numerous voids following complete fibre degradation. Chen et al. (2014) reinforced fly ash-based geopolymer with sorghum fibre and concluded that addition of fibre decreased the workability and unit weight of geopolymer pastes. It was reported that fibre content up to 2% increased both tensile and flexural strengths of the geopolymer composites. The inclusion of fibres changed the failure mode of geopolymer from brittle to ductile. SEM characterization confirmed fibre pull-out and fracture as the main mechanisms responsible for the enhanced ductility, tensile and flexural strengths. Duan et al. (2016) observed a similar trend in a recent study. Fly ash-based geopolymer was reinforced with sawdust and fresh properties, mechanical strength and microstructure were evaluated. A combination of $Na_2SiO_3$ and NaOH with a mass ratio of 8:1 was used as an activator. Fly ash was partially replaced with 0 – 20% sawdust by mass at an interval of 5%. The inclusion of fibre, especially more than 5% affected the workability and setting time. Geopolymers without sawdust exhibit cracks and high porosity ratio after 28 days curing.

### 2.7.3 *Influence of precursor materials on geopolymer-bonded composites*

Materials rich in aluminosilicate oxides in amorphous phases are potential precursors for geopolymer synthesis (Yang et al. 2012; Petermann and Saeed 2012; Alomayri et al. 2013). These include naturally occurring materials, such as natural zeolite (clinoptilolite) (Nikolov et al., 2017), kaolinite, feldspar, albite, stilbite (Arioz et al., 2013) clays, micas, andalousite, spinel (Davidovits 1988), and industrial waste, such as fly ash, granulated blast furnace slag (Nikolov et al., 2017), mine tailings , waste glass, and rice husk-bark ash (Hardjito and Rangan 2014; Sedira et al. 2017). Fly ash and metakaolin, however, have been the principal precursor materials used in geopolymer-bonded lignocellulosic composites as observed in the following research works (Alomayri 2013; Alomayri et al. 2014; Chen 2014; Chen et al. 2014; Duan et al. 2016; Gouny et al. 2013; Gouny et al. 2012; Sarmin 2016; Sarmin and Welling 2015). Metakaolin is the traditionally preferred precursor for making geopolymers because the high consistency in its production makes prediction of characteristics of the final product possible (Petermann and Saeed 2012). It is produced by heat treatment of kaolinite through a calcination process at a temperature range of 400 - 800°C. The optimum condition for producing metakaolin is calcination at 600°C for two hours (Chareerat et al. 2006). The production is energy intensive and leads to depletion of unrenewable natural resources. Fly ash on the other hand is an industrial by-product of coal burning for power generation. It is usually landfilled and pose serious impact on the environment. Its utilization fulfils the objectives of wood and fibre composites production, where environmental sustainability, low cost, durability, and structural integrity of final products are of utmost importance. Metakaolin and fly ash have different morphology, chemical composition, and physical properties, such as particle size distribution and Baine's fineness. These unique characteristics and properties affects their reactivity, which in effect influence the mechanical strength of geopolymers (Petermann and Saeed 2012).

Duan et al (2016) studied the properties of fly ash-based geopolymer reinforced with 5 – 20% sawdust content. The authors recorded comparative compressive strength for both the reference sample samples reinforced with sawdust, irrespective of sawdust content, until curing time of 14 days. As curing progressed, a pronounced increase in compressive strength was observed with the reinforced samples, about 9.6% and 12.1% higher after 28 day and 90 days curing ages. These observations contradict the findings of Sarmin (2016) where the compressive strength of reinforced geopolymer decreased with the addition of wood materials. In the study, fly ash was substituted by 30% metakaolin and the compressive strength decreased by about 50% when 10% wood flour was added: and 75% with the addition of 10% wood particle. In a separate study by Sarmin and Welling (2015)

where mixed softwood particles was incorporated into fly ash-based geopolymer substituted by metakaolin at 0 – 50 %, reduction was also observed in the compressive strength of the composite products. Maximum values were recorded for composites made with 100% fly ash cured at both room and elevated temperature of 80°C. The same trend was observed in the oven-dry density of composites cured at 80°C. The only exceptions occurred when metakaolin was substituted at 10%, 20% and 40%, the composites had slightly higher values when cured under room conditions. The findings of Sarmin (2016) and Sarmin et al (2014) were in agreement with the observations of Chen et al (2014), where the inclusion of sorghum fibres caused reduction in the unconfined compressive strength of fly-ash based geopolymer. However, increase in splitting tensile and flexural strengths was observed with the addition of sorghum fibres up to 2%. From the foregoing it is evident that partial substitution of fly ash with metakaolin in the study led to reduction in strength properties of the final geopolymer-bonded composite. This is different from what is obtainable with geopolymer concrete where addition of metakaolin improves the strength of fly ash-based geopolymer concrete. Chareerat et al (2006) synthesized high calcium fly ash and metakaolin to make geopolymer mortar. Substituting fly ash with about 40% metakaolin increased the compressive strength. A maximum compressive strength of ± 45 MPa was observed when fly ash was substituted with 25% metakaolin. substitution with metakaolin Optimized value of 25% replacement yielded a maximum strength of ± 45 MPa. The reduction in the strength of geopolymer-bonded composites upon partial substitution of fly ash with metakaolin could be due to inherent properties of the lignocellulosic materials as no information about the chemical composition was provided.

### 2.7.4 *Influence of lignocellulosic material, content, and particle geometry on geopolymer-bonded composites*

Lignocellulosic materials have low specific gravity and density, which lead to reduction in the density of the final inorganic-bonded products. The density of a material is an excellent predictor of its properties. Different studies have indicated that lignocellulosic content and particle geometry influence both physical and mechanical properties of inorganic-bonded wood composites. The extent of their influence differs for various lignocellulosic sources. Badejo (1980) reported that the strength properties of hardwood-cement board increased as the flake dimensions increase while Olorunnisola (2007) observed an inverse relationship between the compressive strength and particle size of rattan-cement composites. This suggests that different lignocellulosic materials exhibit different behaviours when encapsulated in inorganic matrix. This is further corroborated by Ajayi and Badejo (2005). The authors investigated the effect of board density on the bending strength and internal bonding of

cement-bonded flakeboards made with two exotic hardwood species, *Gmelina arborea* and *Leucaena leucocephala*. The boards were made with particle size (l x t) of 50 × 2.5 mm and compressed to densities of 1000, 1100 and 1200 $kgm^{-3}$. Board densities and wood species had significant effect on the MOR. The MOR increased with an increase in density for both species, but boards made with *Gmelina arborea* had higher values. Particle size of lignocellulosic materials also affect properties, such as density, water absorption and compressive strength of geopolymer-bonded composites. Sarmin (2016) studied the effects of wood aggregates on the physical and mechanical properties of fly ash-based geopolymer substituted with 30% metakaolin. Density and compressive strength decreased as the particle size increased. Boards made with wood particles also had higher sorption properties. It was deduced that as the wood particles increases uniform dispersion in the matrix becomes difficult as the particles agglomerated. Lignocellulosic content has also been reported to have significant effect on the properties of geopolymer-bonded composites. Chen et al. (2014) reported that the unit weight of geopolymer-bonded composites decreased as the sorghum fibre content increased. The optimum content was found to be 2% of geopolymer precursor. However, particle content as high as 20% have been incorporated in geopolymer matrix. Sarmin (2016) and Duan et al (2016) incorporated 10% and up to 20% wood particles in geopolymer binders, respectively. According to Duan et al (2016) sawdust possess positive effect on compressive strength of geopolymer, especially when more than 10% of is incorporated. The bottom line is that the proposed end use will determine the choice of particle size and content. Another important factor to consider are the inherent properties of the lignocellulosic material being incorporated in the different geopolymer matrices. These studies focussed more on the resultant products, as there was no mention of the chemical composition of the incorporated lignocellulose. Lignocellulose components interact with inorganic binders differently, based on their inherent properties and chemical compositions. Al Bakri *et al.*(2012) investigated the feasibility of making geopolymer bonded wood products using class C fly ash activated with a combination of 12M sodium hydroxide and sodium silicate. The incorporated wood particle was unnamed, and the chemical composition was determined using XRF analysis. This analysis could not quantify the lignocellulosic components, and it becomes impossible to understand how the components influence the final products.

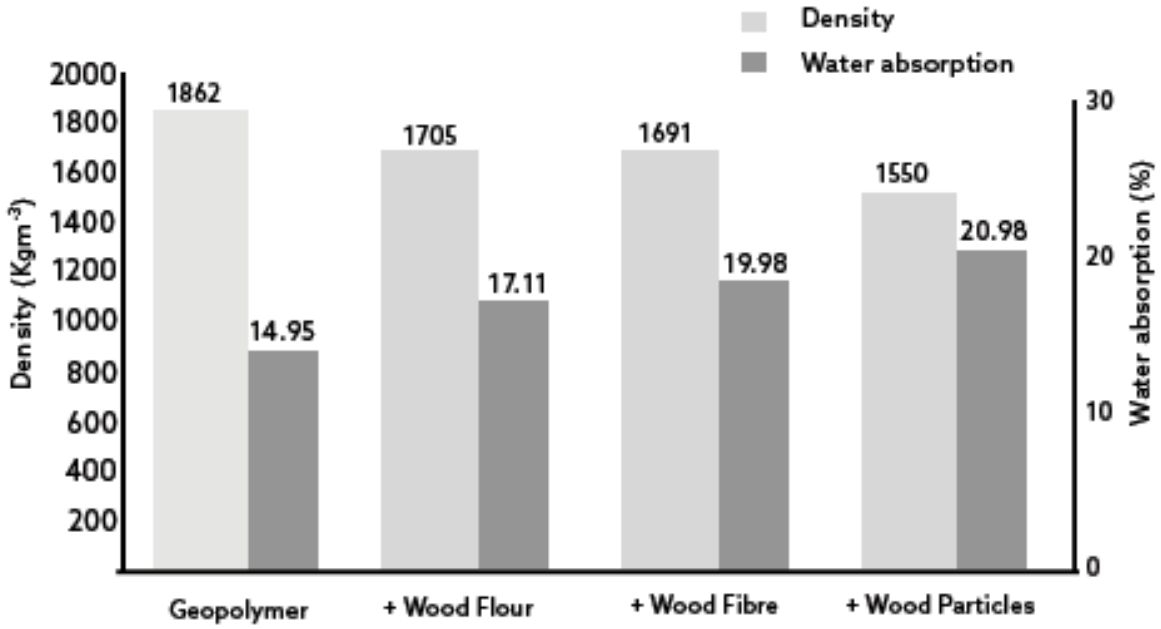


**Fig. 2-4** Variation of density and water absorption as a function of different wood aggregates content for geopolymer composites (Source: Sarmin (2016))

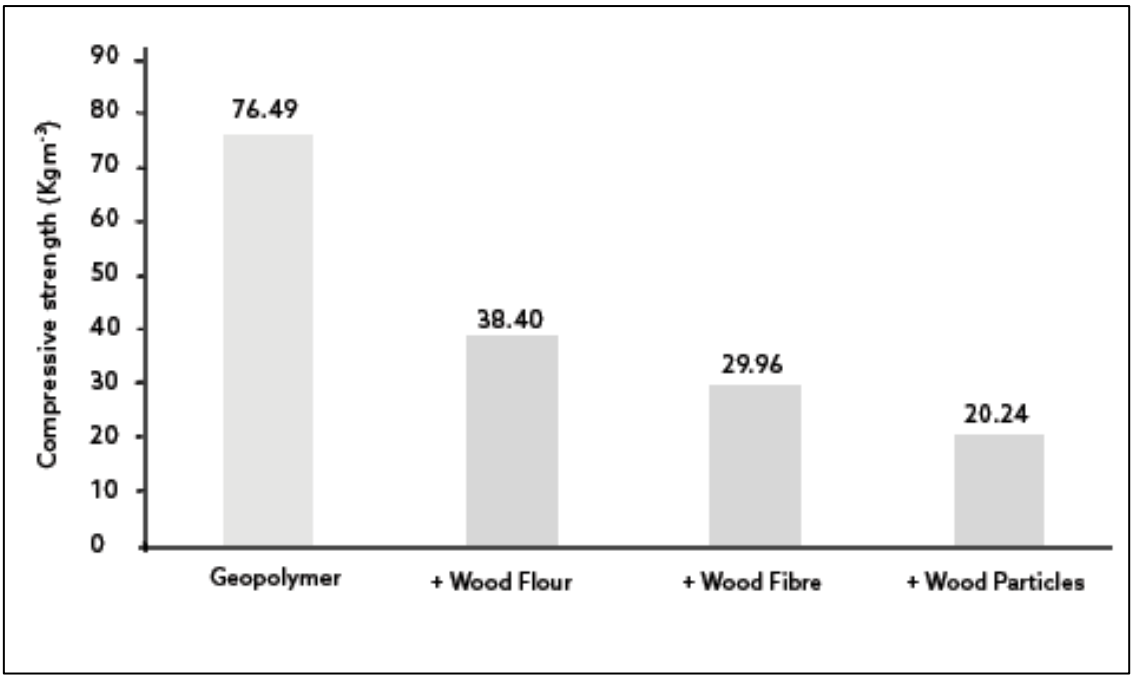


**Fig. 2-5** Effects of wood aggregates on the compressive strength of geopolymer composites (Source: Sarmin (2016))

### 2.7.5 *Curing regimes/patterns*

Curing time and temperature are important factors upon, which the final strength gain of geopolymers depend. Geopolymer concretes can be cured both at room and slightly elevated temperature within the range of 50°C - 80°C. Curing beyond this threshold may lead to deterioration of strength properties (Petermann and Saeed 2012). The understanding of ambient curing technique for geopolymer production is not yet fully developed as there are discrepancies in the available research findings. For example Fernández-Jiménez and Puertas (2002) reported that fly ash based geopolymer did not set when cured at 23°C (conditioned environment) while other researchers (Albitar et al. 2015; Neupane et al. 2016; Rao 2015) have reported the possibility of curing fly ash based geopolymer under ambient conditions . According to Petermann and Saeed (2012), curing at room temperature require longer time while elevated temperature increases the reactivity and the formation of a more crystalline product with a considerable strength gain.

## 2.8 Conclusion

The global awareness of the challenges associated with the production of conventional wood binders has stimulated renewed interest in the search for sustainable alternatives with comparable properties. Geopolymer binders developed from different waste streams have the potential to substitute cement binder in wood composite manufacturing. The final strength of geopolymer concrete products depends on several factors dependent on the source of starting materials, activator type, curing technique and production variables. Previous investigations reviewed in this section had incorporated different biomass materials in geopolymeric matrices, but sufficient information about the performance and product characterization are not available. In order to fully harness the potential of geopolymer binder in wood composites it is imperative that more research focussed on understanding the interactions between chemical components of wood and geopolymer binder be encouraged. Understanding the interactions would help in the formulation of binders for products targeted at a specific end use.

# Chapter 3

# Materials and methods

## 3.1 Materials

### 3.1.1 *Lignocellulose samples*

The lignocellulosic materials used in this study included alien invasive wood species and industrial residue (sugarcane bagasse) from sugar processing plant. The wood species included Long-leaved wattle (*A. longifolia*), Black wattle (*A. mearnsii*) and Port Jackson (*A. saligna*). The Long-leaved wattle was supplied as remnants from processed logs by EC Biomass Fuel Pellets (Pty) Ltd, Port Elizabeth, South Africa. The tree was three years old at the time of harvest. The Black wattle and Port Jackson were harvested during the invasive clearing operations along the Berg river banks in Cape Town and supplied by Casidra, Paarl, Western Cape, South Africa. The trees had all the variabilities inherent in wild growing bush. The sugarcane bagasse (*Saccharum officinarum*) was sourced from TSB Sugars (Pty) Ltd, South Africa.

### 3.1.2 *Geopolymer precursors*

Three geopolymer starting materials used included Metakaolin (MK 40) supplied by Serina Trading, South Africa, Class F fly ash sourced from Ulula Ash, South Africa and ground granulated blast slag (GGBS) from Afrisam, South Africa. The chemical compositions of these materials are presented in Chapter 4.

### 3.1.3 *Chemical activators and other reagents*

A combination of sodium silicate and sodium hydroxide was used to activate the geopolymer materials. Sodium silicate, branded as Silchem 2008 with a silica modulus of two (29.05% $SiO_2$ and 14.17% $Na_2O$) was supplied by PQ Silicas, SA. Analytical grade sodium hydroxide pellets of 98% purity were purchased from Merck Chemical (Pty) Ltd, S.A. Sulphuric acid (72% purity), acetic anhydride (98% purity) and acetic acid (98% purity) used in composition analysis of fibres and fibre treatment were supplied by Kimmix Chemicals, Cape Town, SA.

## 3.2 Methods

### 3.2.1 *Lignocellulose preparation*

Figure 3-1(a – c) shows the lignocellulosic materials as received from the suppliers. The samples were prepared according to Amiandamhen et al. (2016) and the particles are shown in Figure 3-1(d – f) . The invasive wood logs were debarked manually and chipped in a woodchipper. The wood chips and the sugarcane bagasse were then milled using a hammer mill fitted with a 1mm sieve. The milled particles were conditioned at 20°C and 65% relative humidity for 96 h before use for boards and chemical characterization.

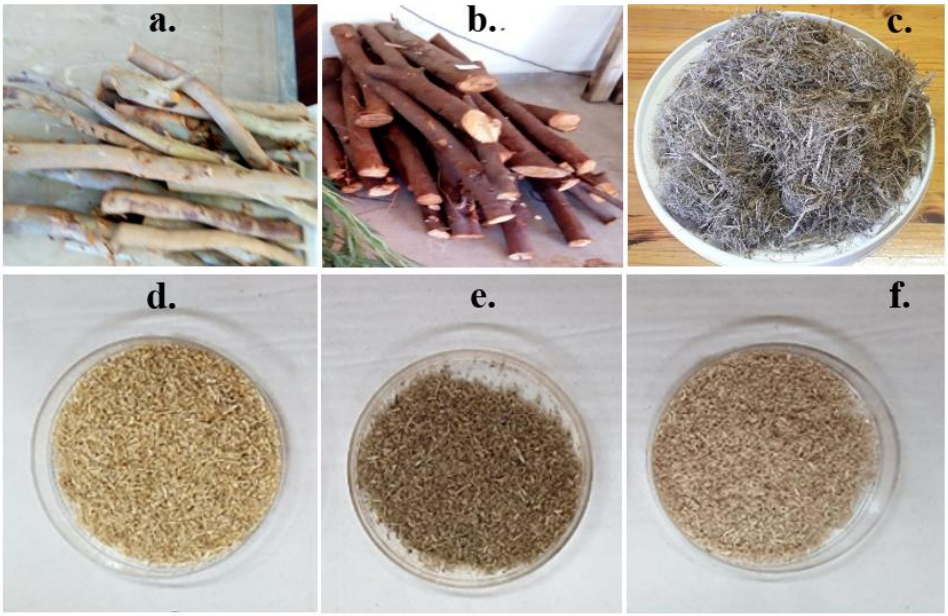


**Fig. 3-1** Lignocellulose materials as received and after milling (a) *A. mearnsii* (b) *A. saligna* (c) bagasse (d) *A. longifolia* particles (e) bagasse particles (f) *A. mearnsii* particles.

### 3.2.2 *Determination of moisture content*

The amount of moisture retained in the lignocellulose samples was determined before used for characterization and board production. It was determined according to the NREL/TP-510-42621(Sluiter et al. 2008) where 2g of lignocellulose samples was placed in a pre-weighed crucible and oven-dried at 105 ± 3°C for 24 h. The crucible was transferred into a desiccator after removal from the oven and allowed to cool for 15 min before recording the oven-dry mass. The moisture content was calculated using the following equation:

$$\boldsymbol{MC}\ (\%) = \frac{\boldsymbol{M_w - M_o}}{\boldsymbol{M_w}} \times \mathbf{100} \qquad \text{Eq. 3-1}$$

Where $M_w$ (g) is the mass of wet lignocellulose and $M_o$ (g) is the oven dry mass of the lignocellulose

### 3.2.3 *Bulk density*

The calculation of the bulk density was carried out in accordance with the procedures given by Miranda et al. (2012). Oven-dried samples were placed in a 25 ml cylindrical container and the bulk density is determined as the ratio of the mass to the volume of the container. The calculation was replicated 3 times for each lignocellulose and the results are shown in Chapter 4.

$$\boldsymbol{Bulk\ density} = \frac{\boldsymbol{M_o}}{\boldsymbol{V_c}} \qquad \text{Eq. 3-2}$$

$M_o$ (g) is the oven dry mass of lignocellulose, $V_c$ ($cm^3$) is the volume of the container

### 3.2.4 *Determination of extractive content*

Lignocellulosic samples sufficiently small to pass through a 0.40 mm screen were prepared according to TAPPI standard method (T257 2012), while the moisture content was determined in accordance with TAPPI standard (T264 2007) . Water and ethanol soluble extractives present in the lignocellulose were determined using TAPPI procedure (T204 2007). Water extraction preceded the ethanol extraction. 2.0 g of air-dry lignocellulose samples were placed into a tarred extraction thimble and weighed to the nearest 1 mg. The extraction thimble containing the lignocellulosic sample was placed in a Soxhlet apparatus connected to a pre-weighed extraction flask filled with 195 ml of water. The extraction was allowed to run for 5-6 h, ensuring no fewer than 24 cycles according to the requirement. The solvent was evaporated and the flask containing the extracts was dried in an oven at 105 ± 3°C for 1 h. The flask was cooled in the desiccator and weighed to the nearest 0.1 mg. The lignocellulose residues obtained after the extraction was used for the ethanol extraction following the same procedure.

.

### 3.2.5 *Klason lignin and monomer sugars*

Compositional analyses to determine the acid insoluble lignin, sugar contents (glucose, cellobiose, xylose and arabinose) were conducted according to the National Renewable Energy Laboratory (NREL) Analytical Procedure (LAP 013) (Ruiz and Ehrman 1996), where 3ml of 72% sulphuric acid was added to 0.3g of lignocellulose in a test tube, then placed in a water bath operating at 30°C. The solution was stirred after every 10min interval until 1h. The acid concentration was diluted to 4% by adding 84ml of distilled water, and then transferred into a flask. The solution was heated in an autoclave operating at 120°C for 90 min. The autoclaved sample was then transferred onto a filtrating crucible and washed with 250 ml boiling water. The residue in the filtrating crucible was oven-dried at 105 ± 3°C to determine the acid-insoluble lignin. Higher pressure liquid chromatography (HPLC) was used to determine the sugar contents i.e., glucose, arabinose, xylose and cellobiose. 10 ml of the hydrolysate was titrated with 1.2 ml 7N KOH, ensuring that the pH is in the range of 3 to 7. The HPLC equipment comprised of a UV1000 detector, spectra system P2000 pump, an auto-sampler (AS3000) and a Shodex RI-101 refractive index indicator.

### 3.2.6 *Determination of ash content*

TAPPI Standard (T211 2012) was used to calculate the ash content of the lignocellulosic samples. 2g of the oven-dried lignocellulosic material was placed in an oven at 575°C for 6 h and the weight of the residue was recorded.

### 3.2.7 *Lignocellulose pre-treatments*

The lignocellulosic samples were subjected to hot water, mild alkalization, and acetylation treatments. All treatments were carried out in a 5-L stainless steel digester equipped with a proportional integral derivative (PID) temperature regulator at a solid/liquid ratio of 1/10 (g/mL) according to Amiandamhen et al. (2018). The influence of each treatment on the fly ash/metakaolin- and slag-based geopolymer wood composites was investigated and is discussed in Chapter 7. Hot water treatment was carried out as described by Ferraz et al ( 2016). The lignocellulose was heated up and kept at 100°C for 1 h. Alkalization treatment is supposed to be less severe than the actual delignification process observed in alkaline pulping, hence the lignocellulose was treated with 1% NaOH solution and heated only up to 60°C for 1 h as described by Oladele et al (2015). Acetylation

was carried out using 1% wt. solution of acetic anhydride with 0.1% wt. $H_2SO_4$ as buffer according to Bledzki et al. (2008). The weight ratio of acetic acid to acetic anhydride was kept at 1.5:1 for all lignocellulose.

### 3.2.8 *Formulation of activating medium*

A combination of sodium silicate ($Na_2SiO_3$) and sodium hydroxide (NaOH) solution at a ratio of 2.5:1 was used, while the ratio of aluminosilicate to activator was varied between 2:1 and 3:1. The preparation of sodium hydroxide solution is an exothermic reaction; hence it was prepared a day prior to mixing with sodium silicate.

### 3.2.9 *Board formation*

The lignocellulosic material, precursors and the activators were measured according to the design of the experiment. The lignocellulose was mixed with precursor materials in a dry state for 3 min before a predetermined amount of activator was added and thoroughly mixed for another 5 min. Additional water was added to keep the water/binder ratio (W/B) at 28 and mixing was further extended until a homogenous mix was achieved. The mixture was transferred into a rectangular mould and cold-pressed at 0.689 MPa for 5 min to obtain a final board dimension of 218 mm × 75 mm × 13mm. The boards were kept in a temperature and humidity-controlled room at 20 °C and 65 % RH until testing.

### 3.2.10 *Curing pattern*

The curing temperature was varied from room temperature to 100 °C based on the composition of the geopolymer starting material. The curing technique was carried out according to Chareerat et al. (2006). Prior to any required temperature according to the experimental design, the boards were left in a conditioning room for 1 h and then wrapped with aluminium foil to prevent excessive loss of water during heat treatment (Figure 3-2). The boards were later left in a temperature and humidity-controlled environment for 27 days, after which they were tested for physical and mechanical properties.

**Fig. 3-2** Geopolymer boards wrapped with aluminium foil prior to curing

### 3.2.11 *Board properties*

The mechanical and physical properties of the boards were tested according to ASTM D1037(ASTM 2013) to evaluate the influence of the production variables on the GWC while the thermal property was evaluated using TGA. The flexural strength to determine the modulus of rupture (MOR) and modulus of elasticity (MOE) was conducted on an Instron machine using a 5-ton load cell at a load rate of 5 mm/min (Figure 3-3).

The physical properties included apparent density, water absorption (WA), thickness and volumetric swelling (TS/VS). The samples for the sorption and dimensional stability were cut from the boards using an angle grinder fitted with a concrete blade into dimensions of 75 mm × 50 mm × 13± 1.2 mm. The mass and dimensions of each sample was measured and recorded before being submerged horizontally in distilled water for 24 h. After removal from water, the samples were suspended and allowed to drain for 10 min to get rid of excess water. The final mass and dimensions were measured, and the water absorption (WA) and thickness/volumetric swelling calculated as a percentage increase in initial mass and thickness/volume.

**Fig. 3-3** Geopolymer boards being tested for flexural strength (3-point bending)

## 3.3 Material and products characterization

### 3.3.1 *Particle size distribution of precursor materials*

The particle size analysis of fly ash, metakaolin and slag was carried out using Saturn DigiSizer 5200 V 1.12 operated at a flow rate of 12.0 l/m and ultrasonic intensity of 60%.

### 3.3.2 *X-ray Fluorescence (XRF) analysis*

The chemical compositions of the fly ash, metakaolin and slag were determined by XRF spectrometry on a PANalytical Axios Wavelength Dispersive spectrometer fitted with a Rh tube and with the following analysing crystals: LIF200, LIF220, PE 002, Ge 111 and PX1. The analysis was carried out at the Central Analytical Facilities, Stellenbosch University, South Africa.

### 3.3.3 *Fourier Transform Infra-Red (FTIR) analysis*

Fourier Transform Infra-Red spectroscopy (FTIR) was performed using Thermo Scientific Nicolet iS10 Spectrometer equipped with a Smart iTR attenuated total reflectance (ATR) accessory to qualify the nature of bonding exhibited by the lignocellulose, precursors and the resulting geopolymer bonded composite products. Spectra were collected in ATR mode at a resolution of 4 cm-1 and 32 scans per

sample within the absorption bands in the region of 4000 – 650cm. The collected data was further processed using OMNIC Software v9.2.86 by Thermo Scientific.

### 3.3.4 *X-ray Diffraction (XRD) of precursors and geopolymer composite*

X-ray diffraction (XRD) was carried out using a Bruker D2 Phaser diffractometer, employing CuKα (λ = 1.5418 Å) at 30 kV and 10 mA. The diffraction intensities for the precursors and the resulting geopolymer composite products were captured with a Lynxeye detector with 2θ scans in the range 4 -50° with a 0.020° step size.

### 3.3.5 *Thermogravimetric Analysis (TGA)*

The thermal stability of each lignocellulose sample and the resulting GBWC were evaluated using a TGA Q50 thermogravimetric equipment. About 5 mg of each grounded sample was placed on a balance fitted in the furnace compartment and heated at a rate of 20 °C/min from room temperature to 800 °C under nitrogen flow. The results were analysed using a TA Instruments Universal Analysis 2000 software version 4.5A. The software generated the derivatives of the weight loss against temperature thermograms to show the different decomposition stages.

### 3.3.6 *Scanning Electron Microscope (SEM)*

Images of the lignocellulose and resulting GBWCs were captured and analysed using a Zeiss EVO® MA15 Scanning Electron Microscope. SEM was carried out to examine the influence of chemical treatments on the surface morphology of the fibres and microstructural characteristics of the final products at a magnification of 1000x.

## 3.4 Experimental design

For the fly ash/metakaolin binding system, the major production variables considered were the curing pattern (CP), PA ratio, molar concentration of NaOH (MCon) and amount of lignocellulosic material (LM). A mixed factorial experiment based on two factors at 2 levels (CP and PA ratio) and two factors at 3 levels (MCon and LM) with three replicates each was laid out using Statistica 13.3 for the board production. The lignocellulose content was kept constant at 25% of the total precursor. For slag-based binder the considered variable were CP, MCon and LM. The factorial experiment was based on one 2-level factor (CP) and two 3-level factors (MCon and LM) with three replicates and designed using Statistica 13.3. The PA and lignocellulose content were kept constant at 2:1 and 25% respectively.

The pre-treatment experiment was established based on a completely randomized design with 3 replications. Three different methods (hot water, mild alkali, and acetic anhydride) were designated as independent variables and the lignocellulose types were investigated separately.

**Table 3-1** Mixed factorial design for fly ash/metakaolin and slag based geopolymer bonded wood composites

| Variables | Description | Levels | | |
|---|---|---|---|---|
| | | Low | Mid | High |
| 1. Concentration (Mcon) | This is the molar concentration of sodium hydroxide | 8(4) | 10(6) | 12(8) |
| 2. Curing pattern (CP) | The curing temperature is in $^{O}$C. Values in parentheses are the levels employed in slag-based geopolymer | 60 (40) | - | 100(60) |
| 3. Precursor/Activator ratio (PA)* | This is the ratio of total precursors (fly ash + metakaolin) to the activator content. | 2:1 | - | 3:1 |
| 4. Lignocellulosic Materials (LM) | Three LM samples were utilized. Their content was kept constant at 25% of the total precursor | *1.* *A. longifolia*** *2.* *A. mearnsii and* 3. Bagasse | | |

***The PA ratio was kept constant at 2:1 for slag based geopolymer | ** A. longifolia was substituted with A. saligna in slag based geopolymer bonded wood composites.*

## 3.5 Data analysis

The data analysis was conducted using Statistica v.13.3. Analysis of variance (ANOVA) was employed to determine if the variable(s) had a significant effect on the board properties. The effects of fibre treatments on the board properties were also evaluated using ANOVA, while the separation of means for comparison was carried out using Duncan's multi-stage test.

# Chapter 4

# Characterization of lignocellulosic materials and precursors

## 4.1 Chemical compositions of untreated lignocellulosic materials (LM)

The composition of untreated *A. longifolia* (AL), *A. mearnsii* (AM), *A. saligna* (AS) and sugarcane bagasse (SCB) particles is shown in Table 4-1. The acacia species had similar chemical compositions. Qin and Huang (2005) reported similarities in the chemical compositions of other acacia species, such as *A. auriculaeformis* (AA), *A. crassicarpa* (AC) and *A. mangium* (Ama). The only noticeable difference is the hemicellulose content of AS which is much lower than AL and AM samples. It is also much lower than the hemicellulose components of AA, AC and AMa (Qin and Huang 2005). The composition of SCB is quite different from the acacia species. It had higher ash, extractive contents and a considerably lower bulk density than the acacia species.

**Table 4-1** Compositional analyses of the untreated lignocellulosic material

| Parameters (%) | Lignocellulosic materials | | | |
|---|---|---|---|---|
| | *A. saligna* | *A. longifolia* | *A. mearnsii* | SCB |
| Lignin | 25.47(1.34) | 24.41(2.52) | 23.85(1.25) | 26.84(2.18) |
| Hemicellulose | 13.13(1.14) | 19.05(0.86) | 20.29(0.11) | 10.75(1.01) |
| Cellulose | 34.47(0.66) | 31.54(0.48) | 33.72(0.13) | 23.78(0.46) |
| Water Extractives | 5.26(0.40) | 5.51(0.17) | 5.52(0.75) | 9.72(0.10) |
| EtOH Extractives | 0.55(0.02) | 0.54(0.04) | 0.61(0.09) | 1.72(0.02) |
| Total Extractives | 5.81(0.31) | 6.08(0.11) | 6.37(0.58) | 11.49(0.07) |
| Ash | 0.88(0.02) | 0.67(0.02) | 0.71(0.03) | 3.99(0.62) |
| Moisture content | 6.50(0.08) | 6.94(0.09) | 7.43(0.01) | 5.90(0.04) |
| Bulk density ($kg/m^3$) | 178.81(5.09) | 181.43(5.48) | 162.38(2.59) | 119.66(3.48) |

*-values in parentheses are the standard deviations*

## 4.2 Pre-treatment of lignocellulosic materials (LM)

The chemical composition of wood and other lignocellulosic materials affects inorganic bonded composites differently. For example, the sugars and hemicelluloses promote the formation of impermeable layers around non-hydrated cement grains, depriving them access to water, leading to a

delayed setting or total incompatibility with cement (Quiroga et al., 2016). In phosphate composites they cause dimensional instability due to high affinity for moisture (Amiandamhen et al. 2018), while they slow down reaction kinetics in geopolymer boards (Ye et al. 2018). The degree of inhibition or incompatibility is dependent on the type and concentration of the sugars present. Alien invasive trees are usually fast-growing species, which thrive without any silvicultural treatment. According to Quiroga et al. (2016) faster tree growth leads to a high concentration of sugars and hemicelluloses, which are responsible for the inhibition and incompatibility of wood and cement. The pre-treatment methods employed were aimed at reducing the inhibitory substances and modifying the fibres surfaces for better fibre-matrix compatibility.

### 4.2.1 *Influence of pre-treatment on fibre yield*

The lignocellulose yields for each treatment method are shown in Table 4-2. AS had the highest yield for both hot water and alkali pre-treatment with a fibre recovery of 94.65% and 90.12%, respectively. AM had the highest yield for acetylation treatment. Figure 4-1 (a) shows that there was a significant difference between the treatment methods. Hot water treatment had the highest mean yield while the alkalization had the lowest mean yield for all LM. These are in line with the findings reported by Amiandamhen et al. (2018) that the lower yield observed for alkalization method was due to partial removal of some lignocellulose components. Figure 4-1(b) shows that a significant difference in yield also existed between the LM. AS had the highest mean yield, while the SCB had the least. Figure 4-1(c) indicates that significant differences existed between the treatment methods for each LM. The mean acetylation yield for AS was significantly lower than the alkalization yield. This indicates that the treatment affected the LM differently.

**Table 4-2** Lignocellulosic yield of pre-treatment method

| LM | Treatments | | |
|---|---|---|---|
| | Hot water | NaOH | Acetic anhydride |
| AM | 89.54 (0.18) | 86.98 (0.41) | 90.31 (0.33) |
| AS | 94.65 (0.10) | 90.12 (0.52) | 90.20 (0.48) |
| SCB | 93.59 (0.26) | 82.86 (0.63) | 86.66 (0.02) |
| AL | 88.23 (0.03) | 80.27(0.33) | 90.94 (0.26) |

*-values in parentheses are the standard deviations*

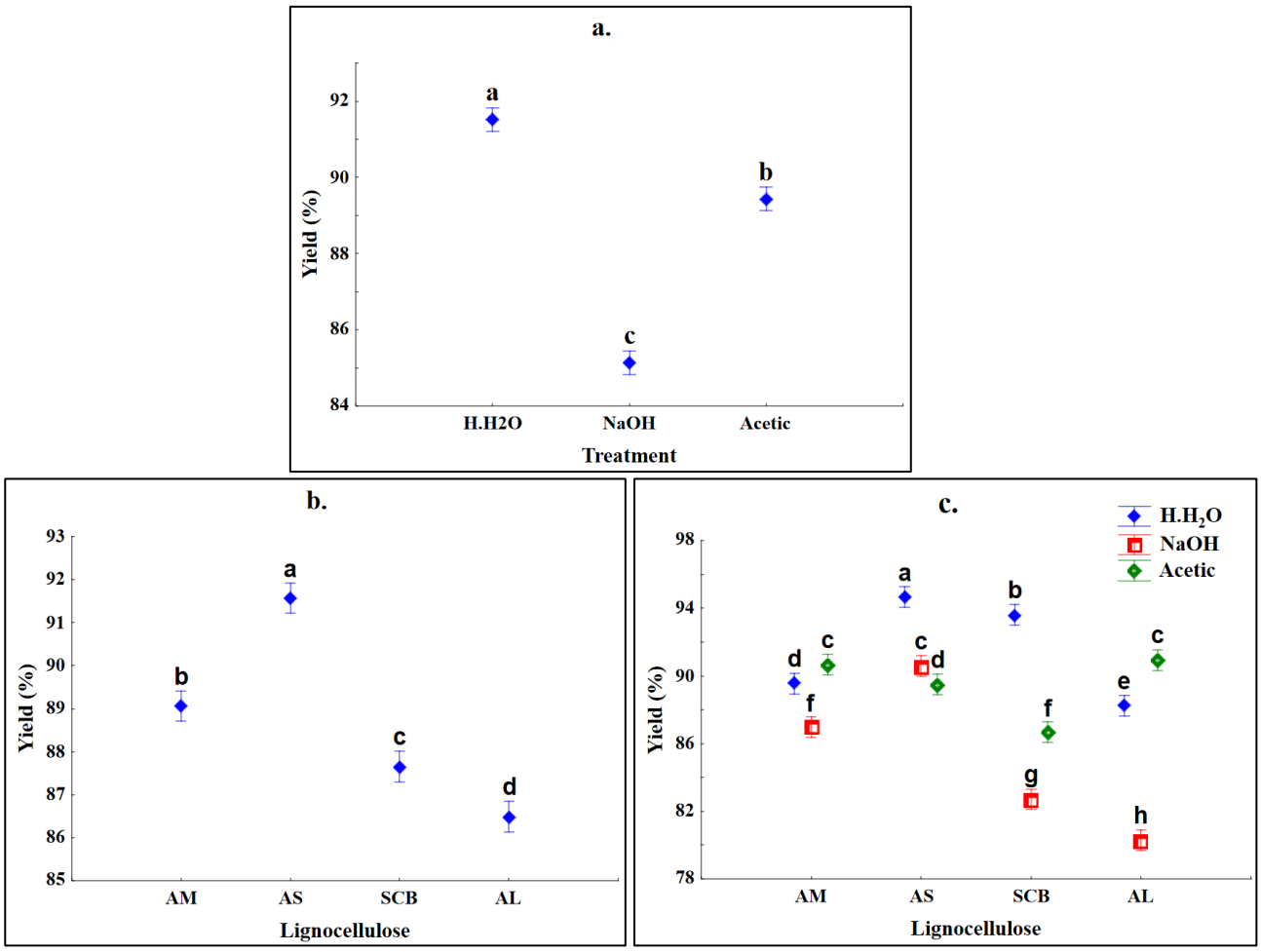


(*vertical lines denote the confidence intervals 0.95*)

**Fig. 4-1** Lignocellulosic yield (%) for (a) each pre-treatment method and (b) each LM (c) effect of pre-treatment on yield for each LM

### 4.2.2 *Influence of pre-treatment on chemical compositions of samples*

The chemical compositions of the treated samples are presented in Table 4-3. It was noted that the reduction of one component caused a proportional increase in the other components. A similar observation was also reported by Amiandamhen et al. (2018) Compared to Table 4-1, all the treatments reduced the extractive content of the samples. Apart from the hot-water treated AL and alkalized AM samples, the treatments also reduced the lignin components of LM. Acetylation caused a reduction in the lignin, extractives, and ash contents of all samples. This is in line with the findings of Amiandamhen et al. (2018). According to Bledzki et al. (2008), the strong sulfuric acid used to speed up the acetylation process to prevent non-uniform results could hydrolyse the fibre structure.

This was supposed to cause an increase in the lignin content, but the reverse was observed. This suggest that the few drops of sulfuric acid added as a buffer was not sufficient to cause condensation of lignin. The alkalization treatment was less severe than what is applicable in kraft pulping since the aim was to remove inhibitory substances present in the samples. It proportionally increased the cellulose and ash contents of all samples, but reduced the lignin and hemicellulose components of SCB, AS and AL. The ash contents increased as a result of partial removal of the organic contents which caused a proportional increase in the inorganic content (Amiandamhen et al. 2018). The hemicellulose contents of AM and AL also reduced after alkalization. According to Garrote et al. (1999), hot water treatment breaks down the lignocellulose into monomers and oligomers, leading to partial removal of the lower molecular components. Hot water treatment reduced the hemicellulose and lignin components of AM and SCB which resulted in a proportional increase in the cellulose content. The reduction in the components was confirmed by the FTIR analysis discussed in Section 4.3. The ANOVA of the effect of treatment methods on the chemical composition is presented in Table 4-4.

**Table 4-3** Compositions of treated samples (%)

| LM | Treatment | Lignin | Cellulose | Hemicellulose | Extractives | Ash |
|---|---|---|---|---|---|---|
| | Hot water | 23.59(2.55) | 35.86(4.73) | 12.93(1.51) | 2.01(0.40) | 0.28(0.06) |
| *A. mearnsii* | Acetylation | 23.12(0.54) | 35.01(1.03) | 19.39(0.09) | 1.82(0.24) | 0.21(0.02) |
| | Alkalization | 24.05(0.86) | 35.18(0.45) | 13.24(0.07) | 2.12(0.16) | 3.22(0.19) |
| | Hot water | 26.26(0.91) | 23.97(0.40) | 9.22(0.64) | 5.21(0.34) | 1.81(0.32) |
| Bagasse | Acetylation | 24.79(0.65) | 26.67(0.65) | 11.46(0.44) | 4.04(0.13) | 1.90(0.14) |
| | Alkalization | 15.28(2.18) | 26.06(0.19) | 11.55(0.33) | 3.61(0.19) | 4.10(0.25) |
| | Hot water | 25.37(1.24) | 35.43(0.95) | 13.54(0.21) | 1.66(0.18) | 0.30(0.02) |
| *A. saligna* | Acetylation | 24.44(0.71) | 37.32(0.89) | 13.39(0.44) | 1.60(0.17) | 0.27(0.01) |
| | Alkalization | 23.71(0.22) | 36.67(0.05) | 13.28(0.07) | 1.80(0.09) | 3.38(0.12) |
| | Hot water | 25.98(4.53) | 33.61(1.91) | 14.01(1.41) | 2.02(0.17) | 0.37(0.03) |
| *A. longifolia* | Acetylation | 23.79(0.72) | 32.94(0.80) | 18.32(0.80) | 1.98(0.20) | 0.23(0.02) |
| | Alkalization | 24.00(0.34) | 32.95(1.40) | 11.15(0.10) | 2.71(0.31) | 3.26(0.04) |

*-values in parentheses are the standard deviations.*

**Table 4-4** ANOVA of the effects of treatment on the chemical compositions of LM

| | Chemical compositions (%) | | | |
|---|---|---|---|---|
| Effect | Cellulose | Lignin | Extractives | Hemicellulose |
| Treatment | 0.638412 | 0.001720* | 0.000283* | 0.000000* |
| LM | 0.000000* | 0.075060 | 0000000* | 0.000000* |
| Treatment **LM | 0.679698 | 0.001130* | 0000000* | 0.000000* |

*- *denotes significant values (p<0.05)* | **- interaction between factors.

Figure 4-2(a) indicates that acetylation yielded highest mean cellulose content, but not significantly different from the other treatments. In Figure 4-2(b), it had the highest mean hemicellulose content which is significantly different from the other methods. Acetylation essentially stabilizes the cell walls by plasticizing the cellulose fibres. It replaces the hydroxyl groups in the cellulose and hemicellulose chains with acetyl groups which have higher molecular weight. This could explain why it resulted in higher recovery of cellulose and hemicellulose. Figure 4-2(c) shows that hot water extraction had the highest mean lignin content, but not significantly different from acetylation. Alkalization, however, had a significant degradation effect on the lignin component. Figure 4-2(d) indicates that hot water had a significant effect on the recovery of extractives, but no significant difference existed between alkalization and acetylation.

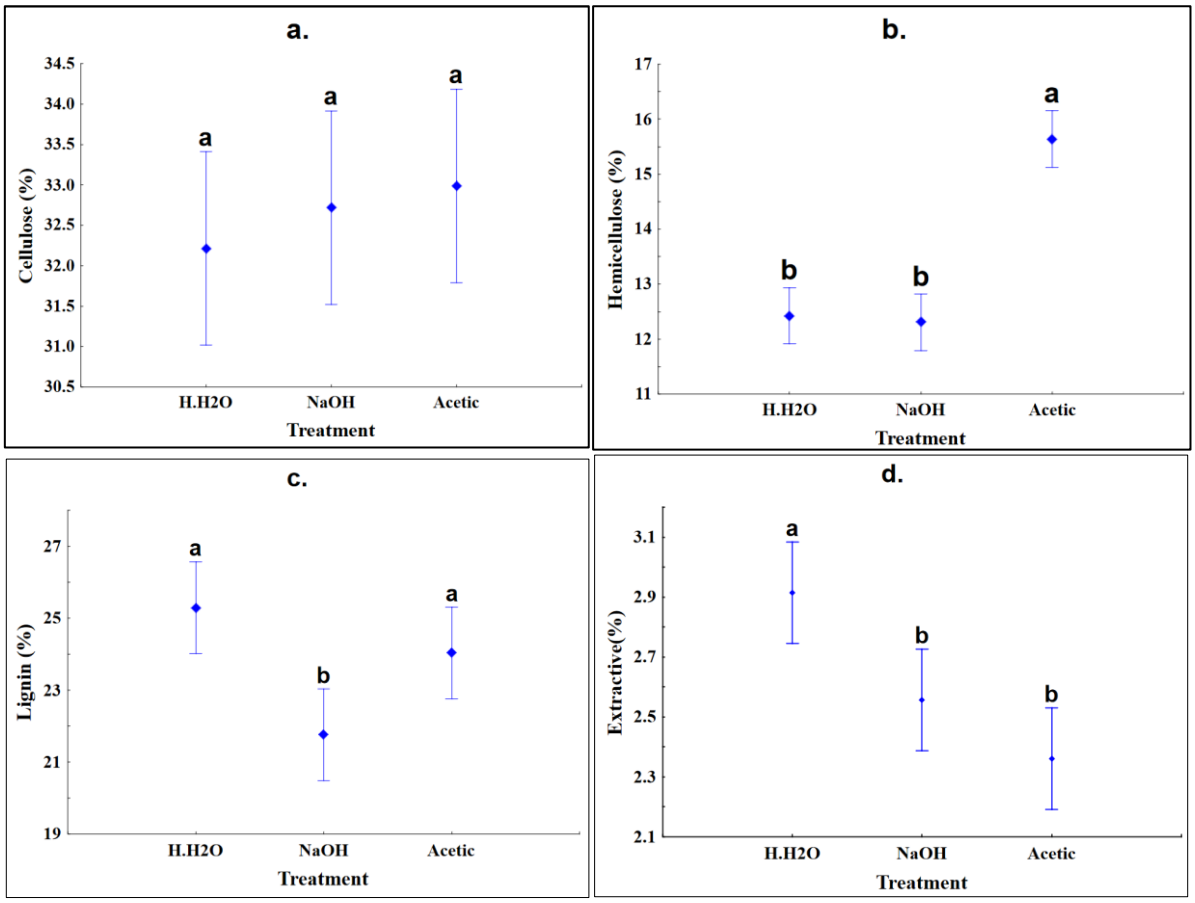


(*vertical lines denote the confidence intervals 0.95*)

**Fig. 4-2** The effects of pre-treatment methods on chemical composition of all samples (a) cellulose (b) hemicellulose (c) lignin and (d) extractives

Figure 4-3 shows the difference between the treatment methods for each lignocellulose sample. The treatment methods did not have any significant effect on the chemical components of AS, but their effects on the lignin, hemicellulose and extractive contents of SCB were significant. Acetylation had significant effects on the hemicellulose contents of AM and AL, while alkalized AL is significantly different from acetylation and hot water treatment. The treatments are expected to have positive effects on the final properties of the board as they all caused a proportional increase in the cellulose contents of the LM.

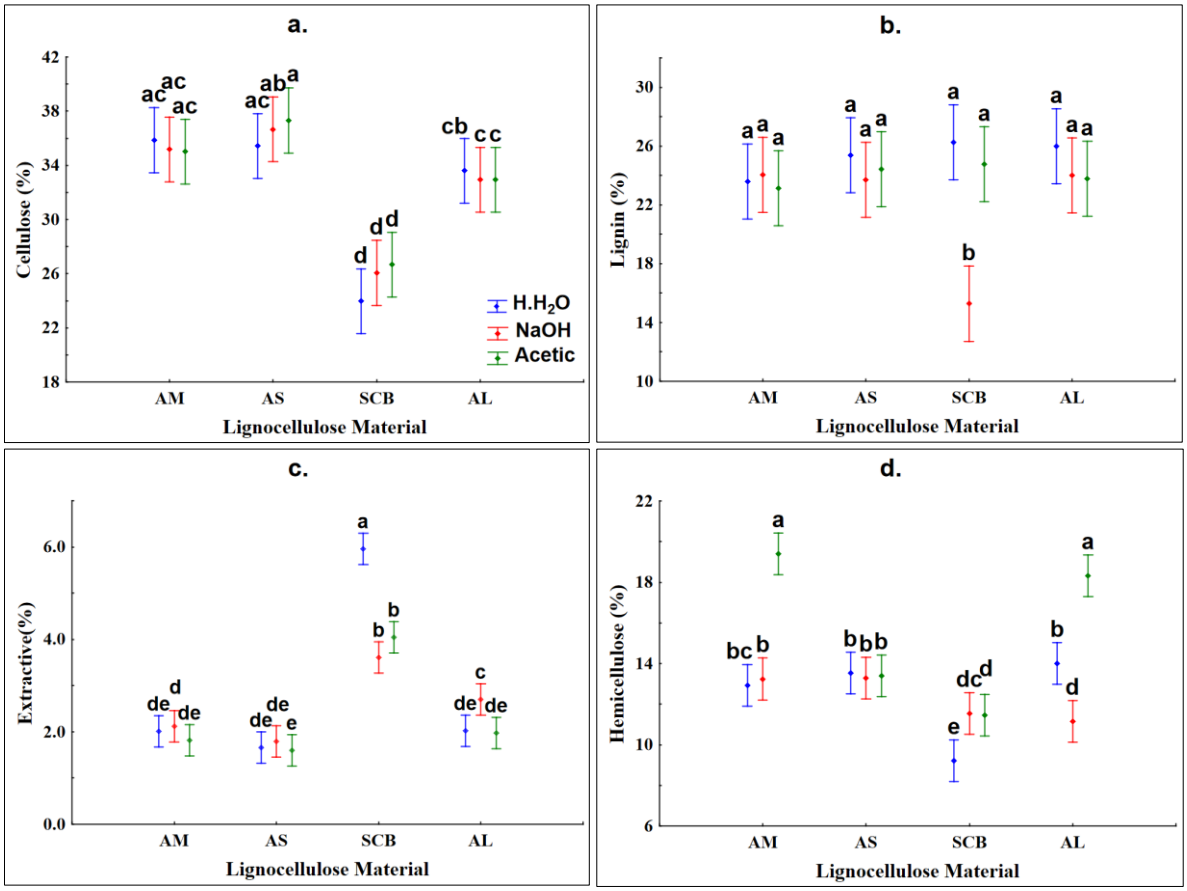


**Fig. 4-3** Effects of treatment methods of the chemical composition of each sample (a) cellulose (b) lignin (c) extractives and (d) hemicellulose

## 4.3 FTIR of LM

### 4.3.1 *Untreated LM*

The lignocelluloses have similar IR spectra within same band numbers as shown in Figure 4-4. The strongest bands are found around 3360cm$^{-1}$ and 1023cm$^{-1}$ in all the samples. The band around 3360cm$^{-1}$ is assigned to axial vibration of the hydroxyl (-OH) group of cellulose (Ibraheem et al. 2016), while the band at 1023cm$^{-1}$ indicates a C-C bond of β-glucosidic linkages between sugar units in hemicelluloses and cellulose (Hajiha et al. 2014). The peak at 2916cm$^{-1}$ represents a symmetrical vibration of C-H bond (Liu et al., 2004; Amiandamhen et al. 2018). Since the bagasse fibre has been processed, which could have altered the position of the absorption bands, this peak could also be attributed to a C-H aliphatic axial deformation in $CH_2$ and $CH_3$ groups from cellulose, lignin and hemicellulose as it is only 4cm$^{-1}$ less than the absorption band reported by Cristina et al. (2012). The peak around 1737cm$^{-1}$ is attributed to the carbonyl (C=O) stretching of acetyl groups of hemicellulose (Cristina et al. 2012; Liu et al. 2004). The peaks around 1235 – 1254 cm$^{-1}$ are assigned to the C -O

stretch of the acetyl group of lignin (Hajiha et al. 2014; Liu et al. 2004), while the peak at 1422cm$^{-1}$ indicates the $CH_2$ symmetric bending of cellulose (Hajiha et al. 2014; Sawpan et al. 2011)

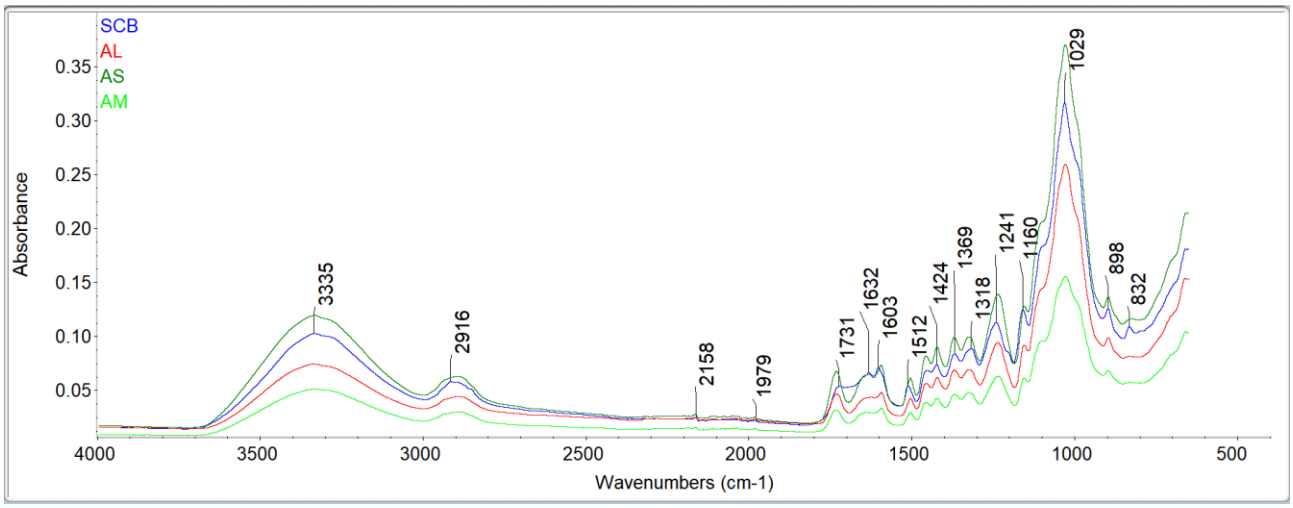


**Fig. 4-4** FTIR spectra of untreated lignocellulosic materials

### 4.3.2 *Treated LM*

The FTIR spectra of the treated samples are presented in Figures 4-5 to 4-8. The spectra of untreated samples were higher than those of the treated samples. This supported the HPLC results that some components were removed after pre-treatment. Levelling of the band between 3000 to 3600 cm$^{-1}$ in alkali and hot water treated SCB and AL indicated partial removal of OH groups. The intensity decreased in treated AM and AS, but the broadness was almost unchanged. The intensity of peak around 2916 cm$^{-1}$ attributed to C-H symmetrical stretching also reduced for the treated sample, but the reduction was more pronounced in alkalized and hot water treated SCB and AL. The peak at 1731 cm$^{-1}$ can be attributed to C = O stretching of acetyl groups of hemicelluloses reduced in intensity for acetylated and alkalized AS. This was also observed in hot water and acetylated AL. The peak was non-existent for all alkalized samples. This confirms the removal of hydrolysed hemicellulose components. Similar observations were also made by Pelaez-Samaniego et al. (2014) and Amiandamhen et al. (2018). The C= O stretch of the acetyl group of lignin found around 1235 – 1254 cm$^{-1}$ disappeared in the alkalized SCB while the intensity reduced for other samples. The intensity was almost unchanged for acetylated and hot water treated samples. This supported the HPLC results that alkalization had the lowest mean lignin for SCB.

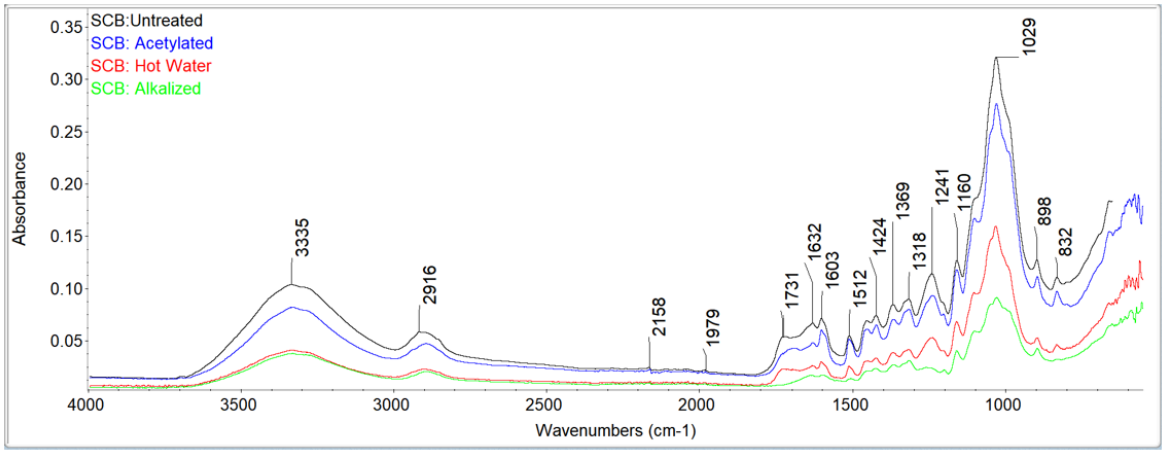


**Fig. 4-5** FTIR spectra of untreated and treated SCB

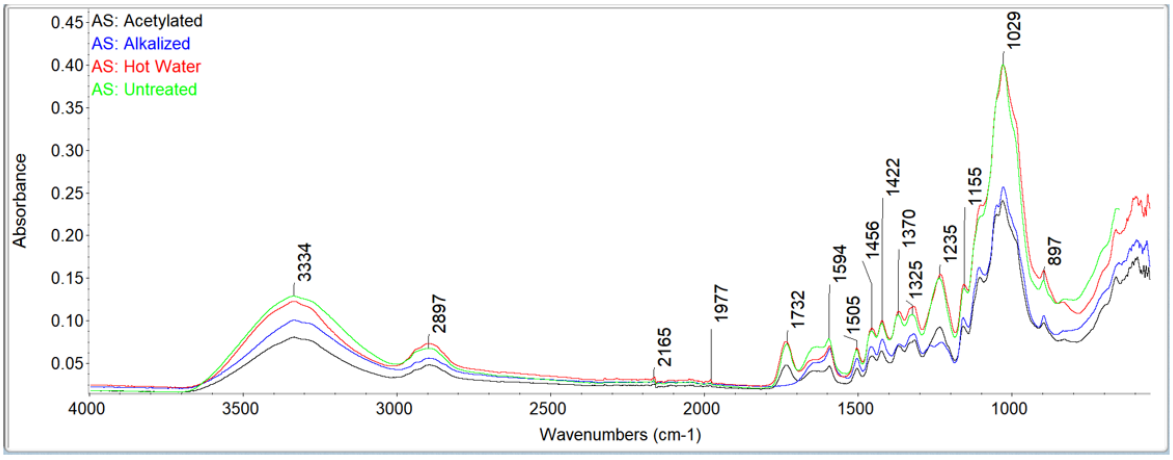


**Fig. 4-6** FTIR spectra of untreated and treated AS

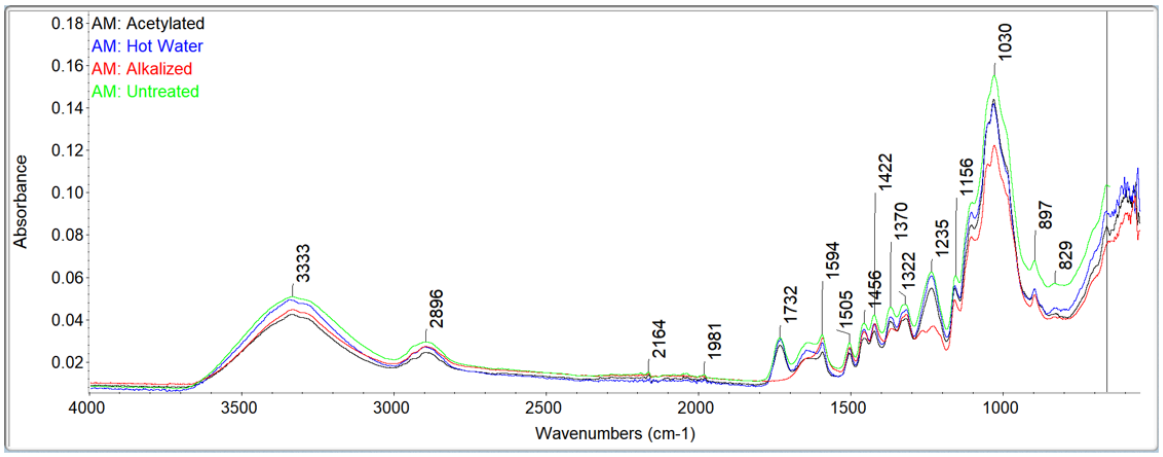


**Fig. 4-7** FTIR spectra of untreated and treated AM

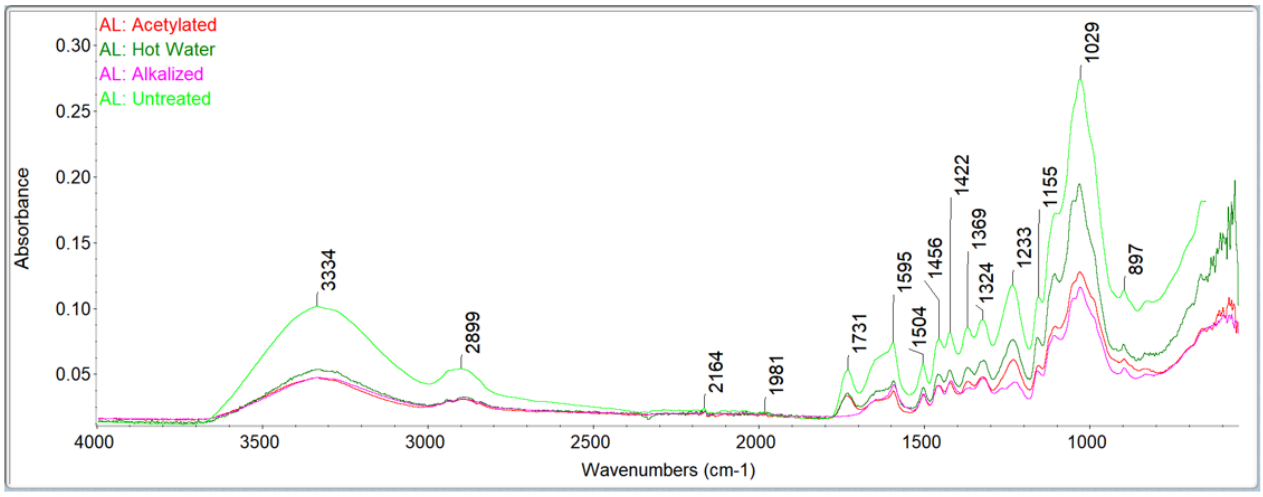


**Fig. 4-8** FTIR spectra of untreated and treated AL

## 4.4 Surface morphology

### 4.4.1 *SEM*

The surface morphology of the samples was examined before and after treatment using Scanning Electron Microscopy and energy dispersive spectroscopy (SEM/EDS). The micrographs of the samples before and after the treatments are shown in Figures 4-9 to 4-12. It was observed that all the treatments caused defibrillation of the fibres, which could improve the fibre-matrix bond and therefore influence the strength development. Alkalization generally removed wax and lignin from the samples leading to cleaner surfaces. Similar observations have been reported in other studies (Amiandamhen et al. 2018; Hajiha et al. 2014). Acetylation makes the sample less hydrophilic by replacing the hydroxy groups on the surface with acetyl groups (Hajiha et al. 2014; Li et al. 2007), while hot water extraction causes fractionation of easily accessible sugars and hemicelluloses (Pelaez-Samaniego et al. 2014; Pereira Ferraz et al. 2016). Figure 4-9 shows that acetylation and hot water treatments removed some waxy substances from AM samples, but some protruding parts are still visible. In Figure 4-10, it was observed that alkalized and acetylated samples had a smoother surface, while minimal difference existed between untreated and hot water extracted AS samples. Figure 4-11 shows that alkalized SCB had smoother surfaces while little difference was observed in hot water extracted and acetylated samples. The highest degree of fibrillation was observed in AL samples (Figure 4-12). The cell wall looks somewhat exploded with the removal of pectin in all treated samples. The alkalized sample appeared to be pulped and was distinctly different from other treated samples. It is expected that these treatments will affect the fibre-matrix bond differently.

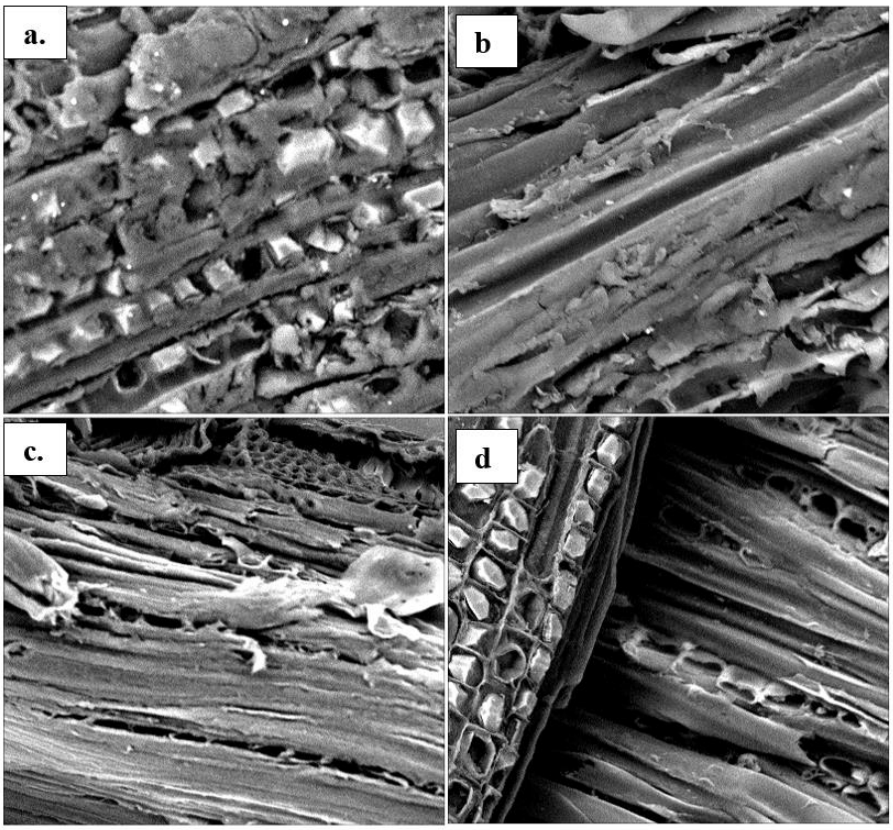


**Fig. 4-9** SEM micrographs of AM (a) untreated (b) acetylated (c) alkalized (d) hot water treated

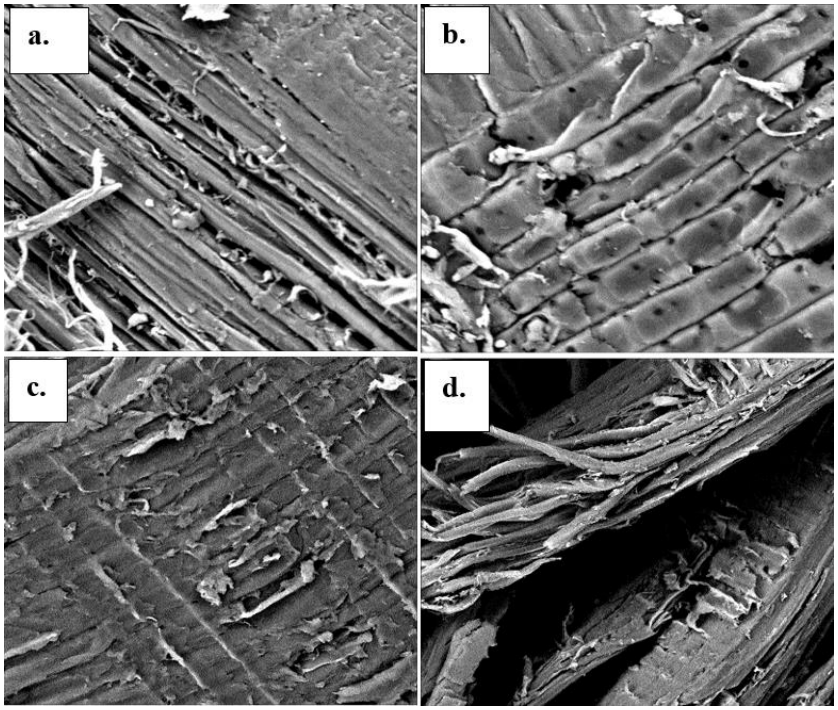


**Fig. 4-10** SEM micrographs of AS (a) untreated (b) acetylated (c) alkalized (d) hot water treated

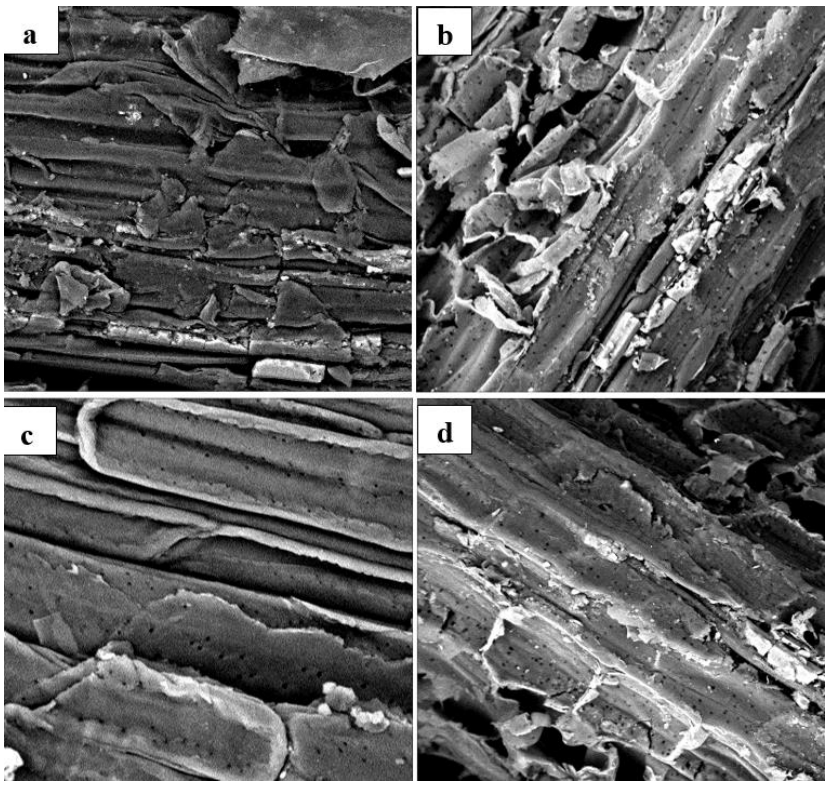


**Fig. 4-11** SEM micrographs of SCB (a) untreated (b) acetylated (c) alkalized (d) hot water treated

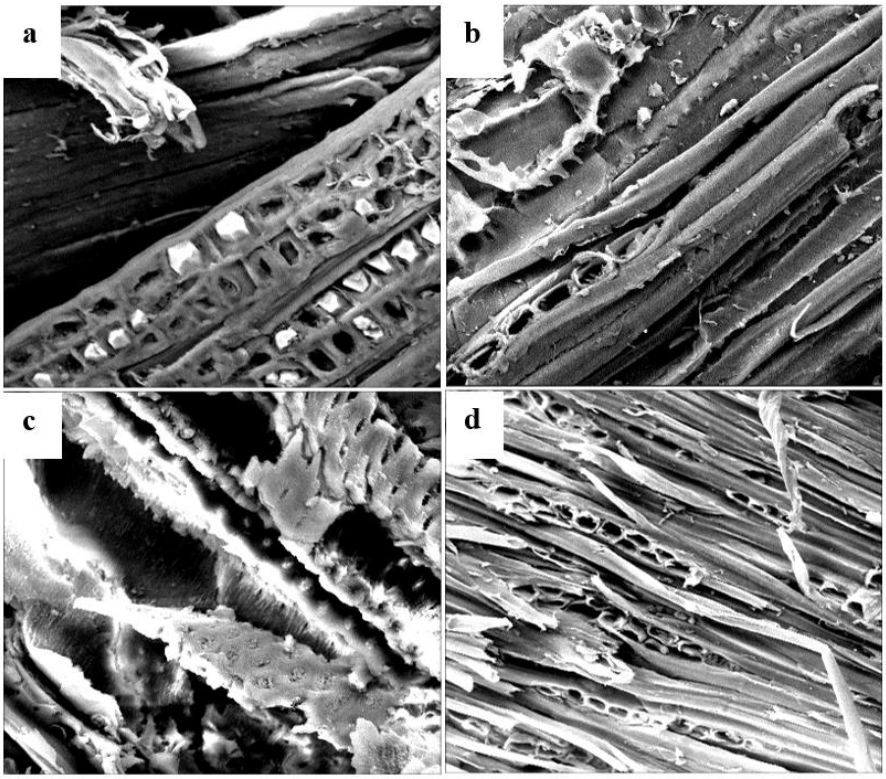


**Fig. 4-12** SEM micrographs of AL (a) untreated (b) acetylated (c) alkalized (d) hot water treated

### 4.4.2 *Energy Dispersive Spectroscopy (EDS)*

The elemental composition of the surfaces of the samples before and after treatments were analysed using EDS. A minimum of two spectra was selected at random and the average was calculated to determine the composition. The surface composition of the samples is presented in Tables 4-5 to 4-8. The hydrophobicity of the sample depends on the C/O ratio. Samples with a higher C/O ratio are less hydrophilic (Amiandamhen et al. 2018). Pre-treatment increased the C/O ratios in all samples. This confirmed the removal of the more hydrophilic lower components indicated by the FTIR and HPLC results. As expected, the treatment methods affected the distribution of the elemental compositions and the C/O ratio of all the samples differently. Apart from AS, acetylation had the highest C/O ratio while hot water extraction had lowest ratio except for AL. The C/O ratio of all the samples was greater than 1.21, indicating that some waxy substances are still present on the surfaces (Amiandamhen et al. 2018).

**Table 4-5** Elemental characterization of treated and untreated AL

| Sample | Elements | | | | | | | | | | |
|---|---|---|---|---|---|---|---|---|---|---|---|
| Treatments | C | O | Na | Mg | Al | Si | K | Ca | Ti | Fe | C/O |
| Untreated | 57.93 | 41.22 | 0.05 | 0.00 | 0.19 | 0.12 | 0.18 | 0.09 | 0.14 | 0.07 | *1.41* |
| Acetylated | 65.70 | 34.02 | 0.02 | 0.03 | 0.04 | 0.05 | 0.04 | 0.07 | 0.01 | 0.02 | *1.93* |
| Alkalized | 62.38 | 36.66 | 0.33 | 0.16 | 0.02 | 0.06 | 0.07 | 0.22 | 0.00 | 0.11 | *1.70* |
| Hot water | 63.68 | 35.96 | 0.00 | 0.05 | 0.02 | 0.02 | 0.01 | 0.11 | 0.05 | 0.10 | *1.77* |

**Table 4-6** Elemental surface composition (%) of treated and untreated AM

| Sample | Elements | | | | | | | | | | |
|---|---|---|---|---|---|---|---|---|---|---|---|
| Treatments | C | O | Na | Mg | Al | Si | K | Ca | Ti | Fe | *C/O* |
| Untreated | 61.83 | 37.70 | 0.05 | 0.04 | 0.03 | 0.02 | 0.21 | 0.03 | 0.03 | 0.04 | *1.64* |
| Acetylated | 66.17 | 33.62 | 0.00 | 0.03 | 0.04 | 0.04 | 0.00 | 0.00 | 0.00 | 0.10 | *1.97* |
| Alkalized | 65.00 | 34.71 | 0.06 | 0.04 | 0.05 | 0.01 | 0.02 | 0.09 | 0.03 | 0.00 | *1.87* |
| Hot water | 62.44 | 36.87 | 0.01 | 0.00 | 0.05 | 0.00 | 0.00 | 0.60 | 0.00 | 0.02 | *1.69* |

**Table 4-7** Elemental surface composition (%) of treated and untreated SCB

| Sample | Elements | | | | | | | | | | |
|---|---|---|---|---|---|---|---|---|---|---|---|
| Treatments | C | O | Na | Mg | Al | Si | K | Ca | Ti | Fe | *C/O* |
| Untreated | 60.12 | 32.96 | 0.04 | 0.11 | 0.10 | 0.94 | 0.09 | 0.07 | 0.01 | 5.57 | *1.82* |
| Acetylated | 65.21 | 33.10 | 0.00 | 0.06 | 0.46 | 0.81 | 0.06 | 0.06 | 0.02 | 0.22 | *1.97* |
| Alkalized | 63.92 | 32.98 | 0.52 | 0.14 | 0.07 | 1.92 | 0.02 | 0.30 | 0.03 | 0.12 | *1.94* |
| Hot water | 65.53 | 34.23 | 0.02 | 0.02 | 0.03 | 0.06 | 0.01 | 0.03 | 0.01 | 0.06 | *1.91* |

**Table 4-8** Elemental surface composition (%) of treated and untreated AS

| Sample | Elements | | | | | | | | | | |
|---|---|---|---|---|---|---|---|---|---|---|---|
| Treatments | C | O | Na | Mg | Al | Si | K | Ca | Ti | Fe | *C/O* |
| Untreated | 56.70 | 43.01 | 0.08 | 0.02 | 0.02 | 0.01 | 0.09 | 0.02 | 0.00 | 0.05 | *1.32* |
| Acetylated | 64.44 | 35.50 | 0.01 | 0.00 | 0.02 | 0.00 | 0.01 | 0.03 | 0.00 | 0.00 | *1.82* |
| Alkalized | 64.73 | 34.57 | 0.47 | 0.02 | 0.02 | 0.01 | 0.03 | 0.09 | 0.04 | 0.02 | *1.87* |
| Hot water | 61.36 | 38.40 | 0.03 | 0.07 | 0.04 | 0.01 | 0.01 | 0.07 | 0.00 | 0.01 | *1.60* |

## 4.5 TGA

The thermal stability of the lignocellulosic materials (LM) was investigated by Thermogravimetric analysis (TGA) under nitrogen flow. The derivative thermographs (DTG) of the LM are shown in Figure 4-13. The LMs exhibited similar thermal behaviour with a presence of peak/shoulders below the main degradation peak. The shoulders appeared at 274.03 °C, 275.43°C, 293.49°C and 274.70 °C for AS, AM, SCB and AL, respectively. The shoulder may be attributed to the degradation of hemicelluloses partially overlapping with cellulose and lignin (Pelaez-samaniego et al. 2013; Sebio-pun and Lo 2012). AM has another shoulder at 225.12°C, which could indicate the decomposition of some volatile components and hemicelluloses of lower molecular weight. This could be attributed to the prior industrial process, which might have removed certain impurities and hence improve the thermal stability of the components.

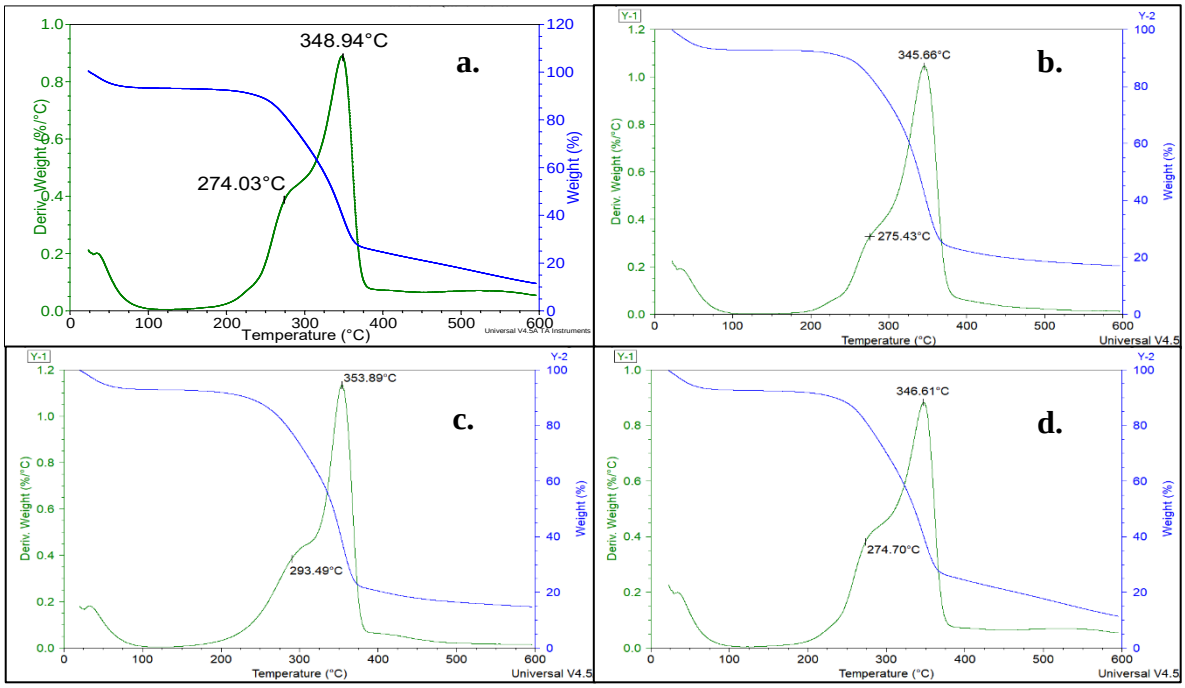


**Fig. 4-13** Thermographs (TG) and derivative thermographs (DTG) of lignocellulosic materials (a) AS (b) AM (c) SCB and (d) AL

## 4.6 Characterization of precursor materials

### 4.6.1 *Particle size distribution and chemical composition*

The particle sizes of fly ash, metakaolin and slag are shown in Table 4-9. Fly ash had finer particles than metakaolin and slag. About 50% of the fly ash particles had sizes less than 14.404µm. Figure 4-14 shows the volume frequency and particle size distributions of the precursors. Most of the particles are within 10 – 40µm for fly ash, 40 – 55 µm for metakaolin and 10 – 45 µm for slag. Precursors with finer particles are more reactive in the activating medium partly due to their larger surface area (Petermann and Saeed 2012) and produce products of superior properties (Chen and Brouwers 2007). The chemical compositions of the precursor materials are presented in Table 4-10. The FA can be classified as low calcium ash according to the ASTM C618 (ASTM 2019), since the sum of its $SiO_2$ and $Al_2O_3$ contents exceeded 70% and the CaO content was less than 20%. The Si/Al ratios of the precursors were 1.31, 1.75 and 2.46 for metakaolin, fly ash and slag, respectively. The precursors meet the preferred properties for the production of geopolymer of optimum binding properties outlined in Fernandez-Jimenez et al (2008). The LOI was less than 5%, less than 10% $Fe_2O_3$, about 40 – 50 % $SiO_2$ and 80 – 90 % of their particles less than or equal to 45µm.

**Table 4-9** Particle size distribution of precursors

| Precursors | Particle size (µm) | | |
|---|---|---|---|
| | $d_{10}$ | $d_{50}$ | $d_{90}$ |
| Fly Ash | 1.383 | 14.404 | 59.804 |
| Metakaolin | 2.775 | 28.052 | 103.736 |
| Slag | 2.361 | 16.554 | 52.742 |

**Table 4-10** Chemical compositions of the precursor materials

| Precursor (%) | $Al_2O_3$ | CaO | $Cr_2O_3$ | $Fe_2O_3$ | $K_2O$ | MgO | MnO | $Na_2O$ | $P_2O_5$ | $SiO_2$ | $TiO_2$ | L.O.I. |
|---|---|---|---|---|---|---|---|---|---|---|---|---|
| Metakaolin | 42.24 | 0.08 | 0.01 | 0.39 | 0.08 | -_ | 0.01 | 0.05 | 0.07 | 55.18 | 1.33 | 1.02 |
| Slag | 15.76 | 33.92 | _ | 0.15 | 1.01 | 8.64 | 0.87 | 0.24 | 0.01 | 38.90 | 0.72 | -1.15 |
| Fly Ash | 31.05 | 5.56 | 0.01 | 2.66 | 0.95 | 1.18 | 0.04 | 0.18 | 0.44 | 54.24 | 1.62 | 2.00 |

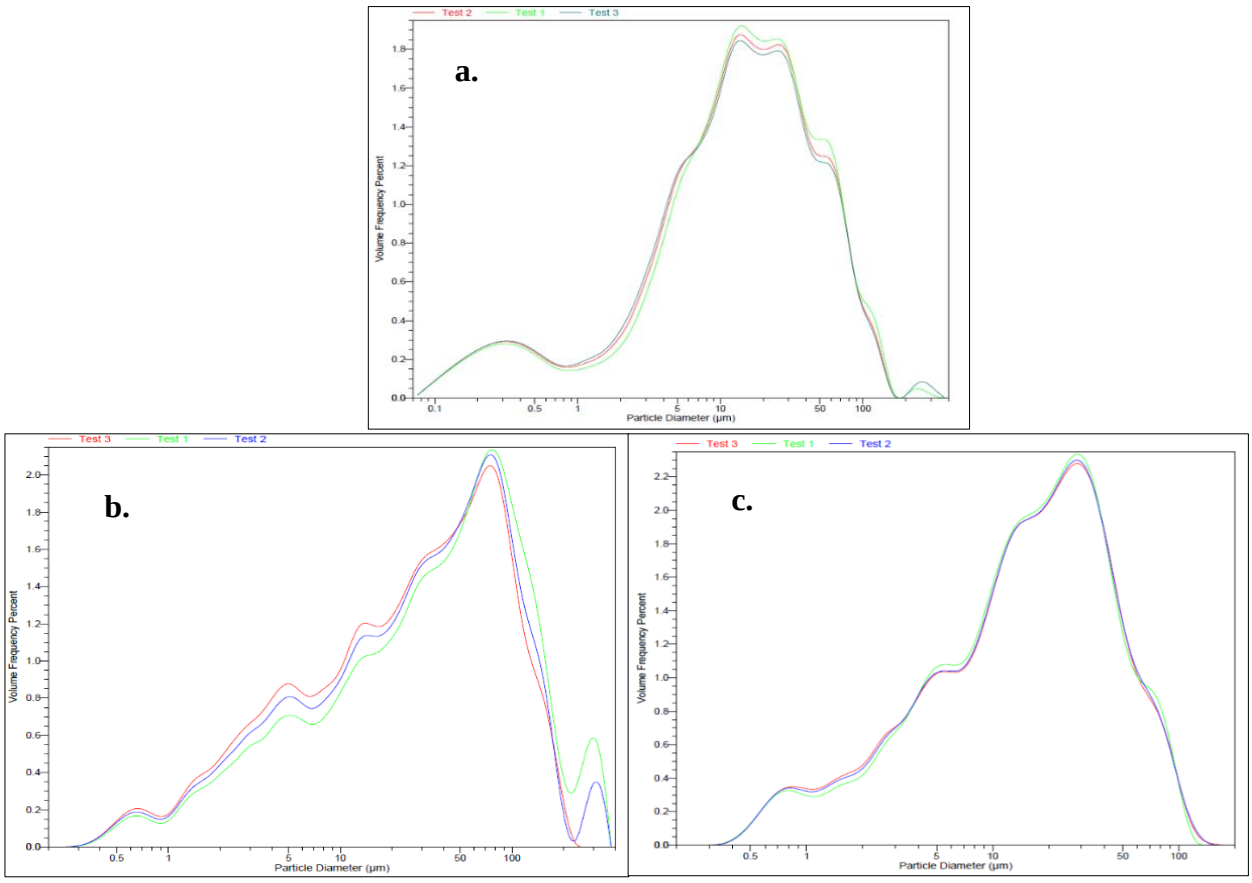


**Fig. 4-14** Cumulative frequency distribution of the precursors (a) fly ash (b) metakaolin and (c) slag

### 4.6.2 *Phase identification and analysis*

The XRD diffractograms of the precursor materials are shown in Figure 4-15. The crystalline phases present in the precursors were identified using the Qualx V2 and X 'Pert Highscore Plus software. Quartz and mullite are the principal crystalline phases present in both fly ash and metakaolin, but their intensities are higher in fly ash. The high peak observed in the diffractograms in Figure 4-15(a), between 15 – 35° 2θ, indicates a high quantity of amorphous contents which could be silica or alumina (Figure 4-15(a)). Figure 4-15(b) shows the diffractogram of slag material. Fewer crystalline phases were present in the slag. The majority of the components are amorphous as indicated by the wide peak present between 20 – 40° 2θ. The minor crystalline phases included quartz, alumina, calcite ($CaCO_3$), magnoan ($MgCO_3$), corundum and magnesite. These support the XRF results presented in Section 4.6.1.

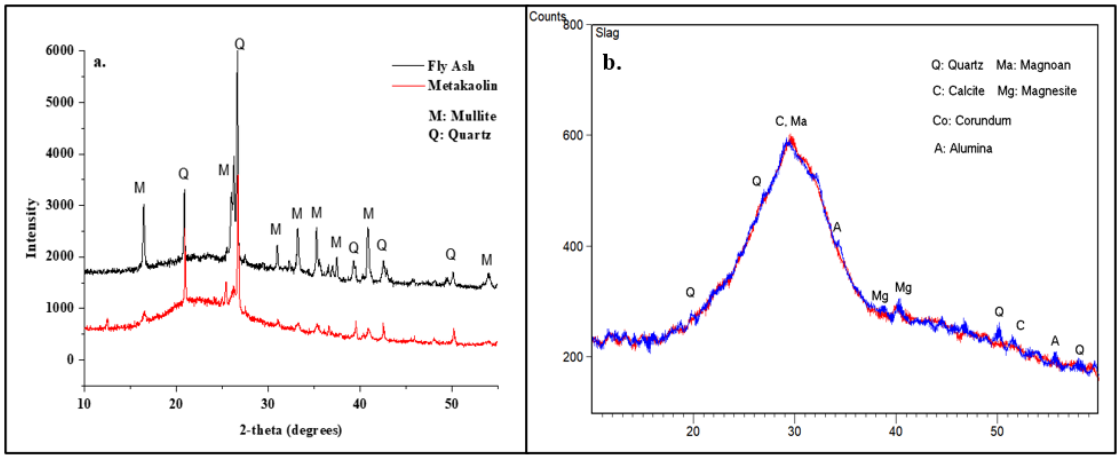


**Fig. 4-15** XRD patterns of the precursors (a) fly ash and metakaolin (b) slag

### 4.6.3 *IR spectroscopy*

The IR spectra of the precursor materials are shown in Figure 4-16. Fly ash had more peaks than metakaolin, but it is important to note that the peaks fall within same band areas. The band between 950 – 1250cm$^{-1}$ is assigned to internal vibrations of Si-O-Si (Davidovits 2008). They also have peaks in the band 500 – 800cm$^{-1}$, which is characteristic of symmetric stretching of the Si-O-Si and Al-O-Si bonds of amorphous or semi-crystalline alumino-silicates (Barbosa et al. 2000; Fauzi et al. 2016). The IR spectrum of the slag material has 3 major broad bands at 680 cm$^{-1}$, 873 cm$^{-1}$, and 1473 cm$^{-1}$ wavenumbers. The peaks at 680 cm$^{-1}$ can be attributed to the stretching vibration of Al – O (Mohassab and Sohn, 2015). According to Barbosa et al. (2000) and Fauzi et al. (2016) peaks found in the range

of 500 – 800cm$^{-1}$ are characteristic symmetric stretching of the Si – O – Si and Al – O – Si bonds of amorphous or semi-crystalline alumino-silicates. The peak at 873 cm$^{-1}$ can also be assigned to the stretching vibrations of Al – O and Si – O (Mohassab and Sohn 2015). The presence of $CaCO_3$ is indicated by the peak at 1474 cm$^{-1}$ (Nasrazadani and Springfield 2014; Ylmén and Jäglid 2013). These prominent peaks support the XRF analysis, which indicated that the main components of the slag material composed of alumina, silica and calcium carbonate.

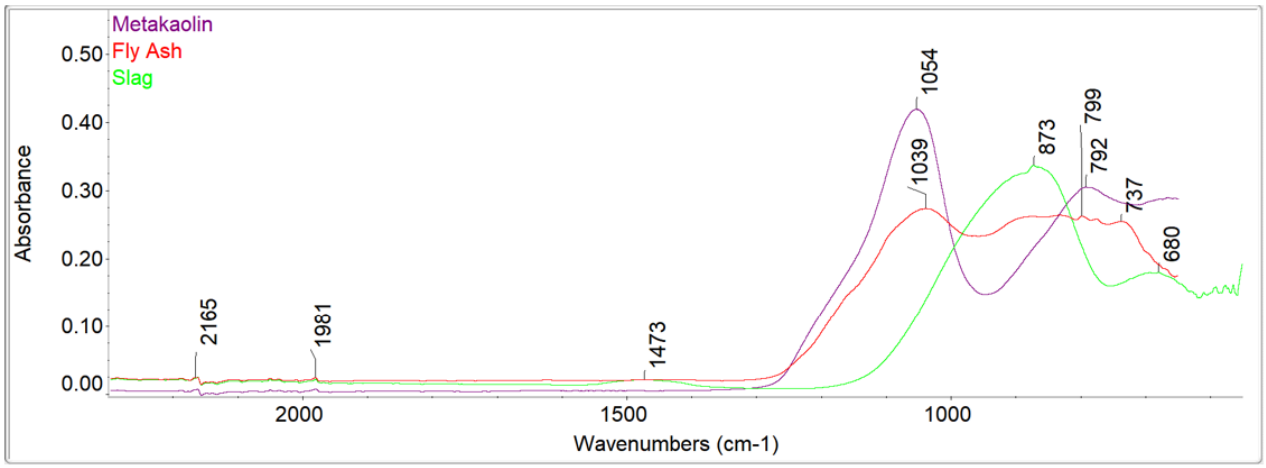


**Fig. 4-16** IR Spectra of the precursor materials

## 4.7 Conclusions

This chapter provided information about the properties of the materials using different characterization techniques. The chemical compositions of the LM were characterized using the TAPPI and NREL standard methods. The LM were subjected to alkalization, acetylation and hot-water treatments to remove substances that could inhibit bonding with geopolymer matrix and modify the fibres surfaces for better fibre-matrix compatibility. The major findings about LM characterization are summarized as follows:

1 Acacia species had higher bulk density than bagasse fibres. The acacia species had similar chemical compositions which were different than bagasse fibres.
2 Significant difference existed between the fibre yield of pre-treated samples. Hot water treated samples had the highest mean yield, while alkalized samples had the lowest. The treatments had significant effects on the chemical compositions of the samples. The HPLC results indicated partial removal of lower molecular components in the LM. Pre-treatment caused a reduction on the extractive components of all samples. Apart from the alkalized AM,

reduction was also observed in lignin content for all samples. The reduction resulted in a proportional increase in the cellulose content. FTIR confirmed the HPLC results. It indicated partial degradation of lignin and confirmed the removal of hydrolysed hemicellulose after pre-treatment.

3 SEM/EDS analyses confirmed that fibre pre-treatment improved the surface property and hydrophobicity of the samples. It is expected that cleaner surfaces free from waxy substances would influence better fibre-binder bonds.

The geopolymer precursor materials were characterized to ensure that they meet the requirements suggested in the literature for optimum binding properties. The particle distributions of the precursors were determined using PSD technique. The chemical bonds and metallic oxides present in the precursors were determined using FTIR and XRF analyses, respectively. XRD was employed to determine the crystalline phases contained in the precursor materials. The major findings are summarized as follows:

1 Fly ash had finer particles than metakaolin and slag. The volume frequency and particle distributions indicated that the precursors had most of their particles $\leq 45\mu m$.
2 The XRD analysis confirmed that the precursors were composed of high quantity of amorphous contents. The few crystalline phases present in fly ash and metakaolin were identified as Mullite and Quartz. The crystalline phases contained in the slag included quartz, alumina, calcite, magnoan, corundum and magnesite.
3 The XRF results indicated that the fly ash can be classified as Class F fly ash according to the ASTM standards. The ferric oxide, silica and Si/Al ratios of the precursors suggested that they were suitable materials for geopolymerization reactions.
4 The prominent peaks in the IR spectra of the precursor materials indicated the presence of Si – O – Si and Al – O – Si bonds of amorphous alumino-silicates. The slag had an additional peak which confirmed the presence of calcium carbonate. The results supported the XRF analysis.

# Chapter 5

# Investigating the suitability of fly ash/metakaolin-based geopolymer reinforced with South African alien invasive wood and sugarcane bagasse residues for use in outdoor conditions

## 5.1 Board formation

The overview of the design of the experiments for board formation is presented in Table 5-1.

**Table 5-1** Overview of the mix design for board formation

| Runs | Fly Ash (g) | Metakaolin (g) | LM (g) | $Na_2SiO_3$ (g) | NaOH (g) | Water (g) | Conc. (M) | Curing Pattern (°C, h) |
|---|---|---|---|---|---|---|---|---|
| 1 | 120 | 40 | 40 | 57.14 | 22.86 | 14 | 8 | 60, 24 |
| 3 | 120 | 40 | 40 | 57.14 | 22.86 | 15 | 10 | 60, 24 |
| 5 | 120 | 40 | 40 | 57.14 | 22.86 | 16 | 12 | 60, 24 |
| 2 | 135 | 45 | 45 | 42.86 | 17.14 | 24 | 8 | 60, 24 |
| 4 | 135 | 45 | 45 | 42.86 | 17.14 | 26 | 10 | 60, 24 |
| 6 | 135 | 45 | 45 | 42.86 | 17.14 | 28 | 12 | 60, 24 |
| 7 | 120 | 40 | 40 | 57.14 | 22.86 | 14 | 8 | 100, 6 |
| 8 | 120 | 40 | 40 | 57.14 | 22.86 | 15 | 10 | 100, 6 |
| 9 | 120 | 40 | 40 | 57.14 | 22.86 | 16 | 12 | 100, 6 |
| 10 | 135 | 45 | 45 | 42.86 | 17.14 | 24 | 8 | 100, 6 |
| 11 | 135 | 45 | 45 | 42.86 | 17.14 | 26 | 10 | 100, 6 |
| 12 | 135 | 45 | 45 | 42.86 | 17.14 | 28 | 12 | 100, 6 |
| Control | 142.50 | 47.50 | - | 67.86 | 27.14 | - | 10 | 60, 24 |

## 5.2 Physical and mechanical properties of geopolymer bonded boards

The apparent density, water absorption (WA), thickness and volumetric swelling (TS/VS) of the boards are shown in Table 5-2. The samples had comparable densities ranging from 1.12 – 1.28 g/cm$^3$, 1.15 – 1.29 g/cm$^3$ and 1.00 – 1.39 g/cm$^3$ for *A. mearnsii*, *A. longifolia*, and SCB boards, respectively. The boards were categorized as high-density boards, as they were above 1.00 g/cm$^3$ (ANSI, 1999). The addition of LM caused a reduction of about 35% in the unit weight of the pure geopolymer boards

(Table 5-2). The unit weights of the boards were lower than the range reported for fly ash-based geopolymer in the literature, i.e. 14.5 – 15.5 kN/m$^3$ (Chen et al. 2014), 14.50 – 17.10 kN/m$^3$ (Andini et al. 2008) and 11.8 – 15.7 kN/m$^3$ (Cioffi et al 2003). The low unit weight was attributed to the low bulk density of the incorporated LM (Chen et al 2014).

Following 24 h immersion in water, the WA ranged from 20.33 – 31.53%, 22.37 – 35.99%, and 23.23 – 40.82% for *A. longifolia, A. mearnsii,* and SCB boards, respectively; while the TS ranged from 0.10 – 1.08%, 0.51 – 1.08%, and 0.21 – 2.42% for *A. longifolia, A. mearnsii,* and SCB boards, respectively. Unreinforced geopolymer boards absorbed less water than the reinforced geopolymers due to the hydrophilic nature of LM. According to the British standard (EN 634-2 2007) for cement-bonded particleboards, all boards met the TS and VS requirements. However, only a few of the boards from each LM met the WA requirement (Table 5-2).

Flexural strength, as indicated by the static MOE and bending MOR, is an important requirement for boards used for structural applications in outdoor applications. The MOE and MOR ranged from 2293 – 6408 MPa and 3.17 – 7.18 MPa, respectively for *A. mearnsii* boards, 2296 – 7986 MPa and 2.77 – 9.228 MPa for *A. longifolia* boards and 1512 – 4686 MPa and 1.68 – 4.95 MPa for SCB boards. The addition of acacia particles improved the flexural strength of the boards. The boards had comparable flexural properties with fly ash and steel slag-based geopolymer reinforced with synthetic fibres reported by Guo and Pan (2018). SCB fibres only slightly improved the MOE and caused a reduction in the MOR of the boards compared to the control. This is due to the low bulk density of the SCB and the high volume included in the matrix. However, the boards had better flexural strength than those reported by Amiandamhen et al. (2018b) using similar wood species in phosphate matrix. The boards produced also performed better than those reported by Chen et al. (2014) using sorghum fibres in fly ash-based geopolymer. The flexural strength compares well with the results of Duan et al. (2016), where a sawdust content of 20% showed maximum flexural strength of about 10 MPa and 12 MPa after 28 and 90 days curing, respectively. According to EN 634-2:2007, there are two classes of boards based on the static MOE (Class 1 & Class 2) and a minimum MOR of 9 MPa is required for each class (Table 5-2). Within the experimental conditions in this study, only a few boards of *A. longifolia* boards met all the minimum requirements.

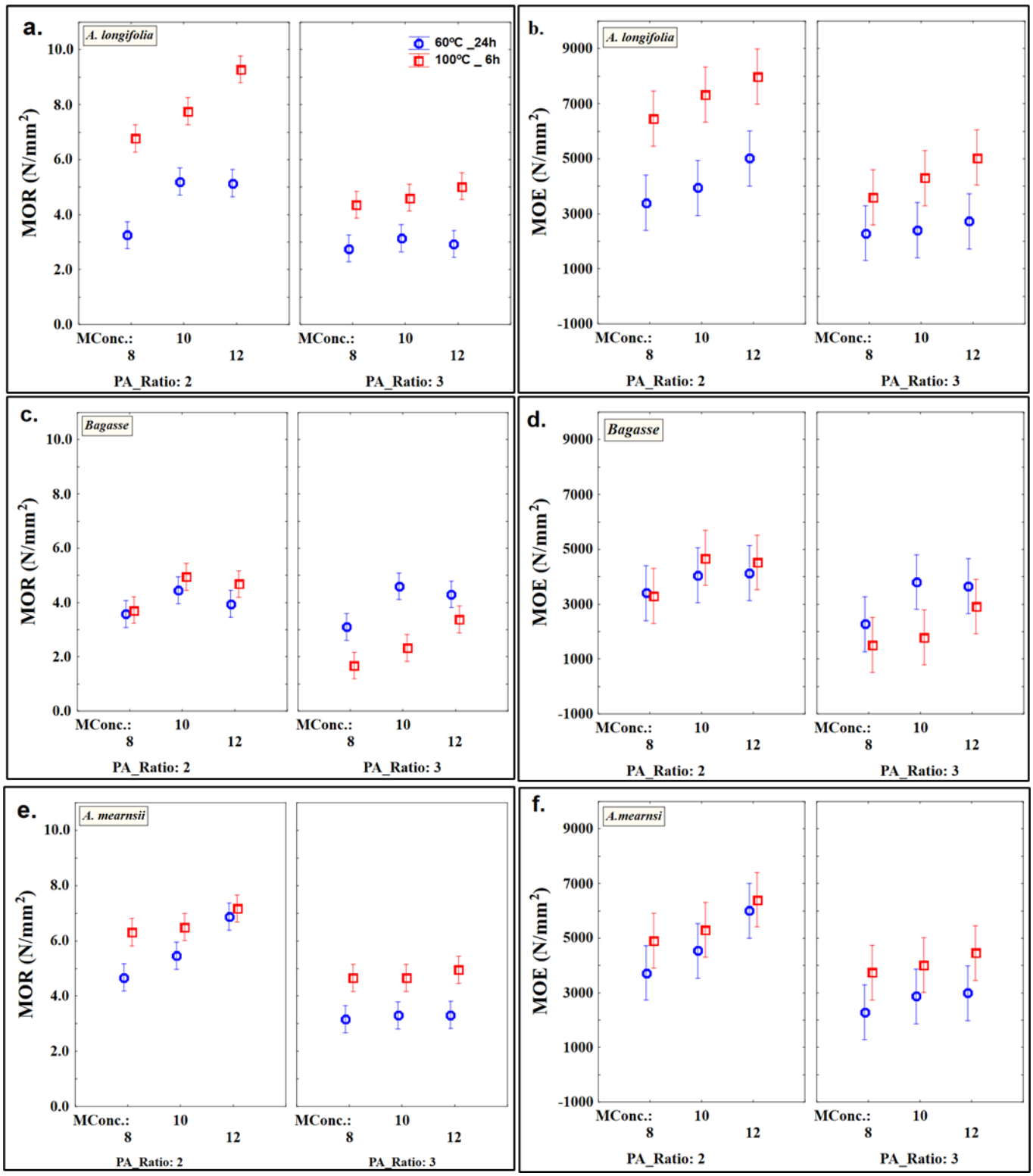


(*vertical lines denote confidence interval 0.95*)

**Fig. 5-1** The mechanical properties of all boards (a) MOR of AL (b) MOE of AL (c) MOR of SCB (d) MOE of SCB (e) MOR of AM and (f) MOE of AM

**Table 5-2** Physical and mechanical properties of the boards and EN 634-2:2007 requirements of cement-bonded particleboards for outside applications

| Properties | Units | Boards | | | | Standards | |
|---|---|---|---|---|---|---|---|
| | | *A. mearnsii* | *A. longifolia* | *SCB* | *Control* | EN 634-2:2007 | ANSI* |
| MOE | MPa | 2293 – 6408 | 2296 – 7986 | 1512 – 4686 | 3790 – 4096 | Class 1: ≥ 4500<br>Class 2: 4000 | 1034 |
| MOR | MPa | 3.17 – 7.18 | 2.77 – 9.28 | 1.68 – 4.95 | 5.14 – 5.20 | ≥ 9.0 | ≥5.50 |
| Density | g/cm$^3$ | 1.12 – 1.28 | 1.15 – 1.29 | 1.00 – 1.39 | 1.55 – 1.58 | ≥ 1.0 | <0.64 |
| Unit weight | kN/m$^3$ | 10.98 – 12.54 | 11.27– 12.64 | 9.80 – 13.62 | 15.19 – 15.48 | - | - |
| Water Absorption | % | 22.37 – 35.99 | 20.33– 31.53 | 23.23 – 40.82 | 10.11 – 10.82 | ≤ 25 | - |
| Thickness Swelling | % | 0.51 – 1.08 | 0.10 – 1.08 | 0.21 – 2.42 | 0.079 – 0.085 | ≤ 15 | - |
| Volumetric swelling | % | 0.80 – 1.68 | 0.15 – 1.64 | 0.21 – 2.61 | 0.094 – 0.132 | ≤ 15 | - |

* *Grade 1-L-1 low density particleboard*

## 5.3 Effect of curing pattern and LM on physical properties

Increasing the curing temperature up to 100 °C has been reported to have positive effects on the properties of geopolymer products (Yuan et al. 2016). Figure 5-2 (a) shows that there is a significant difference between the curing patterns employed in this study. Boards cured at 60 °C had a higher mean density than those cured at 100 °C. This observation is in agreement with findings in the literature (Sarmin and Welling 2015; Tran et al. 2009). The authors reported a reduction in the density of geopolymers as the curing temperature increased. Curing beyond 100 °C caused the formation of numerous cavities, resulting in decreased density and strength. However, Figure 5-2(b) shows that the trend varied with different LM. Curing at 100 °C for 6 h resulted in a slightly higher mean density than 60 °C curing for both *A. longifolia* and *A. mearnsii* boards. Statistical analysis ($p$<0.05) revealed that the curing pattern had no significant effect on the density of boards for both species, which indicates that the two curing conditions employed in this study did not deteriorate the internal structure of the acacia boards. In contrast, curing at 100 °C for 6 h caused a reduction in the density of SCB boards by about 15.59%. SCB has a low bulk density, which implies that more particles and embodied moisture were incorporated in SCB boards than the other board types. Higher curing temperature causes the formation of microcracks (Görhan et al. 2016), increases the extent of dehydroxylation between T – OH (T: Si or Al) and rate of removal of both free water and pore water resulting in the formation of large voids (Yuan et al. 2016). The formation of large voids was further accentuated by the reduced compressibility (due to high volume), which caused the board volume to

expand, leading to a reduction in board density. An increase in composite volume due to the formation of cavities, as a result of rapid moisture removal at higher temperatures was also reported by Tran et al. (2009). Statistical analysis ($p$<0.05) revealed a significant effect of curing conditions on the density of SCB boards (Figure 5-3(b)).

Generally, boards cured at 100 °C for 6 h absorbed more water and there was no significant difference between curing conditions and TS/VS. However, the influence was different for different LM (Figures 5-2 and 5-3). The effects on the sorption properties of SCB boards followed the same trend as density. Boards cured at 60 °C for 24 h absorbed less water and had better dimensional stability than those cured at 100 °C for 6 h. This can be explained by the fact that the porous morphology due to high-temperature curing exposed more sorption sites on the SCB fibre and the matrix was not compact enough (due to lower compressibility at high fibre loading) to resist the dimensional changes associated with water uptake. The curing pattern had significant effects ($p$<0.05) on the WA, TS, and VS of SCB boards. *A. longifolia* boards cured at 60 °C for 24 h had a lower mean WA but were less dimensionally stable compared with those cured at 100 °C for 6 h, as they had higher mean TS/VS values. The formation of micro cracks and cavities at elevated temperatures provided more channels for water molecules to penetrate the boards (See Figures 5-4(a)). However, the lower TS/VS at 100 °C curing is evidence that the water was only absorbed into the open cracks and the matrix was compact enough to uphold the dimensional integrity of the boards. Curing patterns had a significant effect on TS and VS for *A. longifolia* boards but their influence on WA was insignificant ($p$>0.05). *A. mearnsii* boards behaved differently: boards cured at 60 °C for 24 h absorbed more water and had higher mean TS but lower VS values than those cured at 100 °C for 6 h. The disparity could be as a result of the difference in the cellular and chemical composition of the species. Statistical analysis revealed no significant influence of curing pattern on the sorption properties of *A. mearnsii* boards.

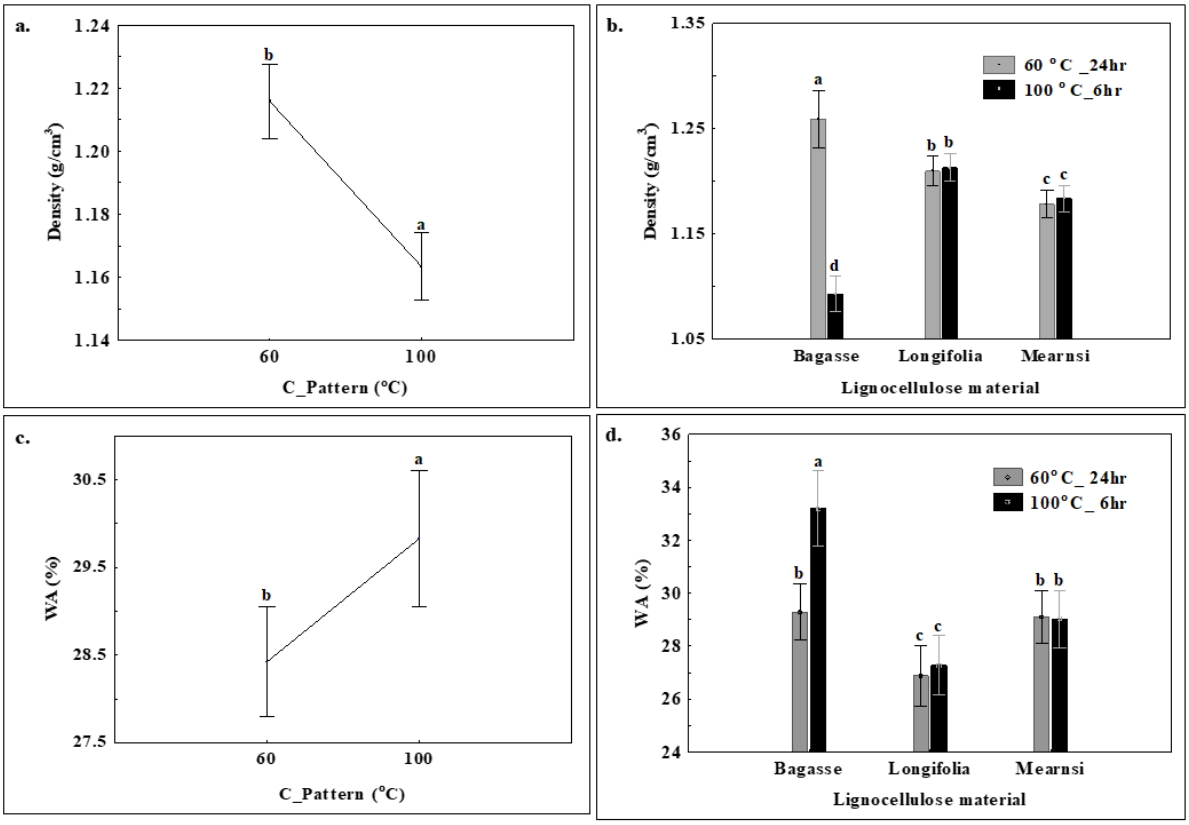


**Fig. 5-2** Effects of curing pattern on (a) density for all boards (b) density for each LM (c) WA for all boards (d) WA for each LM

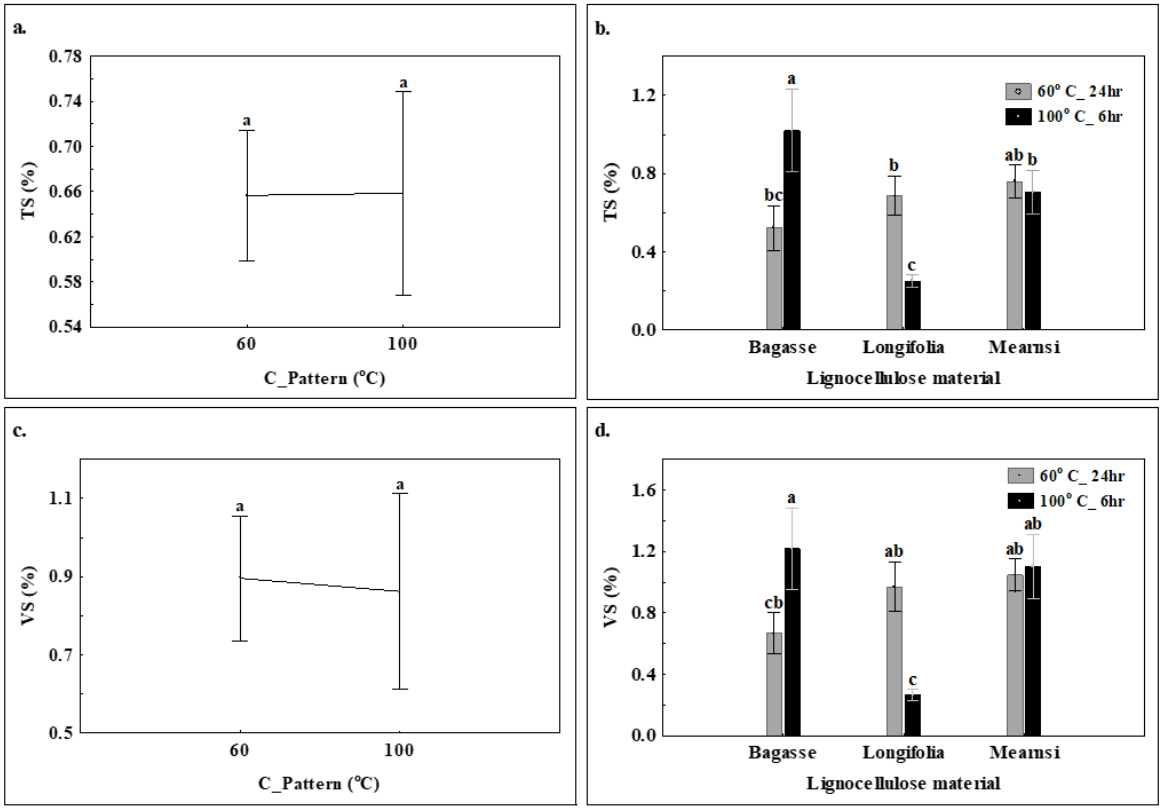


**Fig. 5-3** Effects of curing pattern on TS - (a) for all boards (b) for each LM; - and VS (c) for all boards, (d) for each LM

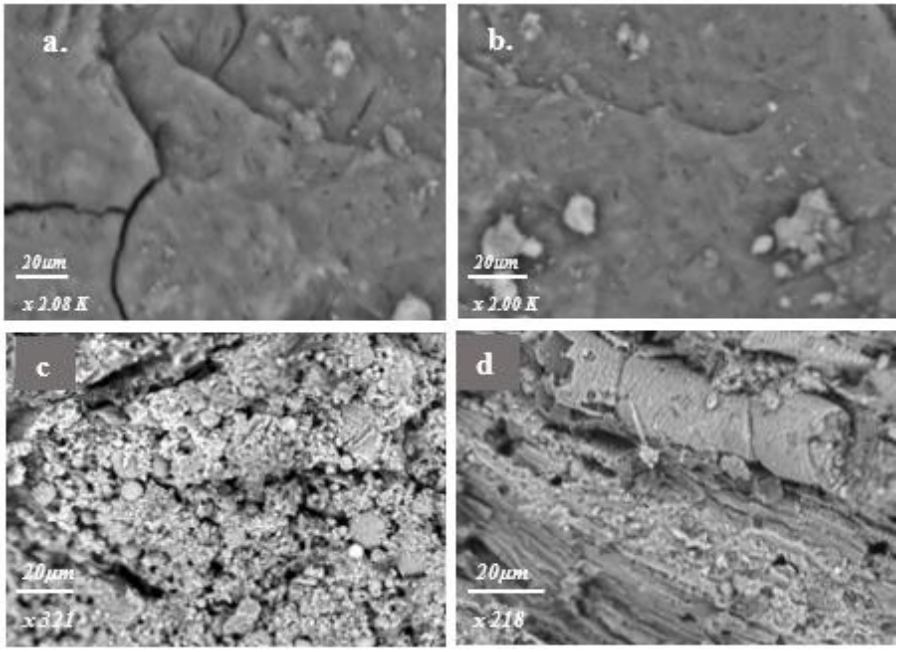


**Fig. 5-4** SEM images showing (a) formation of micro-cracks and channels at high temperature curing in AL board (b) densified pore structure (c) fractured surface of SCB board (d) mineralized fibres of AM boards

## 5.4 Effect of PA ratio and activator concentration on board properties

The effects of PA ratio and activator concentration on the physical and mechanical properties of the boards are presented in Figures 5-5 and 5-6, respectively. The PA ratio and activator concentration are critical factors, which greatly influence the formation and evolution of the overall strength of geopolymer products (Petermann and Saeed 2012). While keeping the weight ratio of $Na_2SiO_3$ and NaOH fixed at 2.5:1, the PA ratio of 2:1 produced alkali dosage (%$Na_2O$/binder) of 10.19, 10.98 and 11.72% with 8M, 10M and 12M NaOH, respectively; compared to the dosages of 6.79, 7.32 and 7.81% recorded for PA ratio of 3:1. Irrespective of LM type and activator concentration, a PA ratio of 2:1 had higher mean density, MOE, MOR and lower WA than a PA ratio of 3:1. The improved properties are due to the higher alkali dosage, which enhanced the dissolution stage of the geopolymerization kinetics and subsequently aided the densification of the pore structure as seen in Figure 5-4(b).

The effect of alkali dosage on the strength development of geopolymers has been reported in the literature. According to Soutsos et al. (2016), increasing the alkali dosage affected the properties of fly ash-based geopolymers until an optimum value of 12.5%, beyond, which the strength decreased. The alkali dosages used in this experiment were below this optimum value. The MOE and MOR of acacia boards improved as the molar concentration of the activator increased. There is an exception with SCB boards where the strength properties decreased when the molar concentration increased from 10M to 12M. This could be explained by the presence of high extractive content and lignin in SCB, which leached and retarded the dissolution of both silica and alumina species and delayed the nucleation stage of geopolymer synthesis. This might have caused the migration of excess alkali anions into the fibre bundles leading to degradation of the holocellulose. This is in line with the result of Ye et al. (2018) that higher lignin content caused reduction in the strength of metakaolin-based geopolymer.

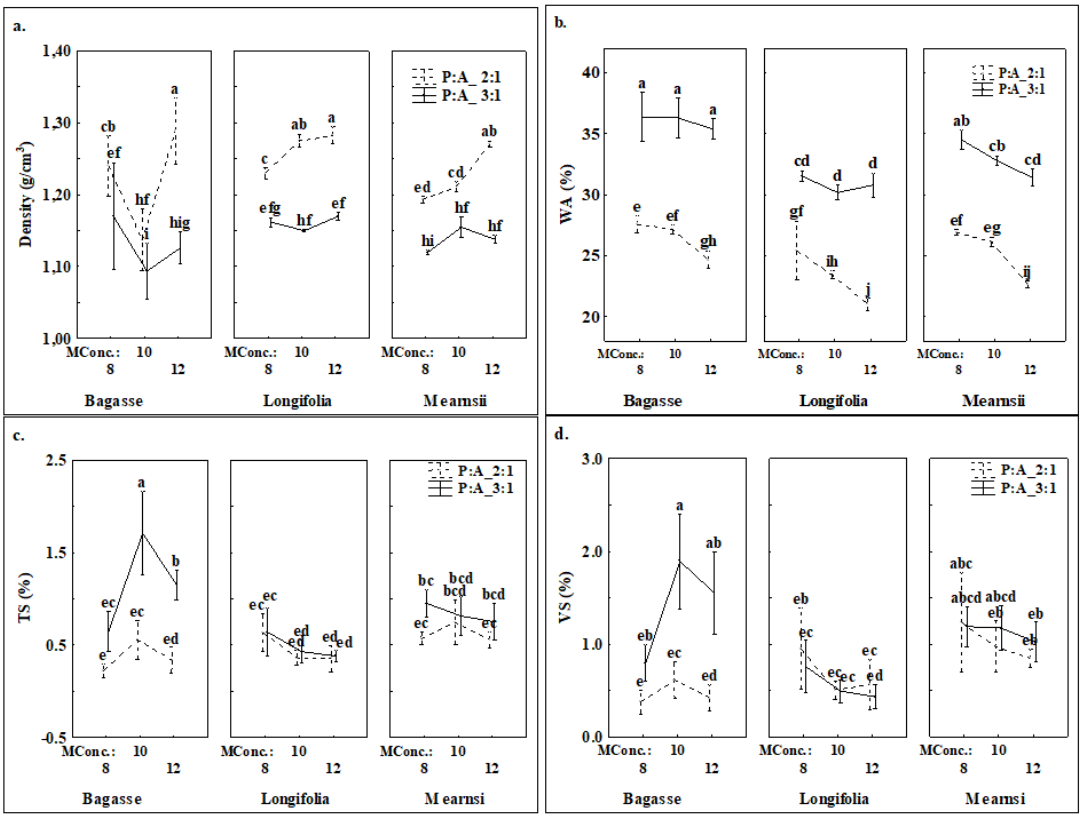


**Fig. 5-5** Effects of PA ratio and molar concentration on (a) board density (b) WA (c) TS (d) VS

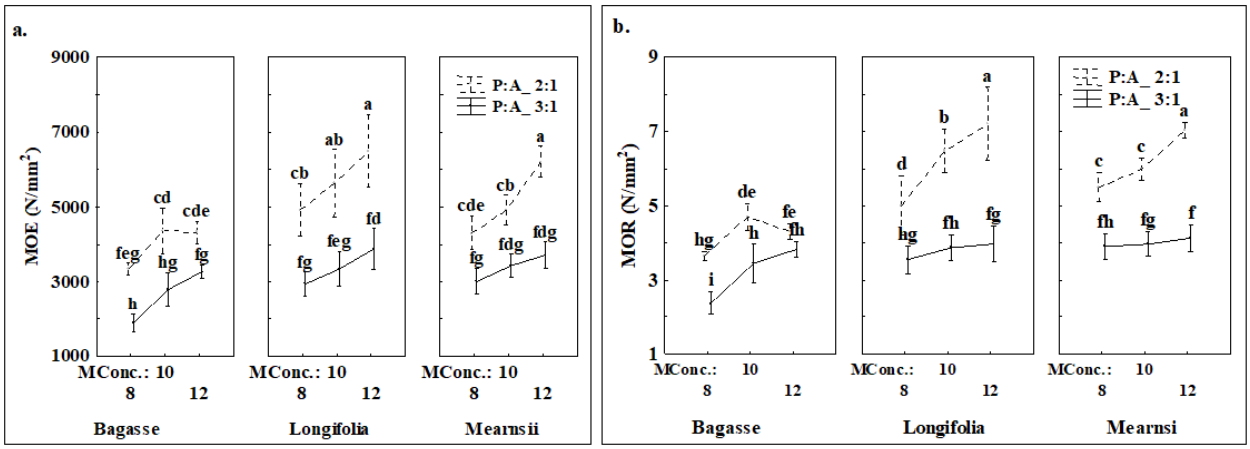


**Fig. 5-6** Effects of PA ratio and activator concentration on MOE and MOR

## 5.5 Effects of curing pattern and LM on mechanical properties of boards

Figure 5-7 shows the effect of the curing pattern on the strength properties of the boards. The effects followed the same trend as was observed with the board density for all LM. SCB boards cured at 60 °C for 24 h had higher mean MOE and MOR than those cured at 100 °C for 6 h, while the reverse was observed with acacia boards. Figure 5-8 shows weak positive correlations observed between

board density and the strength properties. Amiandamhen et al. (2018b) reported a similar observation in phosphate bonded composites where invasive acacia wood was incorporated in the matrix as reinforcement. Irrespective of LM, the curing pattern had significant effects ($p$<0.05) on the strength properties of the boards with the exception of the MOE of SCB boards. Curing at 100 °C for 6 h accelerated the geopolymer kinetics and improved the strength properties of acacia boards. Increasing the curing temperature up to 100 °C has been reported to improve the strength development of low-calcium fly ash (Class F) geopolymers, regardless of the curing duration (Hardjito and Rangan 2005).

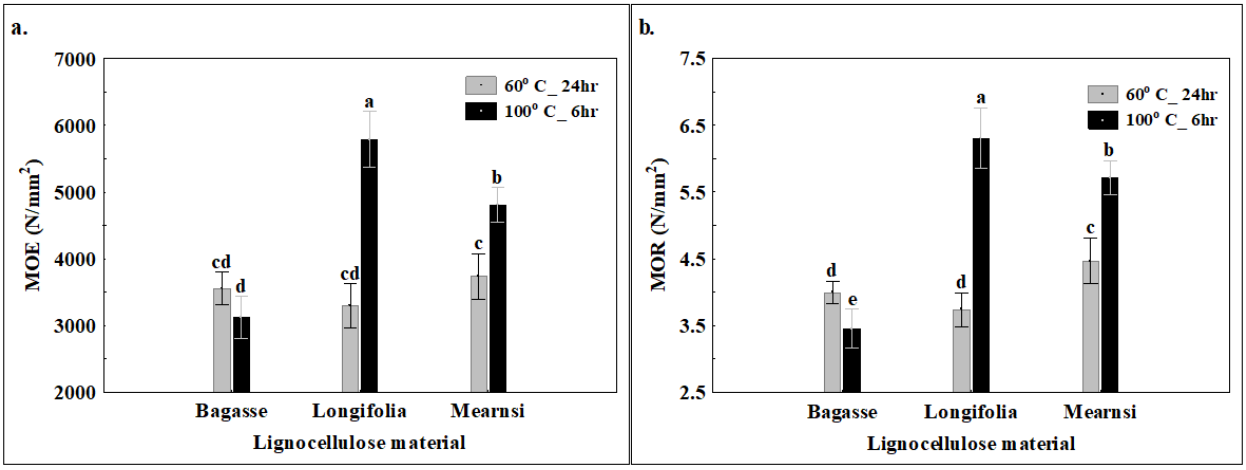


**Fig. 5-7** Effects of curing pattern on (a) MOE (b) MOR

*A. mearnsii* boards cured at 60 °C for 24 h had a higher mean MOE and MOR than *A. longifolia* boards cured at the same temperature, which could be due to its slightly higher cellulose content. Higher cellulose content improves the strength properties of geopolymers as the bridging mechanism of the fibres impedes crack propagation (Ye et al. 2018). However, the trend was reversed when the curing temperature was raised to 100 °C for 6 h. *A. longifolia* boards recorded a significant strength gain compared to *A. mearnsii* boards (Figure 5-7). This could be due to the slightly higher hemicellulose content in *A. mearnsii*, which can degrade in an alkaline environment at higher temperature curing. The SEM image (Figure 5-4(d)) shows that the fibres in *A. mearnsii* boards were mineralized, as the geopolymer matrix can be seen absorbed into the fibre bundles. This caused degradation of hemicelluloses, which was further confirmed by FTIR results. The degraded

hemicelluloses in the alkaline matrix, together with the high extractive content, could cause a reduction in the geopolymerization kinetics.

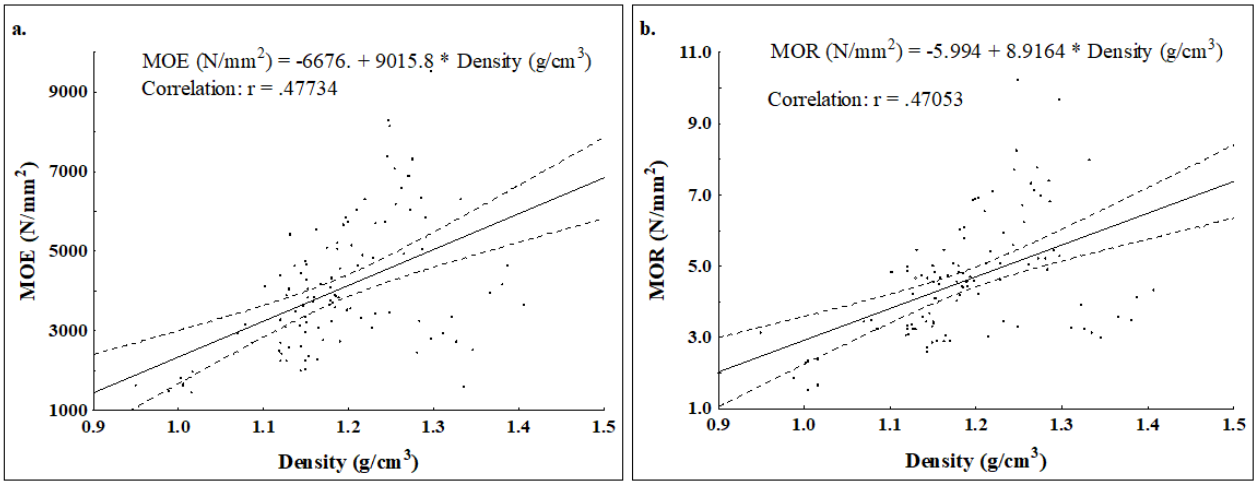


**Fig. 5-8** Relationship between density and (a) MOE, (b) MOR

## 5.6 Characterization of the geopolymer product

### 5.6.1 *FTIR*

The infrared (IR) spectra of the precursor materials are shown in Figure 5-9. Fly ash has more peaks than metakaolin, but it is important to note that the peaks fall within the same band areas. The band between 950 – 1250 $cm^{-1}$ is assigned to the internal vibrations of Si-O-Si (Davidovits 2008). They also have peaks in the band 500 – 800 $cm^{-1}$, which is characteristic of symmetric stretching of the Si-O-Si and Al-O-Si bonds of amorphous or semi-crystalline alumino-silicates (Barbosa et al. 2000; Fauzi et al. 2016). The LM types have similar IR spectra within the same band numbers as shown in Figure 5-10(a). The strongest bands are found around 3360 $cm^{-1}$ and 1023 $cm^{-1}$ in all LM samples. The band around 3360 $cm^{-1}$ is assigned to the axial vibration of the hydroxyl (-OH) group of cellulose (Ibraheem et al. 2016), while the band at 1023 $cm^{-1}$ indicates a C-C bond of β-glucosidic linkages between sugar units in hemicelluloses and cellulose (Hajiha et al. 2014). The peak at 2916 $cm^{-1}$ represents a symmetrical vibration of C-H bond (Liu et al. 2004; Amiandamhen et al. 2018a). Since the SCB fibre has been processed, it could have altered the position of the absorption bands. This peak could also be attributed to a C-H aliphatic axial deformation in $CH_2$ and $CH_3$ groups from cellulose, lignin and hemicellulose as it is only 4 $cm^{-1}$ less than the absorption band reported by Corrales et al. (2012). The peak around 1737 $cm^{-1}$ is attributed to the carbonyl (C=O) stretching of acetyl groups of hemicellulose (Liu et al. 2004; Corrales et al. 2012). These peaks disappeared in the IR spectra of their respective boards (Figure 5-10(b)), indicating the degradation of hemicelluloses in

the matrix. SCB has peaks at 1603 $cm^{-1}$ and 1633 $cm^{-1}$, which could be assigned to C-Ph vibration at peak and C = C bonds found in lignin aromatic structures (Corrales et al. 2012). The C-Ph peak disappeared in SCB boards.

The peak at 1422 $cm^{-1}$ is present in both SCB and the acacia species, indicating $CH_2$ symmetric bending of cellulose (Hajiha et al. 2014; Sawpan et al. 2011). The peak shifted to around 1416 $cm^{-1}$ and the intensity decreased in the geopolymer products, indicating the partial degradation of lower molecular cellulose components. The C–O stretch of the acetyl group of lignin assigned to the peaks found around 1235 – 1254 $cm^{-1}$ (Hajiha et al. 2014; Liu et al. 2004) also disappeared in the composite products. This indicates a partial breakdown of lignin in the alkaline matrix. The major peak found in the geopolymer products is due to the convolution shifts of the Si-O-Si band of the precursor materials (Figure 5-10) and the C-C peak of the LM towards the low wavenumber (Figure 5-10(b)). The shift in the Si-O-Si and Al-O bands towards lower wavenumber indicates that geopolymerization has occurred through partial replacement of silica species by alumina, resulting in a change in the local chemical environment of the bonds (Criado et al. 2005; Davidovits 2008).

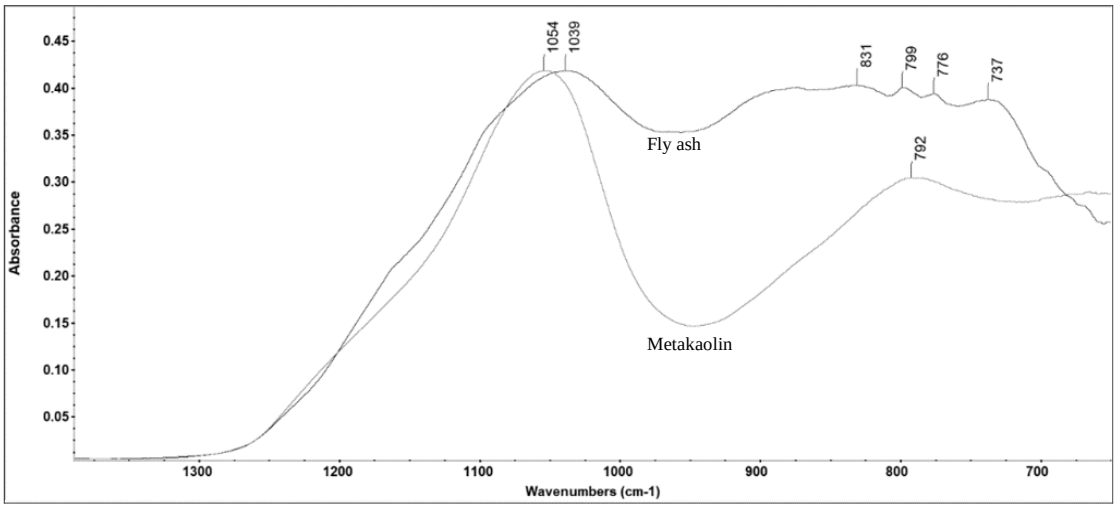


**Fig. 5-9** FTIR spectra of precursor materials

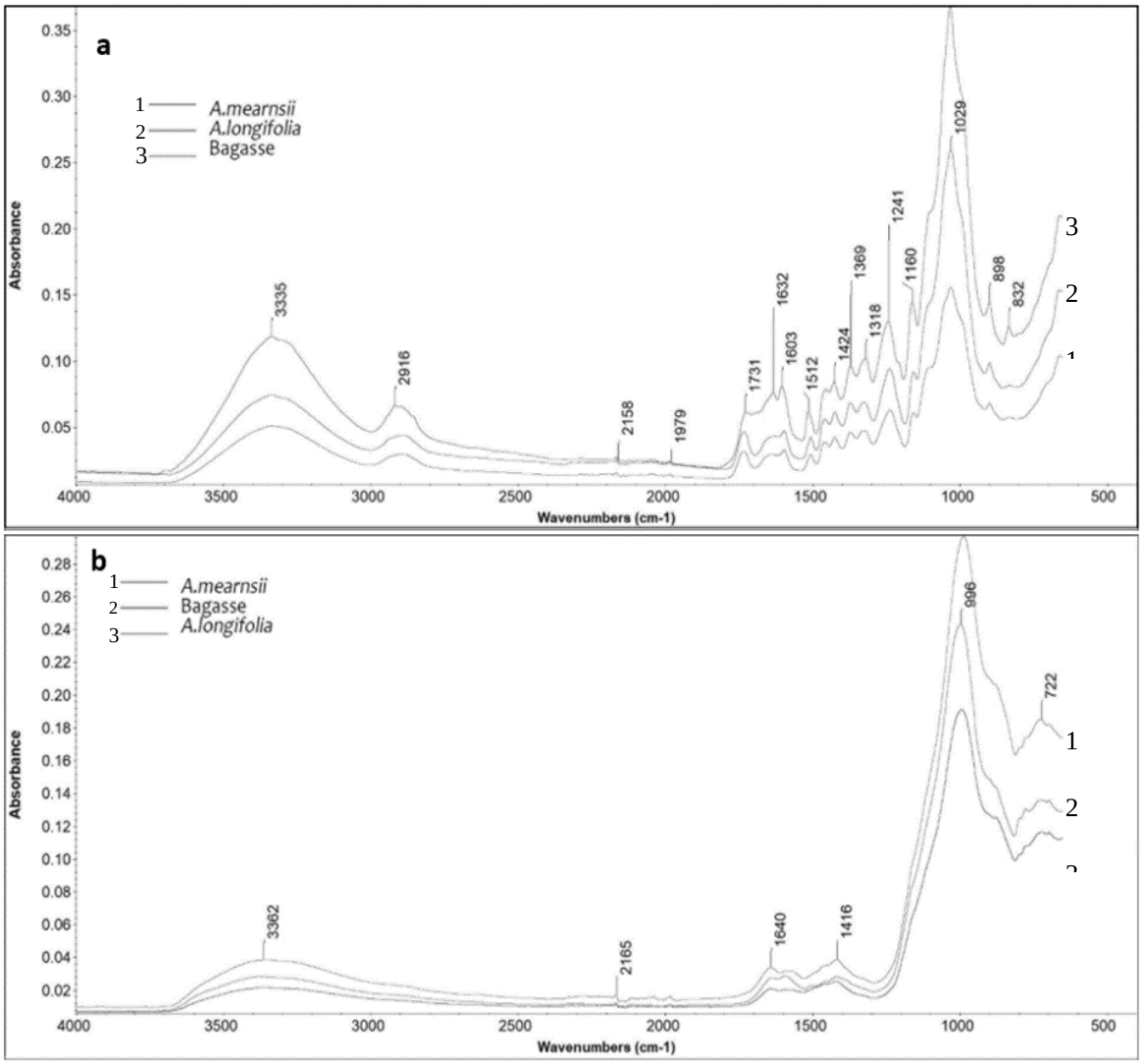


**Fig. 5-10** FTIR spectra of (a) LMs (b) composite products after 28 days

### 5.6.2 *TGA*

The thermal stability of the LM and composite products was investigated by thermogravimetric analysis (TGA) under nitrogen flow. The derivative thermograms (DTG) of the LM are shown in Figure 5-11. The LMs exhibited similar thermal behaviour to the presence of peak/shoulders below the main degradation peak. The shoulders appeared at 272.43 ℃, 274.70 ℃ and 293.49 ℃ for *A. mearnsii*, *A. longifolia* and SCB, respectively. The shoulder may be attributed to the degradation of hemicelluloses partially overlapping with cellulose and lignin (Sebio-Puñal et al. 2012). *A. mearnsii* has another shoulder at 225.12 ℃, which could indicate the decomposition of some volatile components and hemicelluloses of lower molecular weights. The DTG plot of the boards is shown in Figure 5-12. The peak-shoulder disappeared in all boards, which corroborates the FTIR results that the hemicellulose components have degraded in the alkaline matrix.

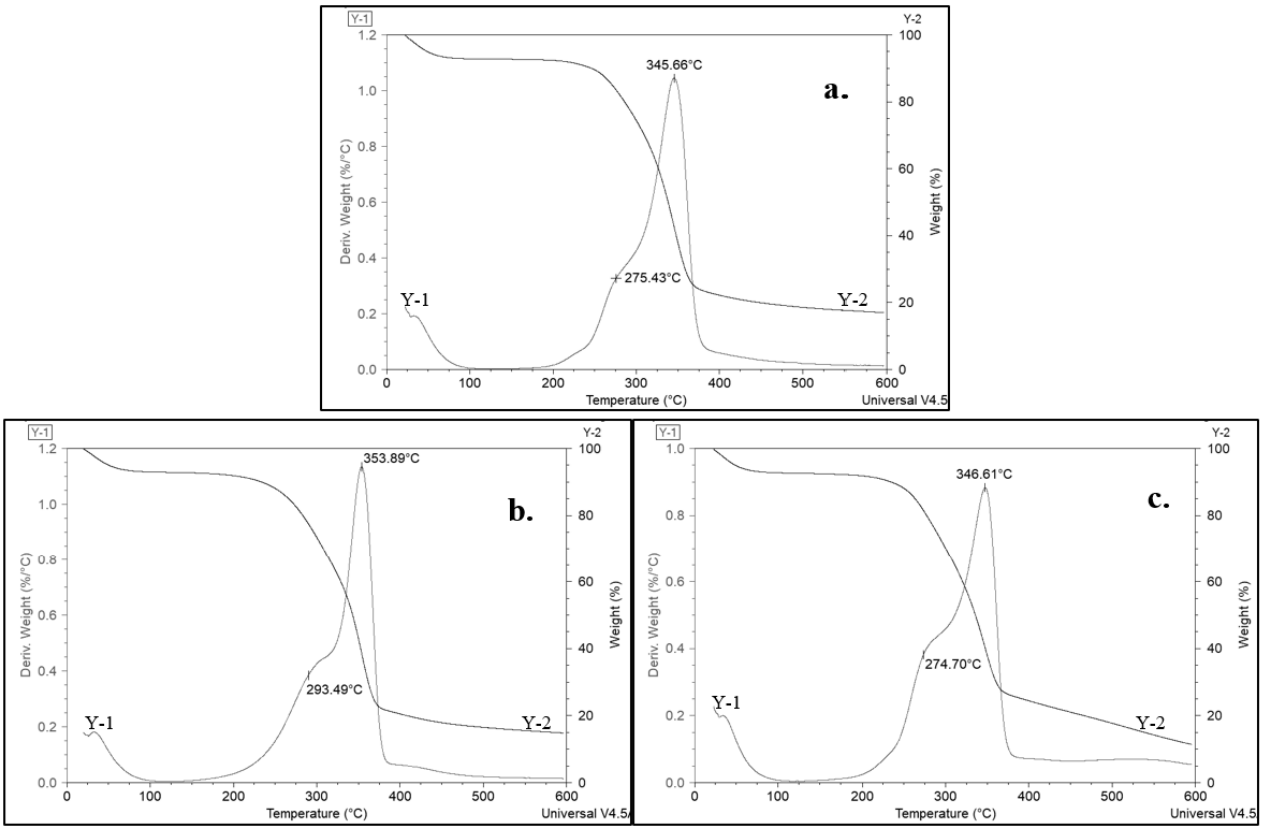


**Fig. 5-11** Thermograms (TG) and derivative thermograms (DTG) of LM: (a) *A. mearnsii*, (b) SCB, (c) *A. longifolia*

The shift in the main degradation peaks towards the lower end of the cellulose degradation range of 275 – 500 °C also confirms the partial degradation of cellulose and lignin (Machado et al. 2018). Other broad peaks found around 425 – 525 °C for *A. mearnsii* and *A. longifolia* could indicate an overlap of lignin degradation and transformation of the amorphous matrix contents into a more crystalline structure. This peak is absent in the SCB board, but its weight loss was increasing until it became steady around 540 °C. The products are thermally stable as the residues are all above 70.

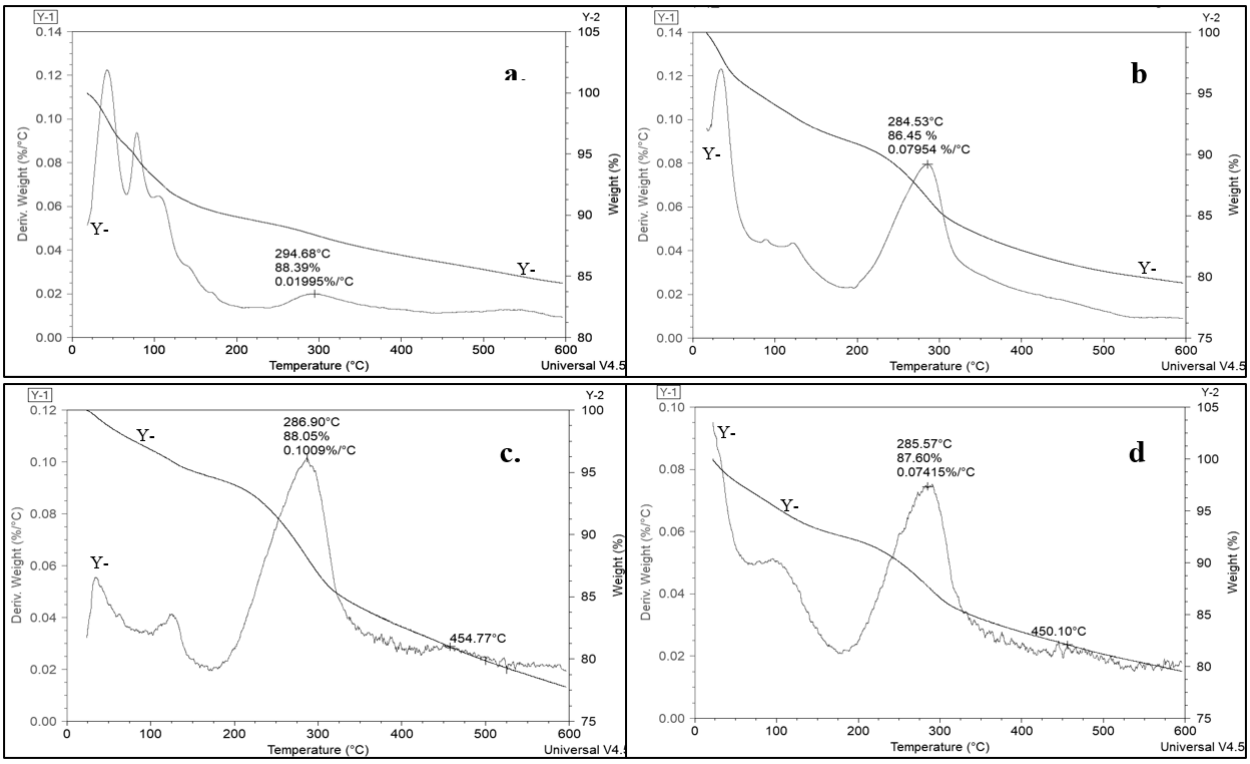


**Fig. 5-12** Derivative and weight loss thermograms of (a) control sample, (b) SCB boards, (c) *A. longifolia* boards, (d) *A. mearnsii* boards

### 5.6.3 *XRD*

The XRD diffractograms of fly ash and metakaolin are shown in Figure 5-13 (a). The high peak observed between 15 – 35° 2θ indicates a high level of amorphous content, which could be silica or alumina. Quartz (00-901-0145) and mullite (00-900-5502) are the principal crystalline phases present in both materials, but their intensities are higher in fly ash than metakaolin. No formation of new crystalline phases was observed in the diffractograms of the composite products shown in Figure 5-13(b), but the intensity of the identified crystalline phases reduced, and the peak shifted towards higher 2θ values. The shift confirms the FTIR results that geopolymerization has taken place (Yuan et al. 2016), and the reduction in intensity indicates that some parts of the crystalline material took part in the reaction (Alomayri 2017). Fewer crystalline phases participated in the geopolymerization reaction of *A. mearnsii* boards as they exhibit higher intensities than those found in the other boards (Figure 5-13(b)). *A. longifolia* and *A. mearnsii* had comparable chemical composition (see Table 4-1), but the difference in the intensities of the crystalline phases in SCB and *A. longifolia* boards are not noticeable, which could mean that *A. mearnsii* contains components that inhibited geopolymerization kinetics.

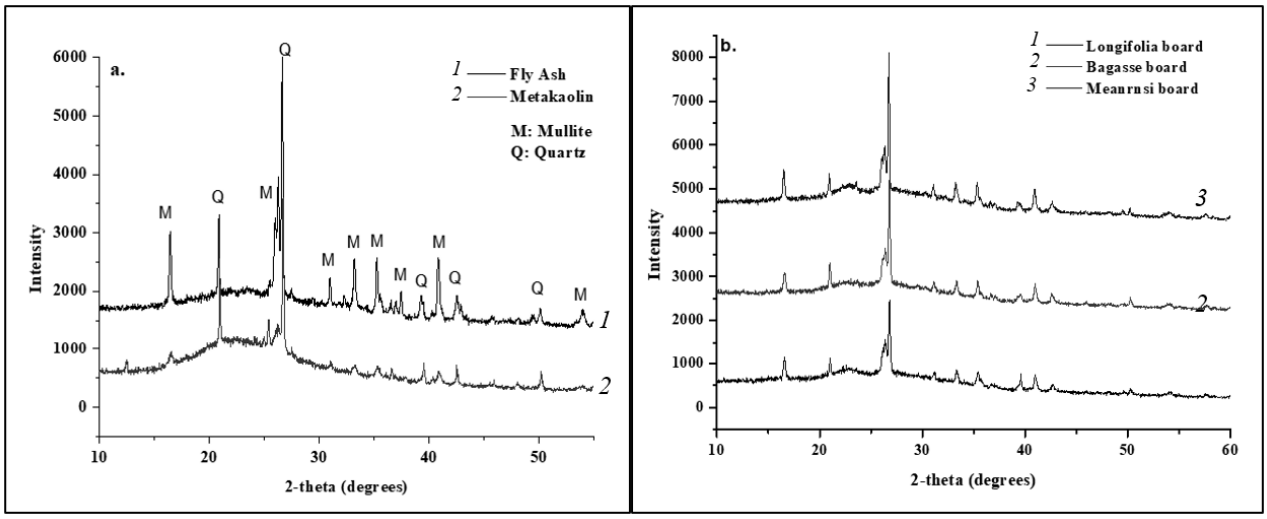


**Fig. 5-13** XRD patterns of (a) precursor materials (b) geopolymer composites

## 5.7 Conclusion

This study has demonstrated the possibility of producing high-density geopolymer panels reinforced with untreated wood particles from South African invasive species and SCB for use in outdoor conditions. The following conclusions can be drawn based on this study:

1 Curing pattern, molar concentration of activator and PA ratio have significant effects on the properties of the geopolymer boards.

2 Increasing the molar concentration of activator and curing temperature results in a denser pore structure and improves the properties of acacia boards. The internal structure of SCB boards deteriorated at higher curing temperature causing low strength development.

3 All geopolymer boards met the sorption requirements of EN 634-2: 2007 for cement-bonded particleboards for outdoor applications. However, only *A. longifolia* boards produced with 12M NaOH, PA ratio of 2:1 and cured at 100 °C for 6 h met the mechanical strength requirements.

4 The boards are thermally stable, as the residue retained at the end of thermal analysis was above 70%.

5 The products have comparable properties to other natural fibre reinforced composites and can be used as alternative materials in similar applications. The development of geopolymer products utilizing industrial residues presents both economic and environmental advantages when compared to conventional composite products. However, there is a concern about the durability of the LM in alkaline matrix. Mineralization of LM due to high dosage of alkali activator was revealed by SEM, while degradation of

hemicellulose and lower molecular wood components was confirmed by FTIR analysis. The degraded products do not prevent geopolymer setting but lower the degree of geopolymerization. Hence, the durability of the product over time needs to be further investigated.

# Chapter 6

# Characterization of unary precursor-based geopolymer bonded composites developed from ground granulated blast slag and forest biomass residues

## 6.1 Board formation

The overview of the mix design for board production is shown in Table 6-1.

**Table 6-1** Overview of board production

| No | Slag(g) | LM (g) | $Na_2SiO_3$(g) | NaOH (g) | $H_2O$ (g) | Conc. (M) | Curing |
|---|---|---|---|---|---|---|---|
| 1 | 160 | 40 | 57.14 | 22.86 | 14 | 4 | 25°C, 24h |
| 3 | 160 | 40 | 57.14 | 22.86 | 14 | 6 | 25°C, 24h |
| 5 | 160 | 40 | 57.14 | 22.86 | 14 | 8 | 25°C, 24h |
| 2 | 160 | 40 | 57.14 | 22.86 | 14 | 4 | 40°C, 6h |
| 4 | 160 | 40 | 57.14 | 22.86 | 14 | 6 | 40°C, 6h |
| 6 | 160 | 40 | 57.14 | 22.86 | 14 | 8 | 40°C, 6h |
| Control | 190 | - | 67.86 | 27.14 | - | 6 | 25$^o$C , 24h |

## 6.2 Physical properties of the boards

The physical and mechanical properties of slag-bonded geopolymer boards are shown in Table 6-2. The boards had densities above 1.0 g/cm$^3$ and were hence classified as high-density boards according to the American National Standard for composite panels ANSI (1999). The unit weights of the control samples ranged from 14.53 – 15.02 kN/m$^3$. The incorporation of biomass caused a considerable reduction in the unit weights. The unit weights of the reinforced boards ranged from 11.59 – 14.53 kN/m$^3$, 11.78 – 14.33 kN/m$^3$ and 12.47 – 14.44 kN/m$^3$ for *A. mearnsii* (AM), *A. saligna* (AS) and sugarcane bagasse (SCB) boards, respectively. These values are in the range observed with fly ash/metakaolin based geopolymer in the previous Chapter, and also lower than the range reported for geopolymers in the literature (Andini et al. 2008; Chen et al 2014; Cioffi et al 2003).

The sorption properties were indicated by water absorption (WA), thickness and volumetric swelling (TS/VS). The WA, TS and VS of the control samples ranged from 10.56 – 12.85 %, 0.04 – 0.07 % and 0.10 – 0.13 %, respectively. The acacia boards had WA of 13.69 – 14.46 % for AS, 17.16 – 17.28

% for AM, while WA of SCB boards ranged from 17.69 – 21.48%. The TS/VS for AS boards ranged from 0.12 – 0.27% and 0.18 – 0.51% respectively. The TS/VS were higher for AM and SCB boards. The ranges were 0.14 – 0.72% and 0.22 – 1.87% for AM; and 0.74 – 2.60% and 0.98 – 3.45% for SCB boards, respectively. The boards were less dimensionally stable compared to the control, but they met the sorption requirements for particleboards according to the British Standard (EN 634-2 2007) and the Indian Standards (IS 1985).

## 6.3 Mechanical board properties

As shown in Table 6-1 the MOE of AM, AS and SCB boards ranged from 1720 – 5078 MPa, 3410 – 7212 MPa and 1175 – 2934 MPa, respectively. The MOR ranged from 5.79 – 7.17 MPa, 6.75 – 9.40 MPa and 5.24 – 7.90 MPa for AM, AS and SCB boards, respectively. According to the British standard (EN 634-2 2007) the minimum MOE and MOR of high-density particleboards are 4000MPa and 9.0MPa respectively, but only AS boards satisfied these requirements (Figure 6-1). The strength properties of AM and SCB were not adequate compared to the EN 634 requirements, but they compared well with the requirements for low-density particleboards grade 1&2, bonded with synthetic resin (ANSI 1999). Hence, AM and SCB boards may be suitable for non-load bearing applications.

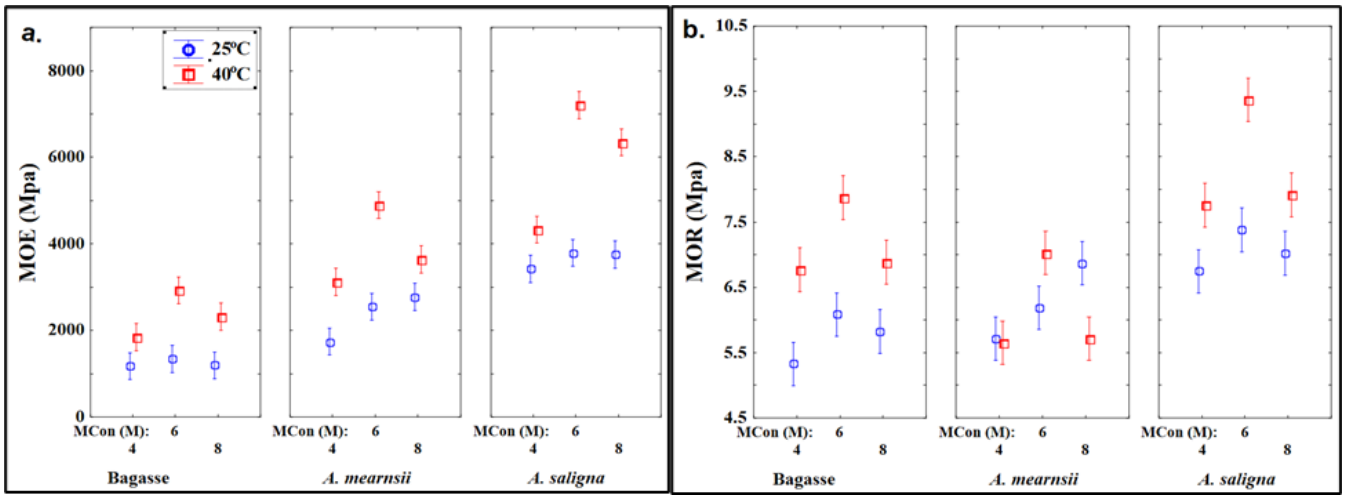


(*vertical lines denote the confidence interval at 0.95*)

**Fig. 6-1** The mechanical properties of all boards (a) MOE (b) MOR

**Table 6-2** Physical and mechanical properties of the boards

| Boards | Board Properties | | | | | | |
|---|---|---|---|---|---|---|---|
| | MOE (MPa) | MOR (MPa) | Density ($g/cm^3$) | Unit weight ($kNm^{-3}$) | WA (%) | TS (%) | VS (%) |
| *A. mearnsii* | 1720 – 5078 | 5.79 – 7.17 | 1.18 – 1.48 | 11.59– 14.53 | 17.16– 17.28 | 0.14 – 0.72 | 0.22 – 1.87 |
| *A. saligna* | 3410 – 7212 | 6.75 – 9.40 | 1.20 – 1.46 | 11.78– 14.33 | 13.69– 14.46 | 0.12 – 0.27 | 0.18 – 0.51 |
| SCB | 1175 – 2934 | 5.24 – 7.90 | 1.27 – 1.47 | 12.47– 14.44 | 17.69– 21.48 | 0.74 – 2.60 | 0.98 – 3.45 |
| Control | 2926 – 3691 | 4.83 – 5.96 | 1.48 – 1.53 | 14.53– 15.02 | 10.56– 12.85 | 0.04 – 0.07 | 0.10 – 0.13 |
| BS EN 634* | ≥ 4000** | ≥ 9.0 | ≥ 1.0 | - | ≤ 25 | ≤ 15 | ≤ 15 |
| ANSI** | 1034 | 5.5 | < 0.64 | - | - | - | - |

**Class 1: ≥ 4500 MPa | Class 2: 4000 MPa. | ** Grade 1-L-1 low density particleboard*

## 6.4 Influence of production variables on physical properties

The effects of all production variables on the physical properties are shown in Figure 6-2. The LM, MCon and curing temperature had significant effects on the density, WA, and TS/VS of the boards. Figure 6-2(a – b) show that only the interaction between MCon and LM had significant effects on the density and the WA of all boards. The interactions between MCon – LM and MCon – Temp had a significant effect on the TS, while the interaction between the variables had no significant effects on the VS.

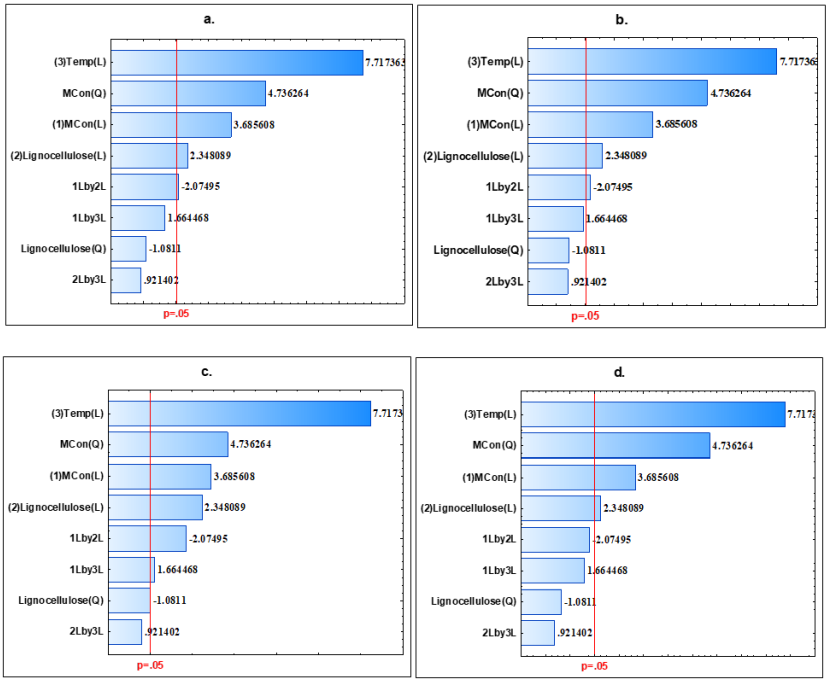


(*1-Mcon, 2-LM, 3- Curing temperature, L- Linear effect, Q-Quadratic effect. Bars that cross the p-line are significant*)

**Fig. 6-2** Pareto charts (ANOVA) showing the effects of production variables and their interactions on the physical properties (a) density (b) WA (c) TS (d) VS

### 6.4.1 Effect of lignocellulosic material on board density

Similar to fly ash/metakaolin based geopolymer composites in Chapter 5, lignocellulosic materials (LM) affected the boards differently. The influence of lignocellulosic material (LM) on the board density is shown in Figure 6-3. AS boards had the highest mean density, which could be attributed to their higher bulk density. Higher bulk density lowered the volume of incorporated particles. This enabled the particles to be fully encapsulated in the matrix and lowered the possibility of compressibility issues at high fibre loading. According to Simatupang and Geimer (1990), and as observed by Amiandamhen et al. (2017) improved properties of mineral bonded composites require full encapsulation of wood/fibres in the matrix. Statistical analysis ($p \leq 0.05$) revealed that LM had a significant effect on the board density. AM had a higher bulk density than SCB (see Table 4-1), but the mean density of their respective boards was not significantly different. The main reaction product of alkali activated slag is C – A – S – H (Calcium alumino silicate hydrates). Slag-based geopolymer contains C – S – H (calcium silicate hydrates) (Song et al. 2000) and some wood species contain chemicals that inhibit the formation of C – S – H (Quiroga et al. 2016). It was observed in the previous chapter that AM contained some components, which retarded the geopolymerization kinetics of fly ash/metakaolin. These inhibitory components could have delayed the formation of C – S – H, leading to compromised microstructures, thus lowering the board density.

### 6.4.2 *Effects of LM on sorption properties*

Figure 6-4 shows how the LM affected the sorption properties of the boards. SCB boards were the least dimensionally stable with the highest WA, and TS/VS. SCB had low bulk density, therefore more volume per unit was used to produce the boards. It was observed that some SCB boards experienced ‘spring back’ effect after removal from the press. This caused the boards to expand and hence lowered their densities. High density indicates sufficient interlocking between the fibre and the matrix, forming a less porous microstructure (Amiandamhen et al. 2018), which explains why AS boards had the best properties. Statistical analyses ($p \leq 0.05$) revealed that WA, TS/VS are significantly different for each LM.

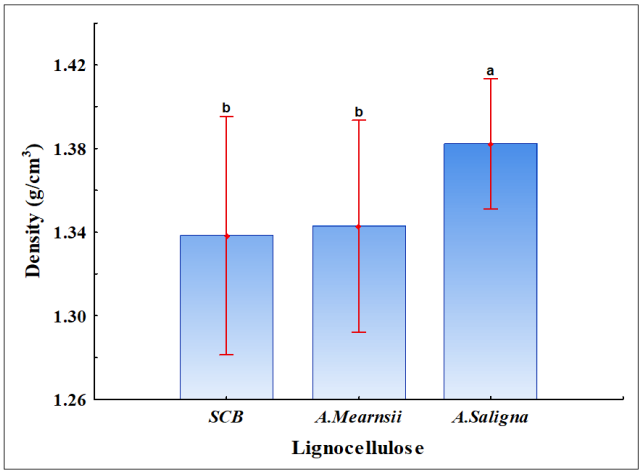


**Fig. 6-3** Effects of LM on (a) density (b) WA (c) TS and (d) VS

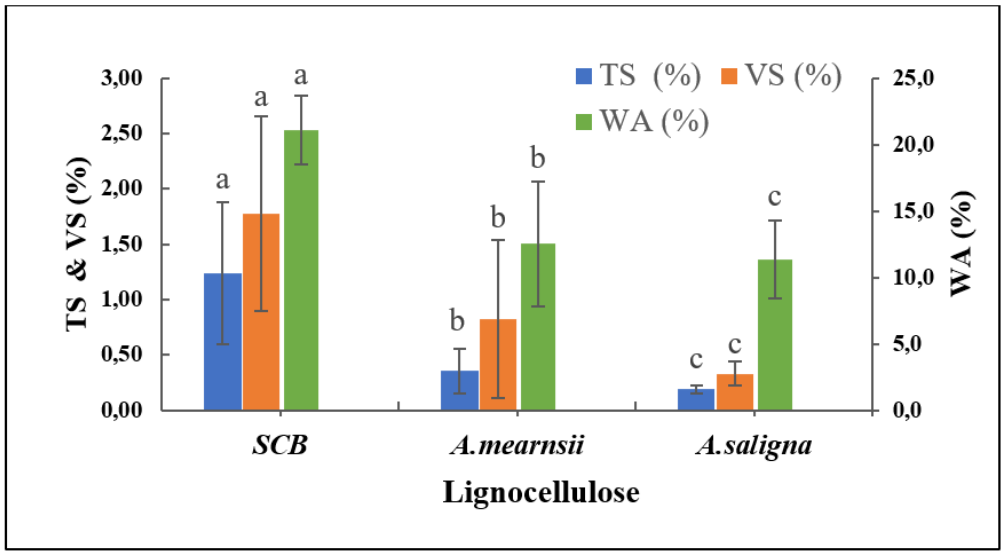


*(vertical lines denote standard deviations, series with same letters are not significantly different)*

**Fig. 6-4** Effects of LM on WA, TS and VS

### 6.4.3 *The effects of molar concentration on board density and sorption properties*

The rate of hydration of slag is dependent on its composition and concentration of alkali activator (Song et al. 2000). The effect of molar concentration of the activator (MCon) on board density and sorption is presented in Figure 6-5. Generally, there was a significant difference between the MCon, with 6M having the highest mean density. The mean board density increased by about 7.6% when the MCon was increased to 6M. The increase was due to higher alkali dosage, which enhanced the reactions at the dissolution stage. Improvement in board composite properties was also observed in fly ash/ metakaolin (FA/MK) geopolymer when the molar concentration was increased (Chapter 5). However, unlike the FA/MK a reduction in mean board density by about 2.86% was observed when

the MCon was increased to 8M. The reduction is attributed to the excess alkali ions, which deteriorated the microstructure of the composite. As seen in Figure 6-5(b) this observation was consistent for SCB and AM boards only, because the density of AS boards slightly increased when the MCon was increased to 8M. However, there was no significant difference between 6M and 8M for AS boards.

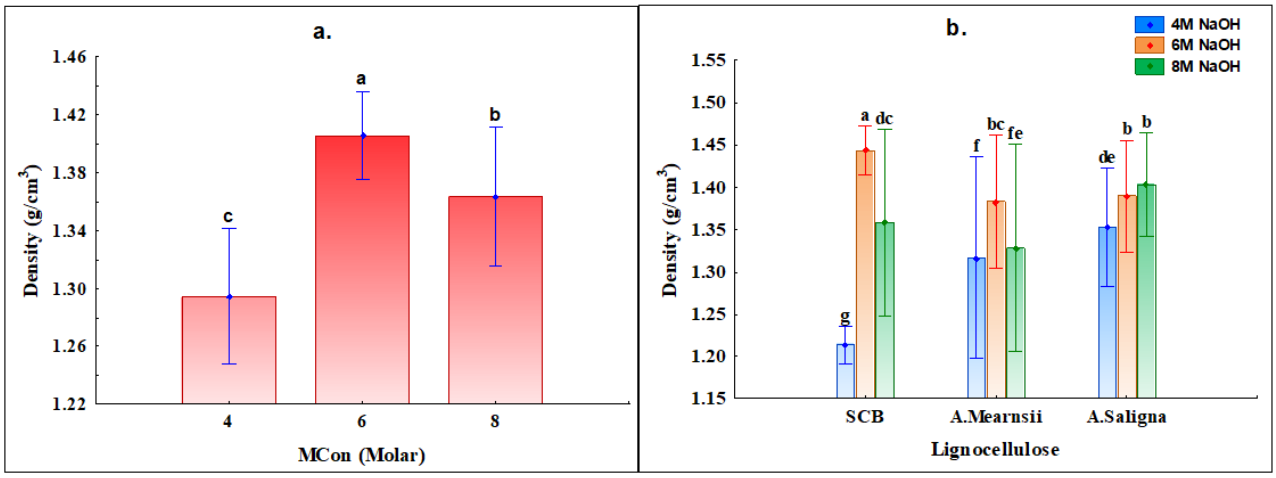


*(vertical lines denote standard deviations, series with same letters are not significantly different)*

**Fig. 6-5** Effect of molar concentration on (a) density of all boards (b) density of each LM

Figure 6-6 shows the influence of MCon on the WA, and TS/VS of the boards. The dimensional stability of the boards followed a similar trend with density. The TS/VS decreased when the MCon increased to 6M and then increased when MCon was increased to 8M. This indicates that the microstructure of the 8M board was not compact enough to withstand the water uptake. The mineralized wood particles at higher alkali dosage (8M NaOH) left large pores, which provided additional channels and exposed more sorption sites for water molecules. The boards produced with 8M absorbed more water and were the least dimensionally stable. A variation however existed in the trend due to differences in the chemical composition of the LM.

Figure 6-6(b) shows the mean WA for each LM. The mean WA for AM boards produced with 6M was higher than those made with 4M and 8M, but their mean TS/VS were lower. The higher WA of AM could be due to its high cellulose and hemicellulose contents, which provided numerous sorption sites for water molecules. However, 6M produced boards with sufficient compact structure to resist the impact of water uptake. A slight but significant difference ($p \leq 0.5$) in WA was observed in AS boards at all MCon levels. 8M boards had slightly higher mean WA and TS than 6M boards, but the VS was lower. Figure 6-6 (c & d) show that there was no significant difference ($p \leq 0.05$) between the mean TS/VS for AS boards made with 6M and 8M MCon.

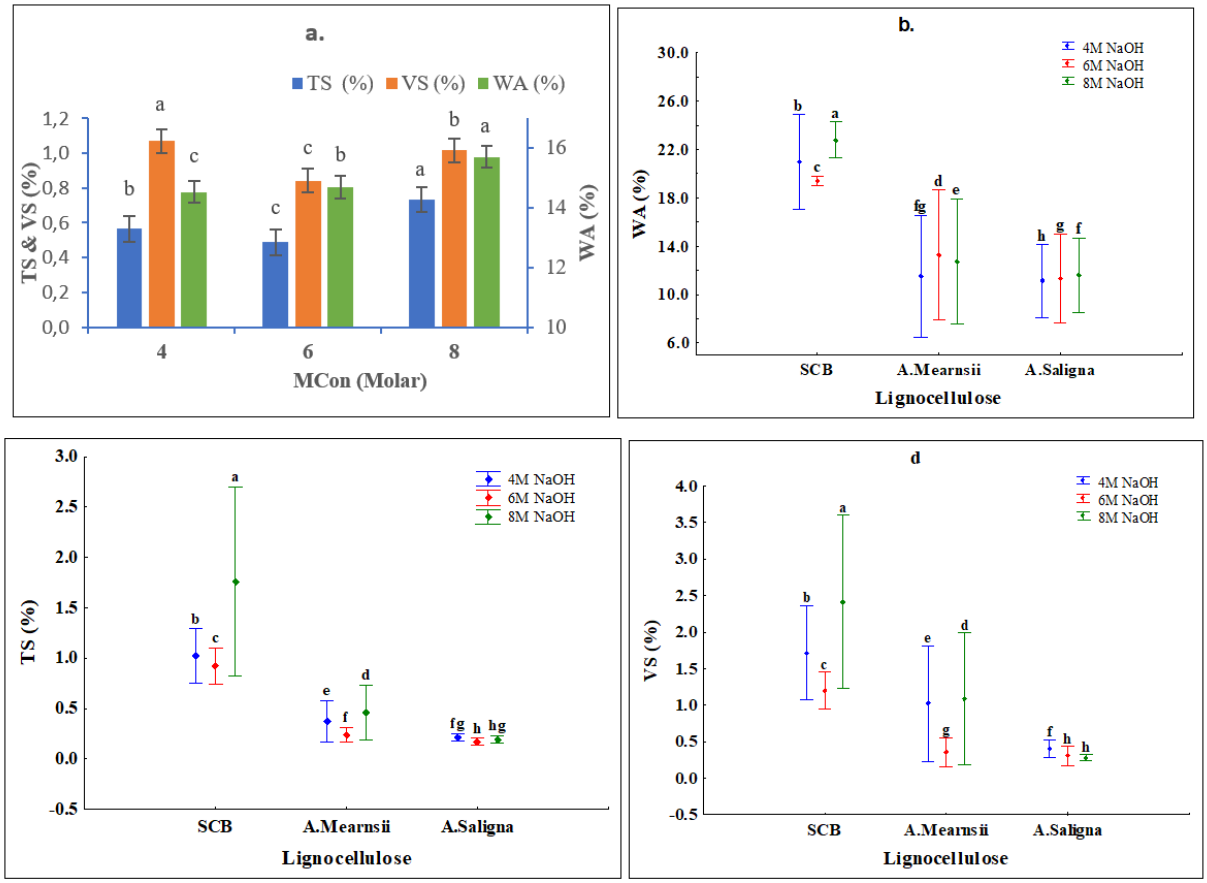


*(vertical lines denote standard deviations, series with same letters are not significantly different)*

**Fig. 6-6** Effects of MCon on sorption properties (a) WA, TS/VS of all boards (b) WA of each LM (c) TS of each LM (d) VS of each LM

### 6.4.4 *The effects of curing pattern on density and sorption properties*

Increasing the curing temperature enhances the reactivity and rate of dissolution of the precursor materials (Petermann and Saeed 2012) . Figure 6-7(a) shows that the curing temperature had a significant effect ($p \leq 0.05$) on the board density. The mean density of the boards increased by about 8.5% when the temperature was increased to 40°C. However, the board density of FK/MK boards in the previous Chapter was reduced when the curing temperature was increased to 100°C. The elevated temperature induced rapid moisture removal causing the formation of numerous micropores. Figure 6-7(b) shows that boards cured at 40°C absorbed more water but were more dimensionally stable than those cured at room temperature. The WA increased by about 44% while the TS and VS decreased by 49% and 58% respectively. The higher temperature improved dissolution of $Ca^{2+}$, $Al^{3+}$ and $Si^{2+}$species and enhanced the polycondensation process to form a compact product. Water, which is a by-product of the condensation stage was driven off quicker at 40°C than 25°C. This created more micropores (not excessive as in the case of FK/MK), which provided more channels for water uptake.

A similar phenomenon was reported by Tran *et al.* (2009). Reduction in TS/VS showed that the fibre-matrix bond was compact enough to resist dimensional changes associated with an increase in WA.

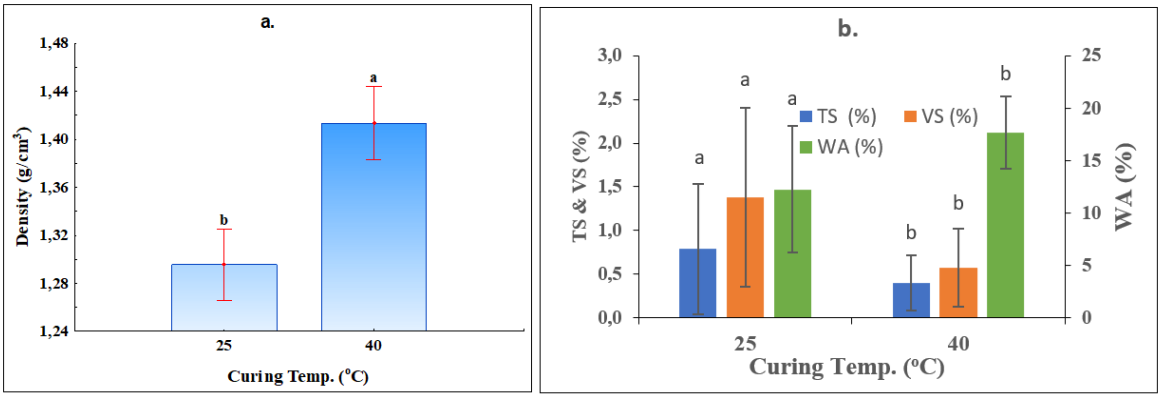


*(vertical lines denote standard deviations, series with same letters are not significantly different)*

**Fig. 6-7** Effects of curing pattern on physical properties (a) board density (b) sorption properties

Figure 6-8 shows how the curing temperature affected the density and sorption properties of each LM. The density and WA of each LM increased as the temperature increased, while the TS/VS decreased. There was a significant difference ($p \leq 0.05$) in the mean density, WA, TS/VS between the curing temperatures for each LM.

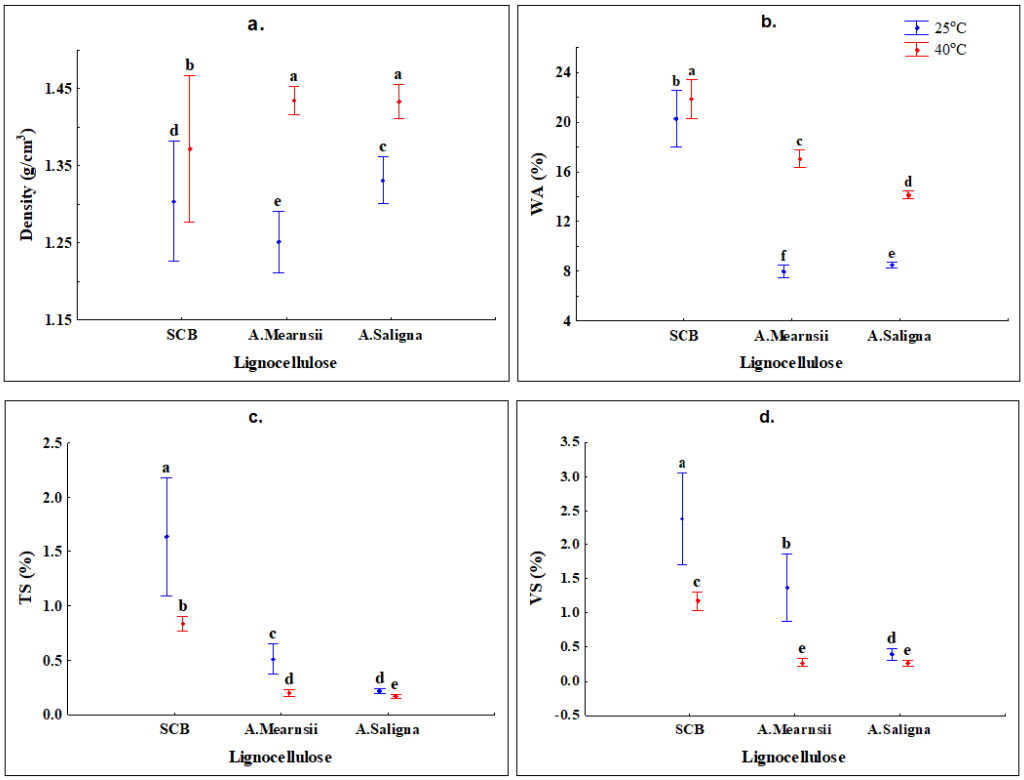


**Fig. 6-8** Effects of curing temperature on (a) density (b) WA (c) TS and (d) VS of each LM

## 6.5 Influence of production variables on the mechanical properties

The pareto chart in Figure 6-9 shows that all the production variables had significant effects on the mechanical properties of the boards. The LM had significant interaction with MCon and curing temperature for MOE (Figure 6-9(a)), but the interaction between MCon and curing temperature was not significant. Figure 6-9(b) shows that only the interaction between LM and MCon had significant effect on the MOR, the other interactions had no significant effects.

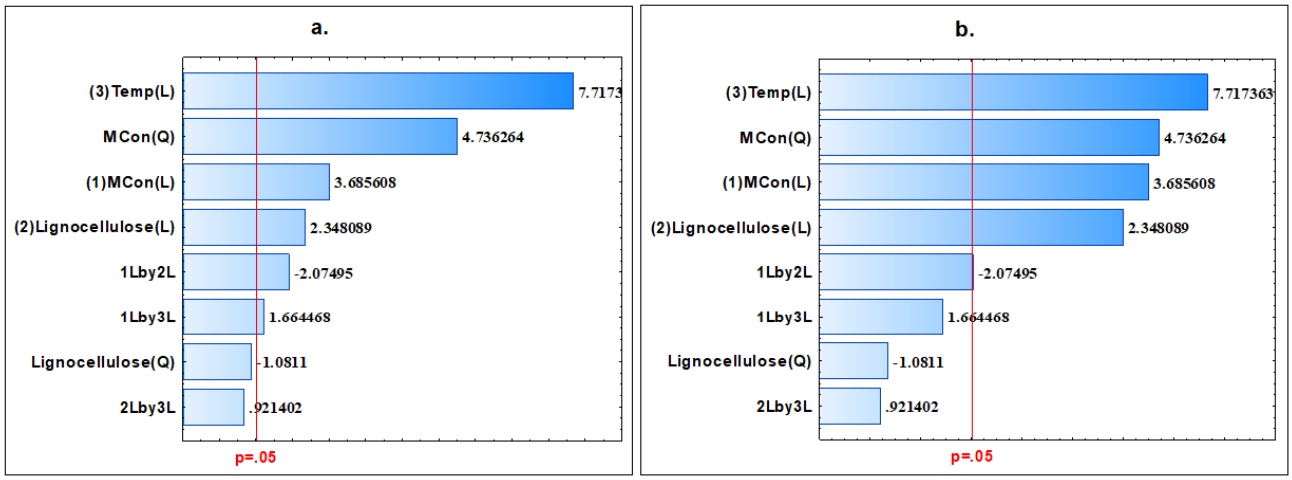


(*1-Mcon, 2-LM, 3- Curing temperature, L- Linear effect, Q-Quadratic effect. Bars that cross the p-line are significant*)

**Fig. 6-9** Pareto charts (ANOVA) showing the effects of production variables and their interactions on (a) MOE (b) MOR

### 6.5.1 *Effect of LM on MOE and MOR*

Figure 6-10(a & b) show that there were significant differences in the strength properties between the LMs. The MOE and MOR followed similar pattern with density for acacia species - AS boards had the highest mean MOE and MOR. This can be ascribed to its higher cellulose and lignin content. Higher lignin and cellulose content improve the strength of composite products by forming strong interfacial adhesion between the particles and the matrix (Bledzki et al. 1998; Bledzki. and Gassan 1999). Figure 6-11 shows a positive correlation between the density and the observed strength properties. The observation was in line with the findings reported in the previous chapter and for phosphate bonded composites (Amiandamhen et al. 2017). However, there was a change in the trend between SCB and AM boards. Although AM boards had a slightly higher mean density than SCB (the difference was not significant), there were significant differences in their mean MOE and MOR. AM boards had a higher mean MOE but lower mean MOR than SCB boards. This could be due to the difference in their chemical compositions. AM contained higher hemicellulose and cellulose, but

lower lignin than SCB. Interaction between these components and binding systems at the different stages of the geopolymerization process could affect the strength properties differently.

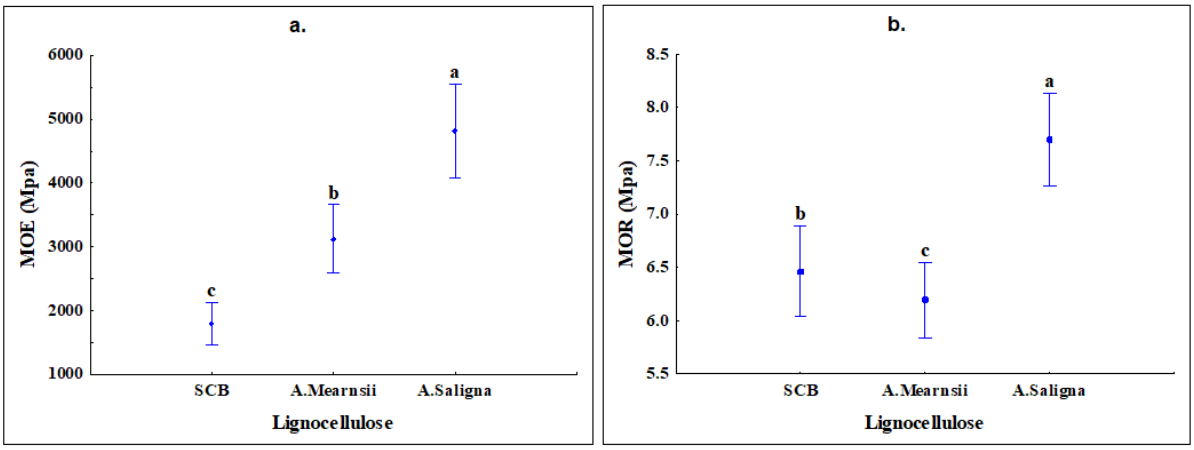


*(vertical lines denote standard deviations, series with same letters are not significantly different)*

**Fig. 6-10** Effects of LM on mechanical properties (a) MOE (b) MOR

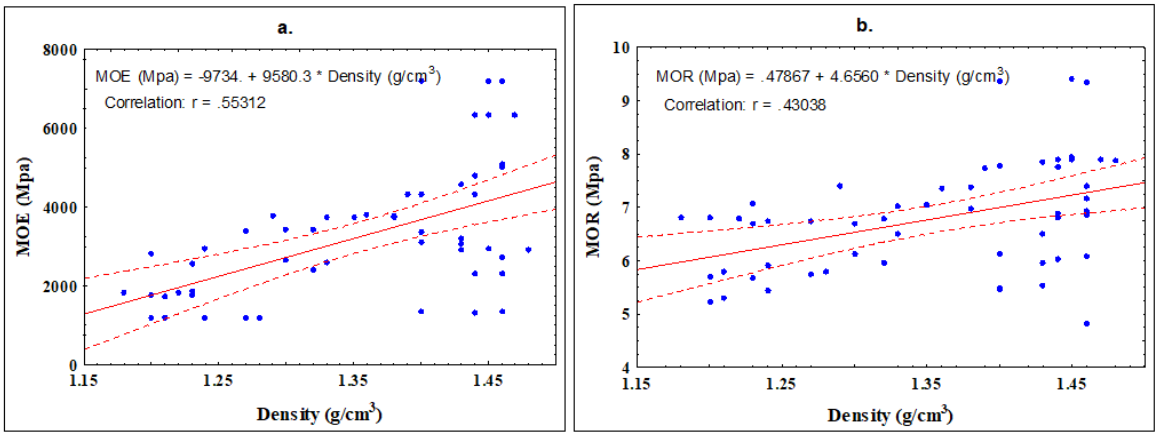


**Fig. 6-11** Relationships between density and (a) MOE and (b) MOR

### 6.5.2 *Effects of MCon on strength properties*

The rate of hydration of slag depends on its composition and the concentration of the alkali activator (Song et al. 2000). Figure 6-12 shows how MCon affected the mechanical properties of all boards. There was a significant difference ($p \leq 0.05$) between the alkali concentration with 6M having the higher mean MOE and MOR Figure 6-12 (a & b). The MOE and MOR increased by about 46% and 16% respectively, when the MCon was increased to 6M. Bilim et al. (2013) also reported an increase in the compressive strength of alkali activated slag with an increase in NaOH concentration. Sufficient dissolution of the anions of slag by the cations in the alkaline activator improved the microstructural

development of the product, leading to enhanced mechanical properties. However, there was a reduction in the MOE and MOR when MCon was increased to 8M. This is attributed to the excessive alkali ions, which mineralized the wood particles, leading to a reduction in the stress-bearing capacity of the particles in the matrix. Efflorescence was noticed on the boards, and the SEM image in Figure 6-13 shows formation of bicarbonate indicating excessive alkali ions. Provis and Van Deventer (2014) posited that efflorescence is not always harmful to the structural integrity of the products, but in this case, it is evident that the excess alkali ions compromised the microstructure of the composites.

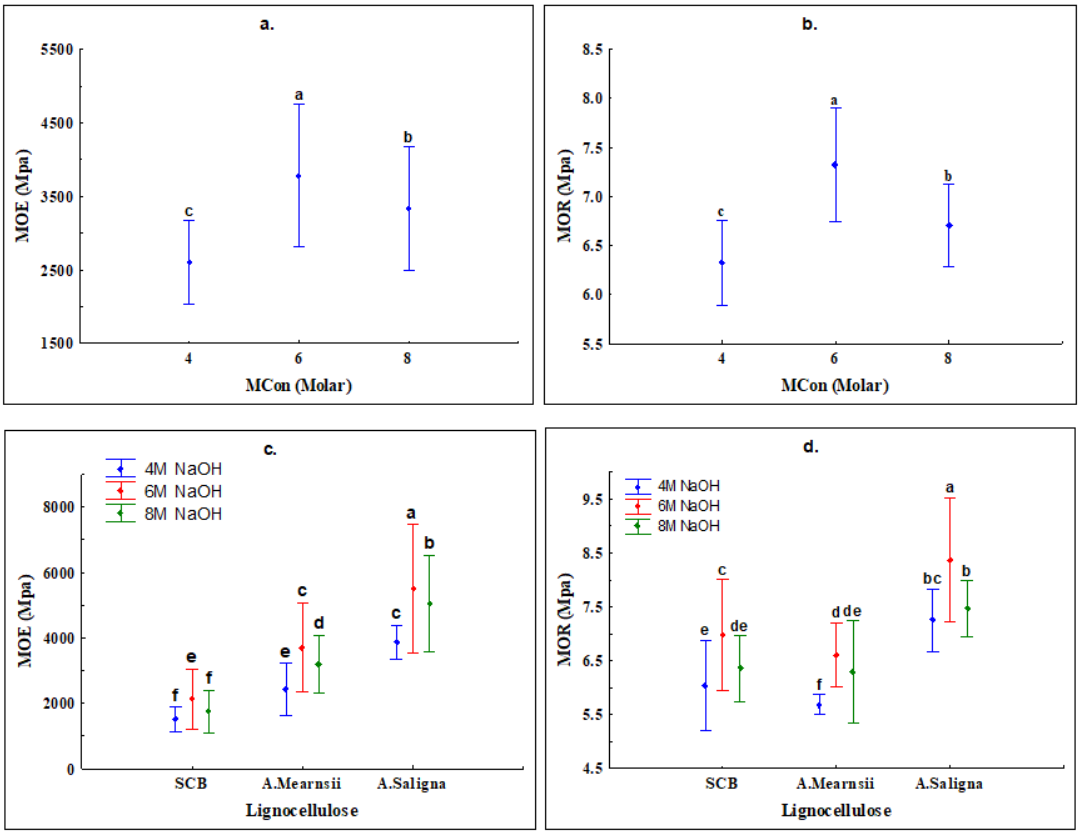


*(vertical lines denote standard deviations, series with same letters are not significantly different)*

**Fig. 6-12** The effects of (a) MCon on MOE (b) MCon on MOR (c) MCon and LM on MOE and (d) MCon and LM on MOR

Figure 6-12 (c & d) indicates that the trend was consistent for the MOE and MOR of each LM. Boards produced with 4M NaOH had the least MOE and MOR, but there was no significant difference in the MOE of SCB boards made with 4M and 8M NaOH. The MOR of SCB and AS boards also exhibited no significant difference between 4M and 8M. Although 6M had a higher mean MOR, there was no significant difference between 6M and 8M for AM boards. The variation is due to difference in their chemical composition.

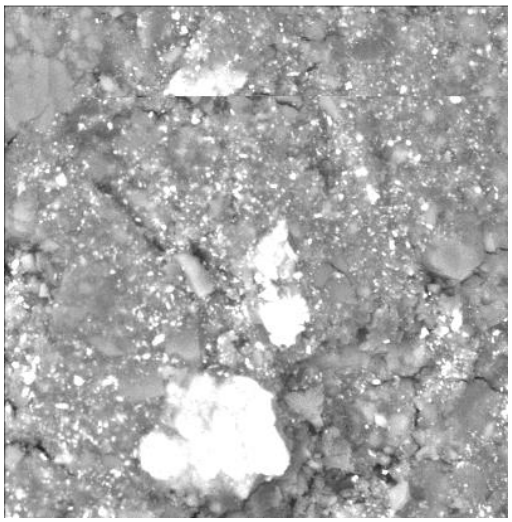

**Fig. 6-13** Formation of bicarbonate in SCB board due to excessive alkali ions

### 6.5.3 *Effects of curing temperature on strength properties*

Curing technique has a significant influence on the strength development of activated slag materials. Figure 6-14 shows that there is significant difference between the curing temperature for both MOE and MOR of all boards. Boards cured at 40°C had higher mean MOE and MOR. The MOE and MOR increased by about 45% and 14% respectively when the temperature was increased to 40°C. Bilim *et al.* (2013) studied alkali activated slag mortars subjected to different curing conditions and reported that heat curing considerably accelerated the early strength development and reduced the high shrinkage of AAS mortar. However, the strength decreased at later age due to dry curing at 50% RH after heat treatment. The SCB and acacia boards were wrapped with aluminium foil prior to curing and left to cool down to room temperature in the oven. This prevented rapid water removal and excessive drying shrinkage, which has been reported to be the main cause of crack development and expansion. Apart from the MOR of AM boards, the mechanical properties of the boards improved at 40°C. AM boards cured at 25°C had a slightly higher mean MOR than those cured at 40°C but the difference was not significant ($p > 0.05$). AS boards cured at 25°C had higher MOE than SCB boards cured at 40°C and not significantly different from AM boards cured at 40°C.

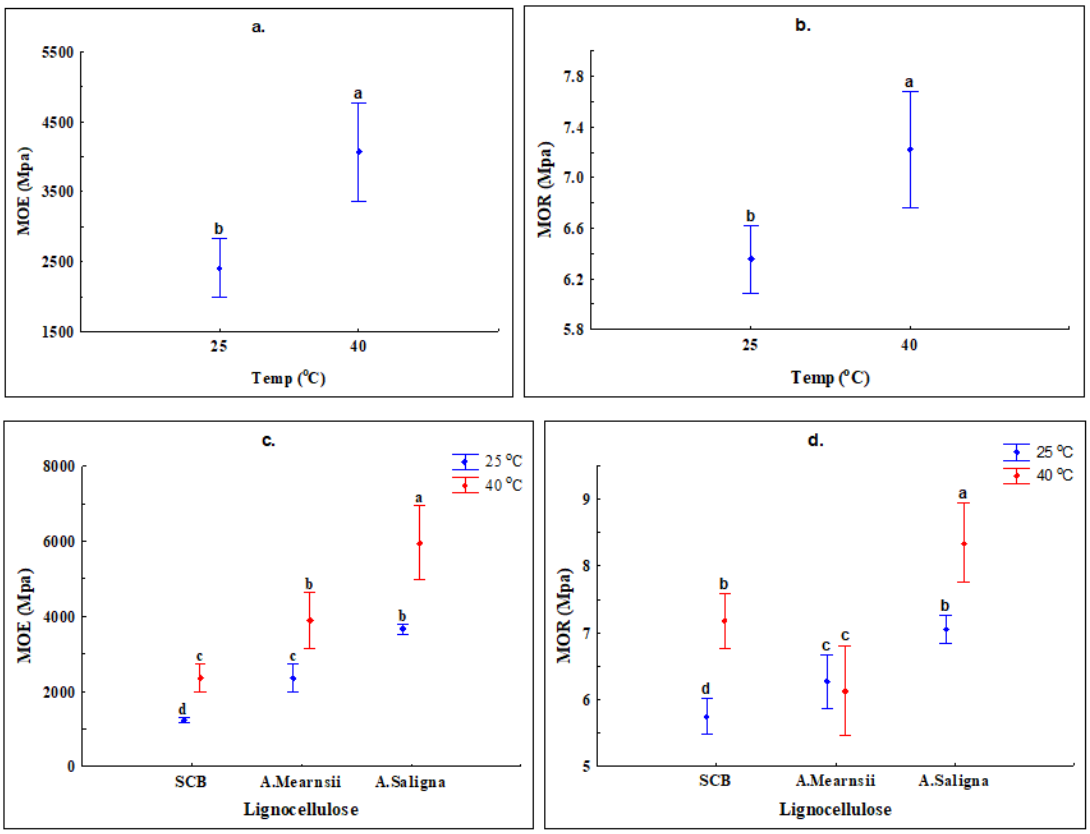


*(vertical lines denote standard deviations, series with same letters are not significantly different)*

**Fig. 6-14** Effects of curing temp on (a) MOE (b) MOR (c) curing temp and LM on MOE (d) curing temp and LM on MOR

### 6.5.4 *Effects of interaction between MCon and curing temperature on the strength properties*

Figure 6-15 shows the influence of the interactions between MCon and the curing temperature on the MOE. Figure 6-15 (a) shows that boards cured at 40°C had higher mean MOE than those cured at 25°C at all levels of MCon. Statistical analyses also revealed that there is significant difference ($p \leq 0.05$) in the MOE between the curing temperature at each MCon level. Boards made with 6M and cured at 40°C had the highest MOE. However, there is no significant difference between 6M and 8M for boards cured at 25 °C ($p > 0.05$). Figure 6-15(b) shows the influence of MCon and curing temperature on each LM. For SCB and AS bords there were no significant difference between 4M, 6M and 8M for boards cured at 25°C. AM boards produced with 4M and cured at 25°C had the lowest mean MOE and was significantly different from those made with 6M and 8M MCon. Curing at 40°C exhibited similar trend for each LM. The highest mean MOE was recorded for each LM produced with 6M MCon.

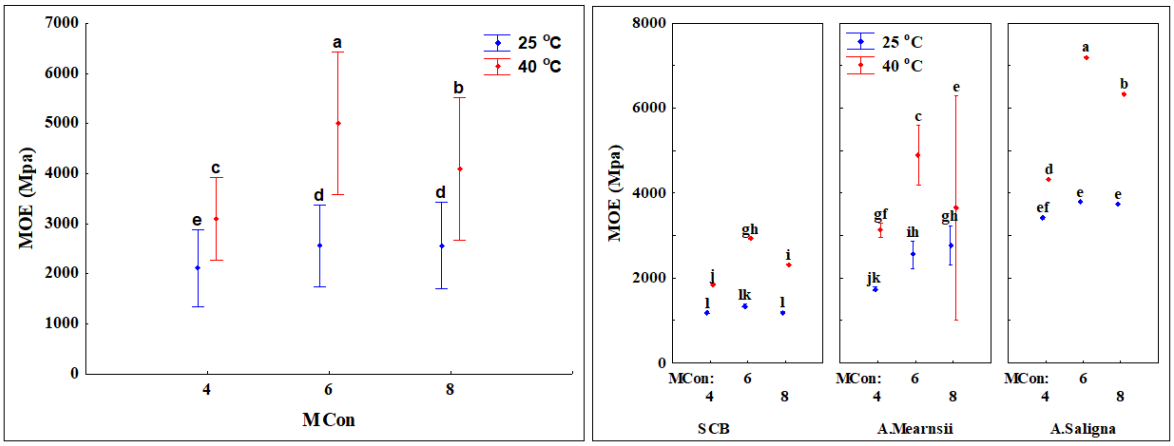


*(vertical lines denote standard deviations, series with same letters are not significantly different)*

**Fig. 6-15** Effects of MCon and Temp on MOE (a) all boards (b) each LM

The influence of the interaction between MCon and curing temperature on MOR is shown in Figure 6-16. Figure 6-16 (a) shows that the mean MOR increased as the curing temperature at each MCon level. However, statistics revealed that the curing temperature had no significant effects on the mean MOR at 8M MCon. It was also observed that the mean MOR of boards made with 4M and cured at 40°C is not significantly different from those produced with 8M.

Figure 6-16 (b) shows that the interactions between MCon and curing temperature affected the MOR of the boards for each LM differently. The mean MOR of SCB and AS boards increased as the curing temperature increased at each level of MCon. For AM boards there was no significant difference in mean MOR at 4M MCon and increasing the curing temperature significantly caused reduction in the mean MOR at 8M MCon.

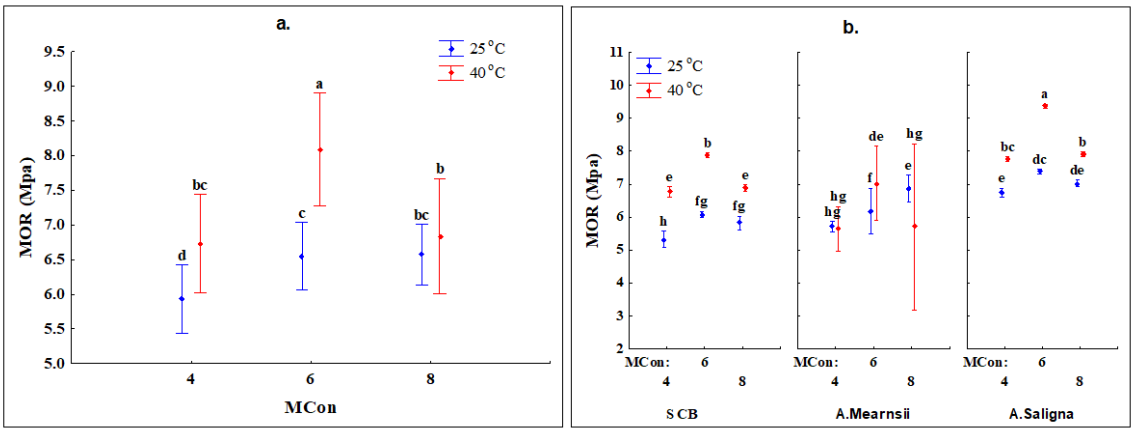


*(vertical lines denote standard deviations, series with same letters are not significantly different)*

**Fig. 6-16** Effects of MCon and curing temperature on MOR (a) all boards (b) each LM

## 6.6 Characterization of products

### 6.6.1 *FTIR analysis*

The IR spectra of the LM has been discussed in Chapter 4. Figure 6-17 shows the IR spectra of the boards. The peak found around 1737 $cm^{-1}$ and 2916 $cm^{-1}$ in the spectra of the LM disappeared in the boards. The peak at 1737 $cm^{-1}$ assigned to the carbonyl (C = O) stretching of acetyl groups of hemicellulose disappeared in the boards for all LM. Likewise, peak around 2916 $cm^{-1}$ attributed to the symmetric vibration of C – H and aliphatic axial decomposition in $CH_2$ and $CH_3$ groups from cellulose, lignin and hemicellulose was not found in the boards of all LM. The peaks in the band 1235 – 1254 $cm^{-1}$, which was attributed to the C – O stretch of the acetyl group of lignin also disappeared. The peaks 1603 $cm^{-1}$ and 1633 $cm^{-1}$ assigned to the C – Ph vibration and C = C bonds of lignin aromatic structure were present only in SCB. These peaks convoluted and shifted to 1636 $cm^{-1}$ in the SCB boards. $CH_2$ symmetric bending of cellulose also shifted from 1422 $cm^{-1}$ to around 1411 $cm^{-1}$ and its intensity decreased in the panels. The shift in this peak and absence of other peaks in the panel indicates partial degradation of lower molecular components of the LM in the alkaline matrix. Similar observations were reported for FA/MK based geopolymer products discussed in Chapter 5. This confirms the assumption that the degraded components of the LM could have interfered with the geopolymer reactions, and thus affect the properties of the composite products. The two prominent bands corresponding to the stretching vibrations of Al – O and Si – O in the precursor material (873 $cm^{-1}$ and 680 $cm^{-1}$) shifted towards the lower wavenumbers. This indicates partial replacement of silica species by alumina as a result of geopolymerization reactions (Criado et al., 2005; Davidovits, 2008).

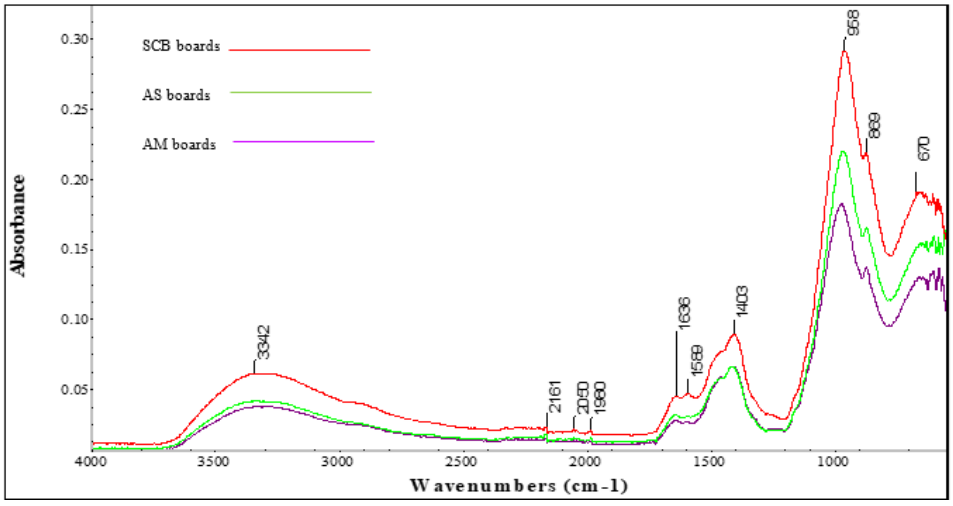


**Fig. 6-17** IR Spectra of slag-based geopolymer bonded boards

### 6.6.2 *TGA*

TGA operated under nitrogen gas was employed to study the thermal stability of the lignocellulosic materials (LM) and the geopolymer bonded composite products. The behaviour of the LM has been discussed in Chapter 4. Figure 6-18 shows the derivative thermographs (DTG) and weight loss of the boards. The DTG peak below 200 °C is attributed to loss of evaporable water. The main degradation peaks in the LM shifted to 276.36 °C, 266.19 °C and 276.48 °C for AS, SCB and AM boards, respectively. These peaks were about 20 °C lower than the main degradation peaks in FA/MK geopolymer bonded boards. The peaks fall within the lower end of cellulose degradation range of 275°C – 500°C (Machado et al. 2018). Similar to the FA/MK boards, the peak-shoulders found in the DTG of LM, which were attributed to the degradation of hemicellulose convoluting with cellulose and lignin component were absent in the DTG of the boards. These corroborate the FTIR results that lower molecular cellulose, lignin and hemicellulose components degraded in the alkaline matrix. Other broad peaks between 350 °C – 475 °C were noticeable in the boards. This could be attributed to the overlap of degradation of crystalline components of LM and change of phases in the microstructure of the matrix at high temperature. These peaks appeared about 100 °C later in FA/MK geopolymer boards. According to Pereira Ferraz et al. (2016), certain impurities, such as inorganic salts could cause degradation of cellulose at lower temperatures. The disparity may be due to the difference in the components of the precursor materials and the geopolymerization products. A peak around 550 °C was present in SCB boards and another peak was building up shortly before the end of the thermal test. This could be attributed to the onset of thermal decomposition of the microstructure of the matrix. The rate of degradation of AM and AS boards were constant at this stage and no peak seemed to be building up. The SCB boards contained higher volume per unit area due to its low bulk density. This could be responsible for the observed early decomposition of the microstructure. However, the products are thermally stable as the residues are all above 75%, a little more than what remained after thermal analysis of FA/MK-based boards.

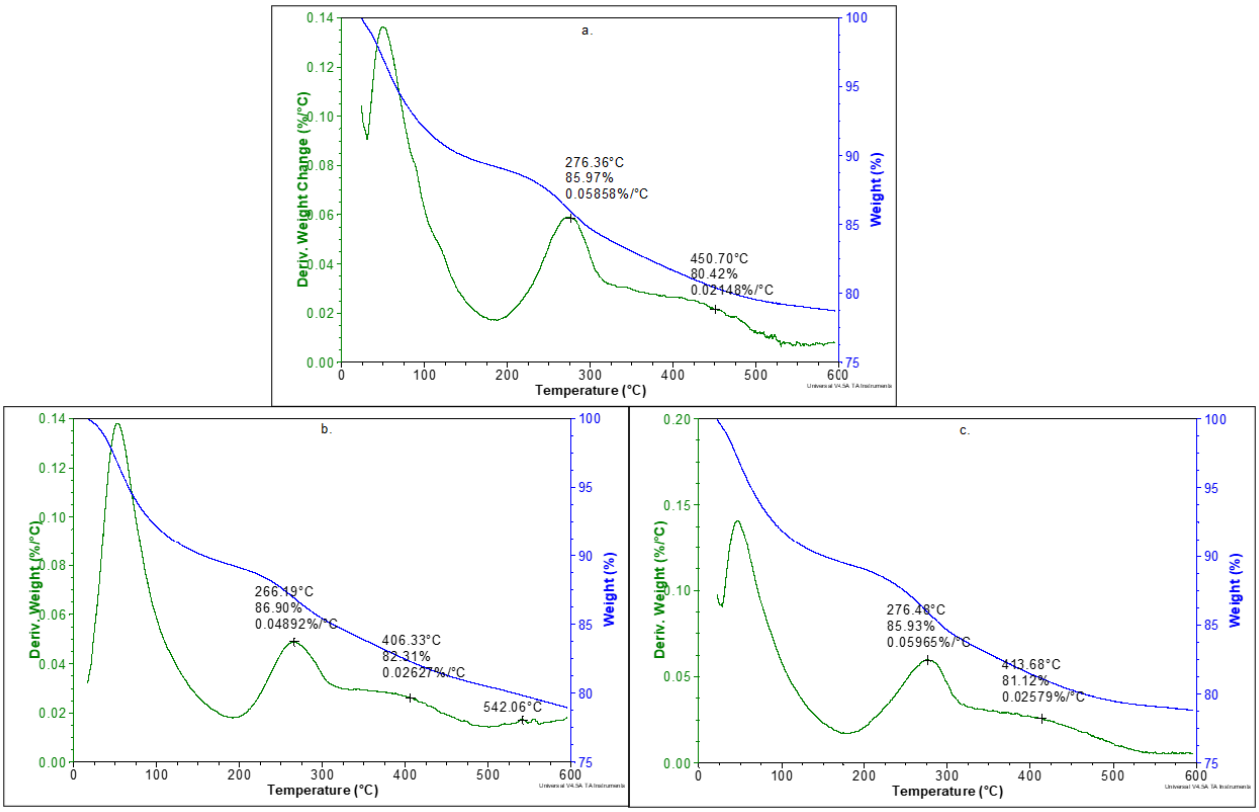


**Fig. 6-18** Derivative and weight loss thermographs of (a) AS boards (b) SCB boards and (c) AM boards

### 6.6.3 *SEM*

SEM was employed to study the morphology and internal structure of the boards under different production conditions. Figure 6-19 shows the micrograph of boards produced with 6M NaOH. The images indicate the formation of amorphous phases with a dense-gel-like matrix. The boards have uniform structures of condensed products believed to be calcium alumino-silicate hydrate (C – A – S – H) surrounded with micro crystals of calcium silicate hydrate (C – S – H ). There are also numerous unreacted slag particles within the dense matrix. The unreacted particles could serve as fillers and improve the board properties. Boards cured at 40°C had a more compact structure with fewer cracks than those cured at 25°C. This was due to the increased reactivity and dissolution of $Ca^{2+}$, $Al^{3+}$ and $Si^{2+}$species at elevated temperature. These results support the physical and strength properties mentioned previously.

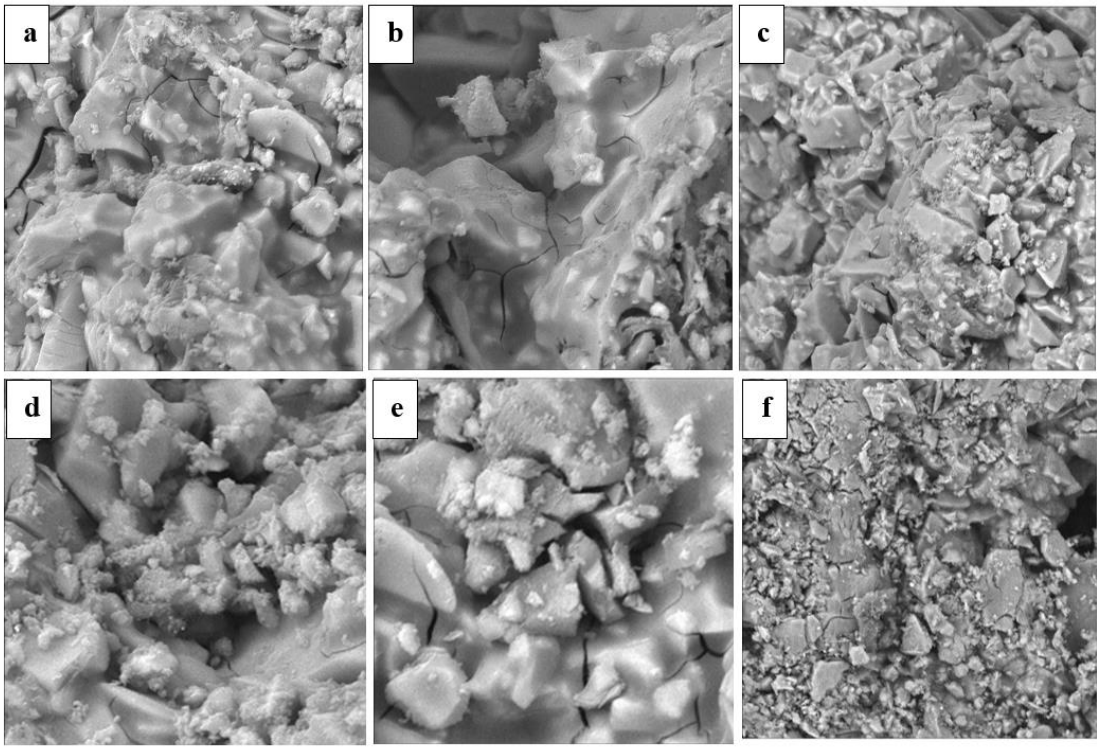


**Fig. 6-19** SEM images of boards made with 6M NaOH and cured at 40°C: (a) AS (b) AM (c) SCB. Cured at 25°C: (d) AS (e) AM (f) SCB

## 6.7 Conclusion

This chapter has demonstrated the feasibility of producing high-density slag-based geopolymer panels using South African alien invasive species and SCB. The proposed product could be used in outside conditions for applications, such as exterior walls, flooring and siding. The major findings in this chapter are summarized as follows:

1 Curing pattern and molar concentration of activator have significant effects on the properties of the slag-based geopolymer boards. And addition of lignocellulosic material improved the flexural properties of the products.

2 Curing at 40°C influenced the reaction kinetics, enhanced microstructural properties, and produced dense geopolymeric matrix, which resulted in improved physical and mechanical properties. Boards cured at 25°C had better strength than phosphate bonded wood composites reported in the literature.

3 Increasing the molar concentration of activator beyond 6M caused formation of bicarbonate and deteriorated the internal structure of AM and SCB boards due to excess

alkali ions. 8M NaOH slightly increased the strength properties of AS boards but the effect was not significantly different than 6M NaOH.

4 FTIR and TGA results confirmed the degradation of lower molecular lignocellulose components in the alkaline matrix. Degraded products could lower geopolymeric reactions, but FTIR confirmed that geopolymerization took place. SEM images also revealed the formation of geopolymer and hydration products, which indicated that the degraded components did not prevent geopolymer setting.

5 All the boards met the sorption requirements for particleboards according to the British and the Indian Standards. The strength properties of the boards were not adequate compared to the British Standard, but they compared well with the requirements for low density particleboards grade 1&2, bonded with synthetic resin (ANSI 1999). Hence, the boards may be suitable for non-load bearing applications in outdoor conditions.

6 The boards are thermally stable, as the residue retained at the end of thermal analysis is almost 80%.

# Chapter 7

# The influence of chemical pre-treatment of fibres on the properties and durability of unary and binary precursor based geopolymer bonded wood and fibre composites

## 7.1 Production conditions

In the unary and binary precursor-based geopolymer bonded composites detailed in chapters 5 and 6, the bending strength of AM and SCB boards were not sufficient according to the BS EN standard. Board characterization also revealed a concern about the durability of products for the intended use due to degradation of the fibres indicated by SEM and the FTIR analyses. In order to improve the properties of the inadequate boards and enhance the durability of the final products, the lignocellulosic materials were subjected to pre-treatment prior to board formation. The pre-treatment techniques and characterization of the lignocellulosic materials before and after treatments are detailed in chapter 4. The conditions for the best performing boards for each lignocellulosic material in chapters 5 and 6 were adopted for this study. The conditions are presented in Tables 7-1 and 7-2.

**Table 7-1** Production conditions for FA/MK-based boards

| Lignocellulose | MCon (Molar) | Curing Condition | PA ratio |
|---|---|---|---|
| *A.mearnsii* | 12 | 100°C, 6h | 2:1 |
| SCB | 10 | 60°C, 24h | 2:1 |

**Table 7-2** Production parameters for slag-based boards

| Lignocellulose | MCon (Molar) | Curing Condition | PA ratio |
|---|---|---|---|
| *A.mearnsii* | 6 | 40°C, 24h | 2:1 |
| SCB | 6 | 40°C, 24h | 2:1 |

## 7.2 FA/MK-based boards: Influence of treatment on properties

A one-way ANOVA using Statistca V.13 was employed to analyse the data for the board properties. The analysis presented in Table 7-3 shows that the treatment methods had a significant effect on the sorption properties of all the boards ($p < 0.05$), while the effect on the flexural strength varied for each lignocellulosic material in FA/MK-based geopolymer. The treatments had a significant effect

on the MOE of AM board, but the effects on density and MOR were not significant. In the slag-based AM boards, the treatment had significant effects on all properties apart from the density. The pattern is a bit different for the SCB boards in both systems. Apart from the density of slag-based SCB boards, the treatment had significant effect on all measured properties. Although the effect of treatment was not significant on the MOR of FA/MK-based AM boards, Duncan's multi-stage range test in Table 7-4 indicated that differences existed between the means. Duncan's multi-stage test shown in Table 7-5 revealed that no difference existed between the mean values of properties not significantly affected by the treatment in slag-based boards.

**Table 7-3** *p – values* for the effects of treatment on board properties

| | FA/MK-based boards | | Slag-based boards | |
|---|---|---|---|---|
| Property | *A. mearnsii* | SCB | *A. mearnsii* | SCB |
| Density | 0.977048 | 0.020677* | 0.811232 | 0.540663 |
| MOE | 0.003051* | 0.023891* | 0.000003* | 0.000046* |
| MOR | 0.054587 | 0.000763* | 0.000105* | 0.000009* |
| WA | 0.000213* | 0.000210* | 0.016649* | 0.000035* |
| TS | 0.000095* | 0.000001* | 0.001814* | 0.000000* |

** - significant values ($p < 0.05$)*

**Table 7-4** Mean comparison using Duncan's multi-stage range test for FA/MK - based boards

| | Properties | | | | |
|---|---|---|---|---|---|
| Boards | Density (g/cm$^3$) | MOE (MPa) | MOR (MPa) | WA (%) | TS (%) |
| **SCB:** | | | | | |
| HWA | 1.284$^{a}$ | 4911.029$^{ab}$ | 8.058$^{a}$ | 20.959$^{b}$ | 0.215$^{b}$ |
| ALK | 1.308$^{a}$ | 4425.215$^{c}$ | 6.979$^{a}$ | 20.370$^{b}$ | 0.151$^{c}$ |
| ACE | 1.238$^{ab}$ | 5081.385$^{a}$ | 7.439$^{a}$ | 19.513$^{b}$ | 0.138$^{c}$ |
| UNT | 1.179$^{b}$ | 4521.944$^{cb}$ | 4.679$^{b}$ | 26.096$^{a}$ | 0.490$^{a}$ |
| **AM:** | | | | | |
| HWA | 1.291$^{a}$ | 6691.328$^{b}$ | 8.495$^{a}$ | 21.403$^{b}$ | 0.217$^{b}$ |
| ALK | 1.294$^{a}$ | 7385.601$^{a}$ | 8.488$^{a}$ | 19.554c | 0.227$^{b}$ |
| ACE | 1.290$^{a}$ | 7472.389$^{a}$ | 7.613$^{ab}$ | 19.403$^{c}$ | 0.148$^{b}$ |
| UNT | 1.278$^{a}$ | 6408.201$^{b}$ | 7.180$^{b}$ | 22.369$^{a}$ | 0.508$^{a}$ |

$^{a,b,c}$ Means in the same column for each board type with similar letters are not significantly different ($p<0.05$) (SCB = Sugarcane bagasse; AM = *A.mearnsii*; HWA= Hot water treated; ALK = Alkalized; ACE = Acetylated; UNT = Untreated)

**Table 7-5** Mean comparison using Duncan's multi-stage range test for slag-based boards

| | Properties | | | | |
|---|---|---|---|---|---|
| Boards | Density (g/cm$^3$) | MOE (MPa) | MOR (MPa) | WA (%) | TS (%) |
| **SCB:** | | | | | |
| HWA | 1.433$^{a}$ | 4399.314$^{a}$ | 8.116$^{a}$ | 14.730$^{b}$ | 0.252$^{b}$ |
| ALK | 1.461$^{a}$ | 3780.044$^{b}$ | 8.336$^{a}$ | 14.593$^{b}$ | 0.235$^{b}$ |
| ACE | 1.451$^{a}$ | 4369.195$^{a}$ | 8.009$^{a}$ | 13.796$^{b}$ | 0.228$^{b}$ |
| UNT | 1.437$^{a}$ | 2962.100$^{c}$ | 4.731$^{b}$ | 19.730$^{a}$ | 0.767$^{a}$ |
| **AM:** | | | | | |
| HWA | 1.446$^{a}$ | 5143.923$^{bc}$ | 7.254$^{b}$ | 13.278$^{ab}$ | 0.145$^{a}$ |
| ALK | 1.460$^{a}$ | 5341.540$^{b}$ | 8.708$^{a}$ | 11.767$^{b}$ | 0.151$^{a}$ |
| ACE | 1.459$^{a}$ | 7111.606$^{a}$ | 8.685$^{a}$ | 12.075$^{b}$ | 0.079$^{b}$ |
| UNT | 1.453$^{a}$ | 4891.048$^{c}$ | 7.026$^{b}$ | 14.527$^{a}$ | 0.147$^{a}$ |

$^{a,b,c}$ Means in the same column for each board type with similar letters are not significantly different ($p<0.05$) (SCB = Sugarcane bagasse; AM = *A.mearnsii*; HWA= Hot water treated; ALK = Alkalized; ACE = Acetylated; UNT = Untreated)

### 7.2.1 *Density*

Figure 7-1 shows the trend in the density of FA/MK-based boards for each treatment method. It was observed that there was no significant difference in the mean density of treated boards for each lignocellulose, but treatment improved the density of the boards. Alkalization had the highest mean density for SCB and AM boards. Apart from hot water extracted AM boards, treatments also increased the density of slag-based boards shown in Figure 7-2. The increase in the density could be due to the improvement in surface properties of the fibres, which influenced better adhesion between fibre and the geopolymer matrix. A similar observation was reported for $Mg^{2+}$ and $Ca^{2+}$ based phosphate bonded panels (Amiandamhen et al. 2018). This observation is expected to impact the strength properties of the boards since there is a positive correlation between density and flexural strength.

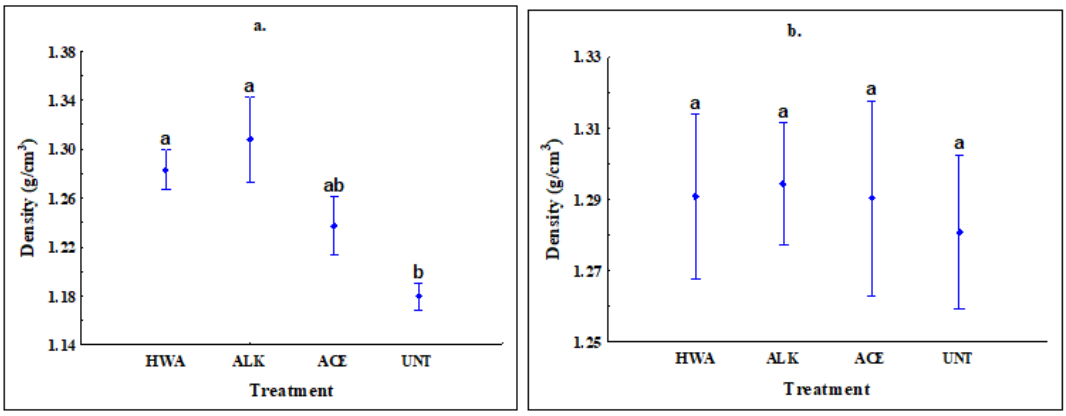


**Fig. 7-1** Trends in density of treated FA/MK- based (a) SCB (b) AM

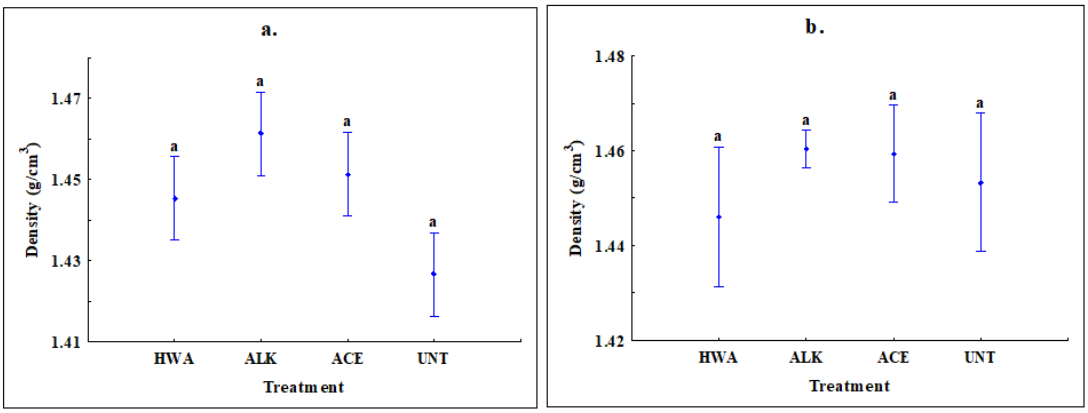


**Fig. 7-2** Trends in density of treated slag- based (a) SCB (b) AM

### 7.2.2 *Flexural properties*

The trends in the MOE of SCB boards are shown in Figure 7-3. Apart from alkalized SCB boards, the MOE of the boards increased after treatment. Acetylated boards had the highest mean MOE in the FA/MK system, while hot water extracted had the highest mean in the slag system. However, there was no significant difference between acetylation and hot water extraction in both systems. The trend is a bit different for AM boards. In Figure 7-4, treated AM boards had higher mean MOE than the untreated in the two precursor systems. Acetylated boards had the highest mean MOE in both systems, but there was no difference between alkalized and acetylated FA/MK-based AM boards.

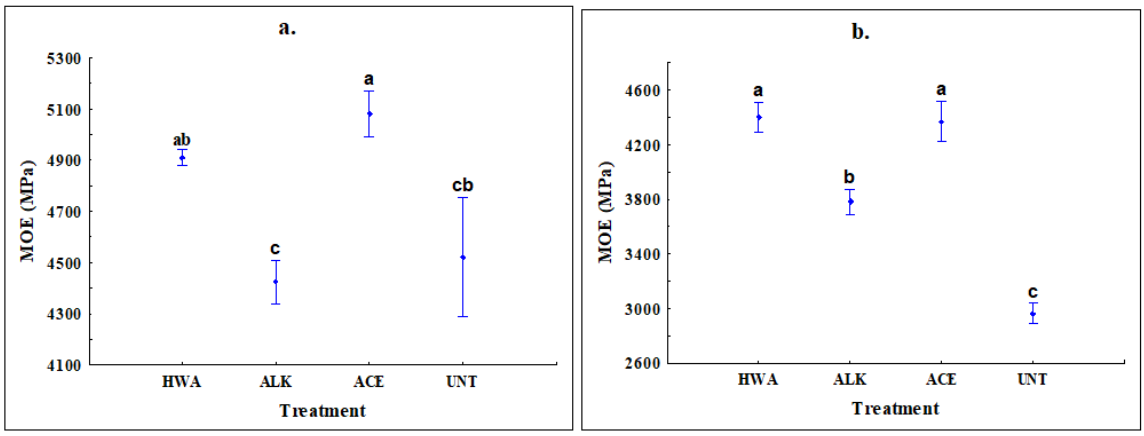


**Fig. 7-3** Trends in MOE of SCB boards (a) FA/MK – based (b) slag-based

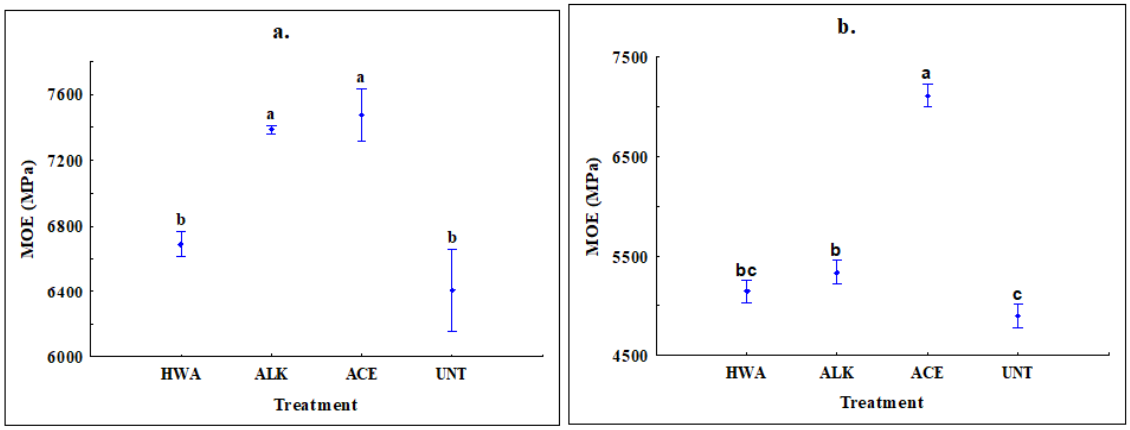


**Fig. 7-4** Trends in MOE of AM boards (a) FA/MK-based (b) slag-based

Figure 7-5 shows the effects of treatments on the MOR of SCB boards. There was no significant difference in the mean MOR for the treated samples for both precursor systems, but alkalized boards had the lowest mean MOR in the FA/MK-based boards. It is important to note that alkalized board also had the lowest MOE for both precursor systems. The decline in the strength properties observed in alkalized SCB board compared to others could be due to the extensive removal of lignin (Chapter 4), which affected the rigidity and lowered the load-bearing capacity of the fibre under stress transfer. Alkalization also resulted in a decrease in MOR of $Mg^{2+}$-based phosphate bonded panels (Amiandamhen et al. 2018). In Figure 7-6, similar to SCB boards, treatment increased the MOR of AM boards in both precursor systems. There was no difference in the mean MOR for treated boards in FA/MK-based system, but the impact was higher in hot water extracted and alkalized boards. In the slag-based system, there was no difference in the mean MOR between alkalized and acetylated boards. However, both are significantly different from untreated and hot water extracted boards.

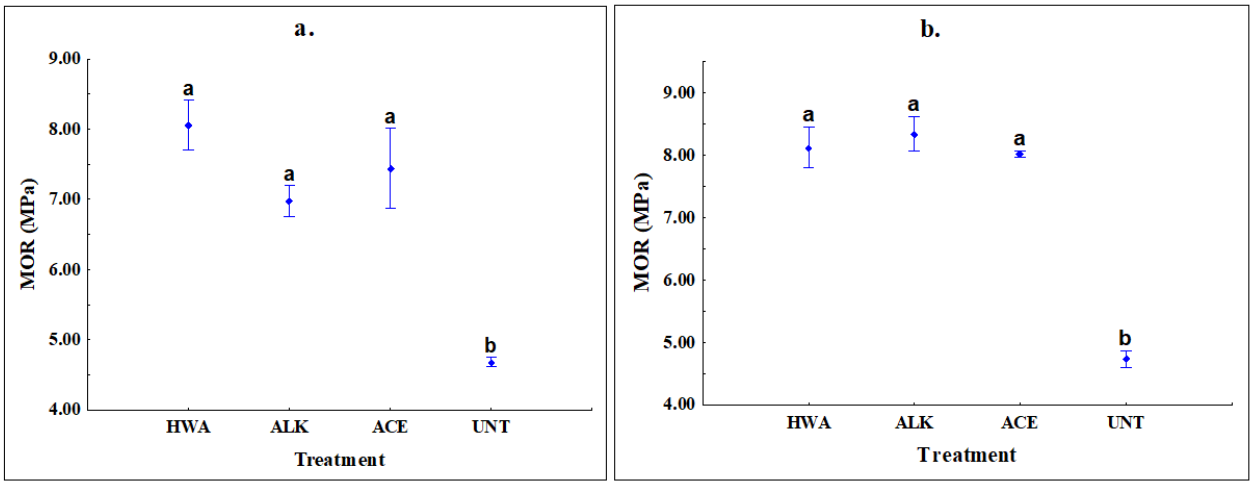


**Fig. 7-5** Trends in MOR of SCB boards (a) FA/MK – based (b) slag-based

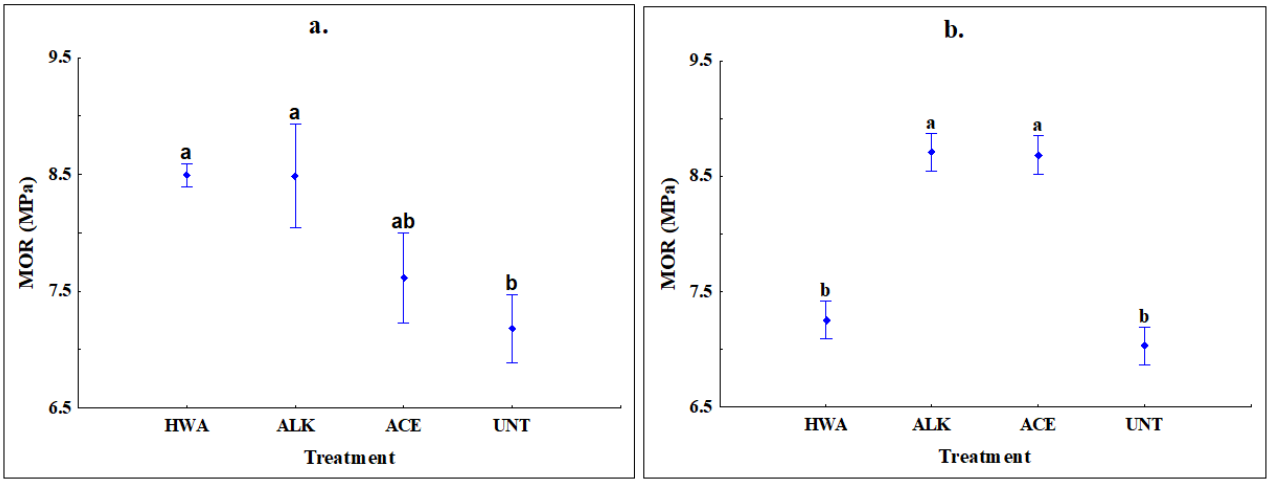


**Fig. 7-6** Trends in MOR of AM boards (a) FA/MK – based (b) slag-based

### 7.2.3 *Sorption properties and dimensional stability*

The WA and TS of SCB boards are shown in Figures 7-7 and 7-8. A decreasing trend in WA and TS can be observed in both slag and FA/MK-based boards. Although there was no difference in the mean WA of treated SCB boards in both systems, acetylated boards had the lowest WA and TS. In Figures 7-9 and 7-10 a similar decreasing trend can be observed in WA and TS of AM boards, apart from the TS of slag-based boards, which exhibited an irregular pattern. Acetylated AM boards had the lowest WA in FA/MK system, while alkalized boards had the lowest WA in slag based. Similar to SCB boards, there was no significant difference in WA between acetylated and alkalized AM boards for both slag and FA/MK matrices. Acetylated AM boards also had the lowest TS in both systems. This

proved that the hydrophilic OH-groups on the fibre surfaces were sufficiently substituted with acetyl groups thereby reducing the available sorption sites. It was also observed that FA/MK-based SCB and AM boards had higher WA than slag-based, but they were more dimensionally stable. This could be attributed to a difference in the production variables. FA/MK-boards were cured at a slightly higher temperature than slag-based. Higher curing temperature increases the rate of geopolymerization, and during polycondensation stage rapid discharge of water (bye-product) leads to formation of numerous micropores and microcracks. It is evident that the higher WA in FA/MK-based boards was due to migration of moisture into the micropores, but not moisture uptake by the incorporated fibres.

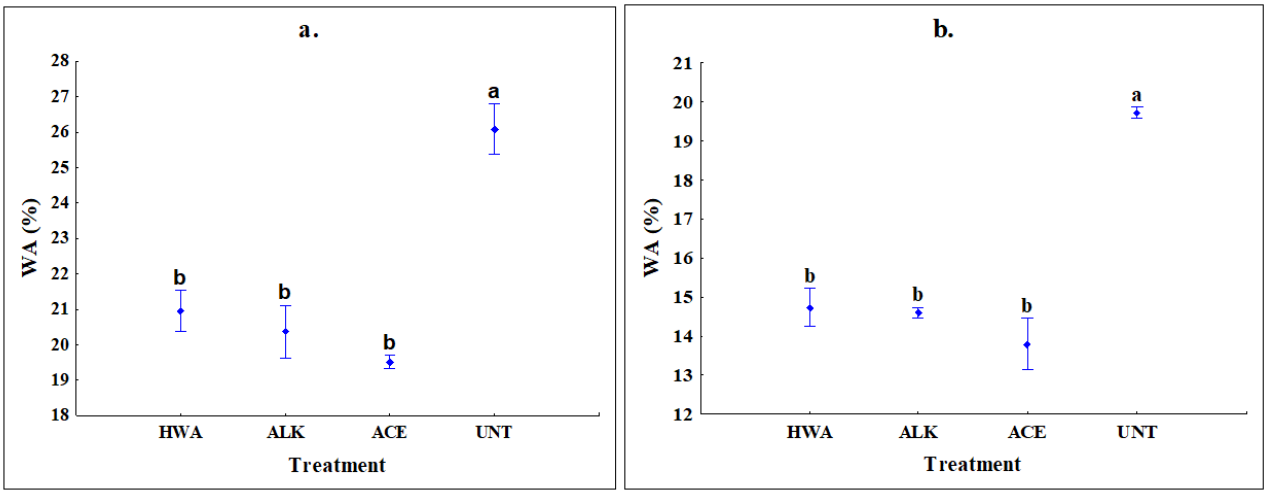


**Fig. 7-7** Trends in WA of SCB boards (a) FA/MK – based (b) slag-based

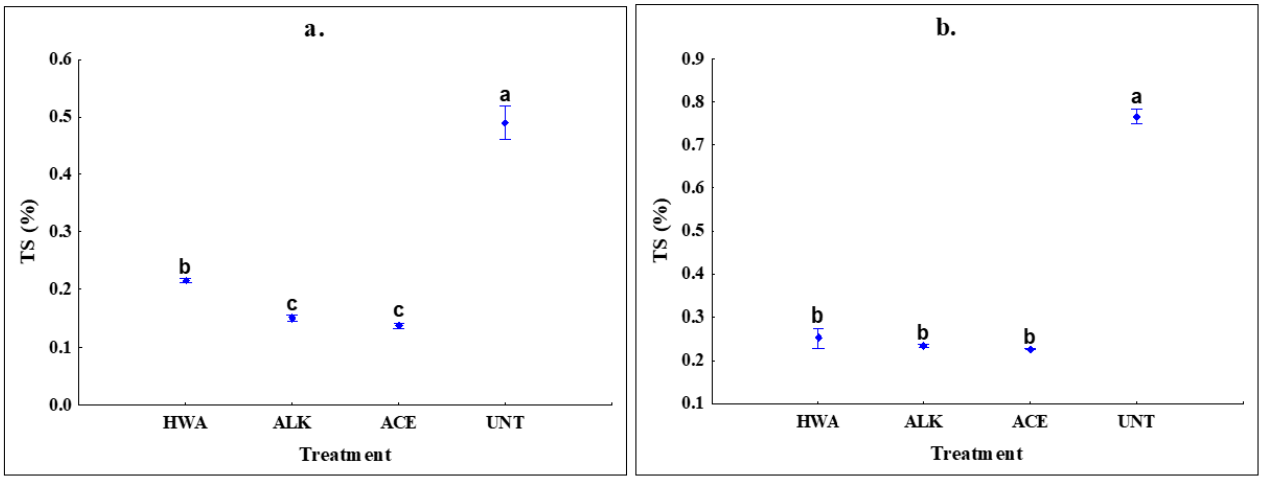


**Fig. 7-8** Trends in TS of SCB boards (a) FA/MK – based (b) slag-based

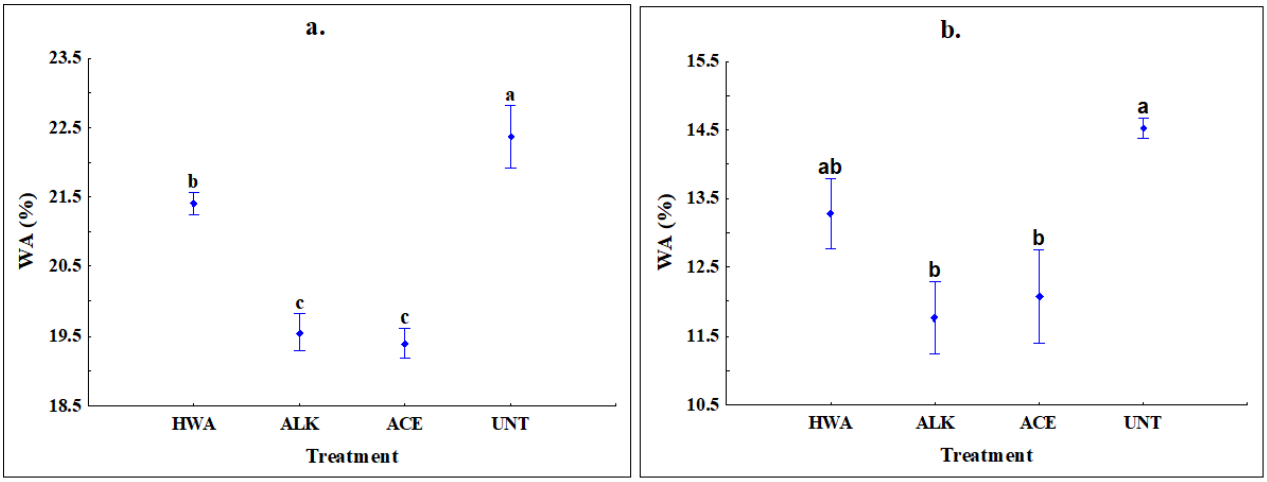


**Fig. 7-9** Trends in WA of AM boards (a) FA/MK – based (b) slag-based

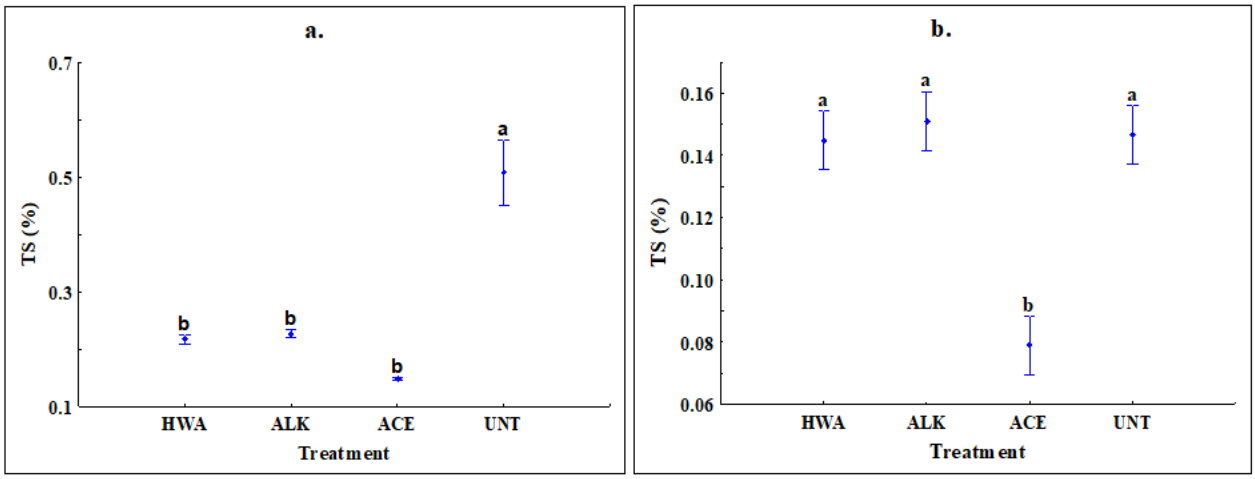


**Fig. 7-10** Trends in TS of AM boards (a) FA/MK – based (b) slag-based

## 7.3 Board characterization

### 7.3.1 *FTIR analysis*

Figure 7-11 shows the IR-spectra of treated and untreated SCB boards in slag and FA/MK-based matrices. The spectra of acetylated boards in FA/MK and slag-based matrices are presented in Figure 7-11(a). Untreated and acetylated SCB boards in FA/MK matrix had similar peaks, but the intensities of the peaks are higher in acetylated boards. Same can be observed for slag-based boards, the peaks in acetylated SCB boards had higher intensities than untreated slag-based SCB boards. The trend is similar in hot water extracted and alkalized boards in both systems as shown in Figure 7-11 (b – c). Peaks corresponding to the lower molecular components were absent in the treated and untreated

boards, but the higher intensities of peaks in the treated samples indicated lower degree of degradation of the lignocellulosic material in the matrices. This resulted in increased geopolymerization kinetics, as evident in the shift of Si – O and Al – O bands towards lower wavenumbers and formation of new peaks within the range of 500 – 800 $cm^{-1}$ (Barbosa et al. 2000; Fauzi et al. 2016). In the untreated slag-based SCB boards, the peaks were 958 $cm^{-1}$, 869 $cm^{-1}$ and 670 $cm^{-1}$. In the acetylated slag-based SCB boards only 670 $cm^{-1}$ shifted to lower wavenumber (653 $cm^{-1}$), 869 $cm^{-1}$ remain unchanged while peak 958 $cm^{-1}$ shifted to 966 $cm^{-1}$. The peaks changed to 970 $cm^{-1}$, 872 $cm^{-1}$ and 653 $cm^{-1}$ in hot water extracted board, with the formation of new peak around 602 $cm^{-1}$. In the alkalized SCB boards the peaks were found at 973 $cm^{-1}$, 867 $cm^{-1}$ and 657 $cm^{-1}$, with new peaks found around 688 $cm^{-1}$ and 622 $cm^{-1}$. The geopolymeric products peaks are found around 985 $cm^{-1}$ and 722 $cm^{-1}$ in the untreated FA/MK-based SCB boards. After acetylation, the peaks changed to 978 $cm^{-1}$ and 726 $cm^{-1}$, with the formation of new peak at 603 $cm^{-1}$. The peaks changed to 981 $cm^{-1}$ and 724 $cm^{-1}$ in alkalized boards, and new peaks formed at 603 $cm^{-1}$, 595 $cm^{-1}$, 587 $cm^{-1}$ and 568 $cm^{-1}$. In the hot water extracted samples the peaks shifted to 985 $cm^{-1}$ and 720 $cm^{-1}$. New peaks were found at 692 $cm^{-1}$, 622 $cm^{-1}$, 599 $cm^{-1}$, 587 $cm^{-1}$ and 566 $cm^{-1}$.

In the IR-spectra shown in Figure 7-12, similar trends were observed for the AM boards in both precursor systems. The peaks in treated samples had higher intensities, peaks corresponding to the presence of geopolymeric products shifted towards lower wavenumbers, and the formation of more geopolymeric products was indicated by presence of new peaks in the range of 500 – 800 $cm^{-1}$. Although, the alkalized AM boards in FA/MK matrix behaved differently. The geopolymer peaks also shifted towards the lower wavenumbers, but the intensities are higher in untreated samples. However, the formation of new peaks could explain the improvement in the properties of the boards observed after alkalization.

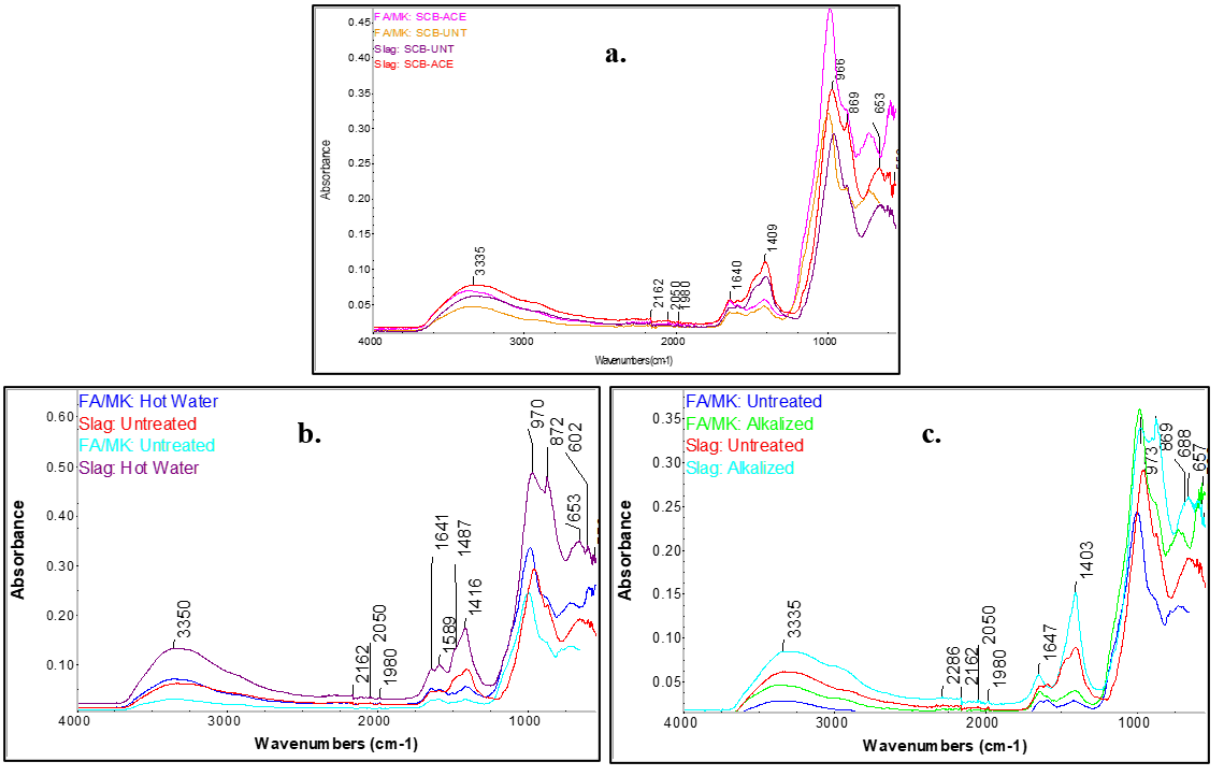


**Fig. 7-11** IR-spectra of treated and untreated SCB boards in slag and FA/MK-based system (a) acetylated (b) hot water extracted (c) alkalized

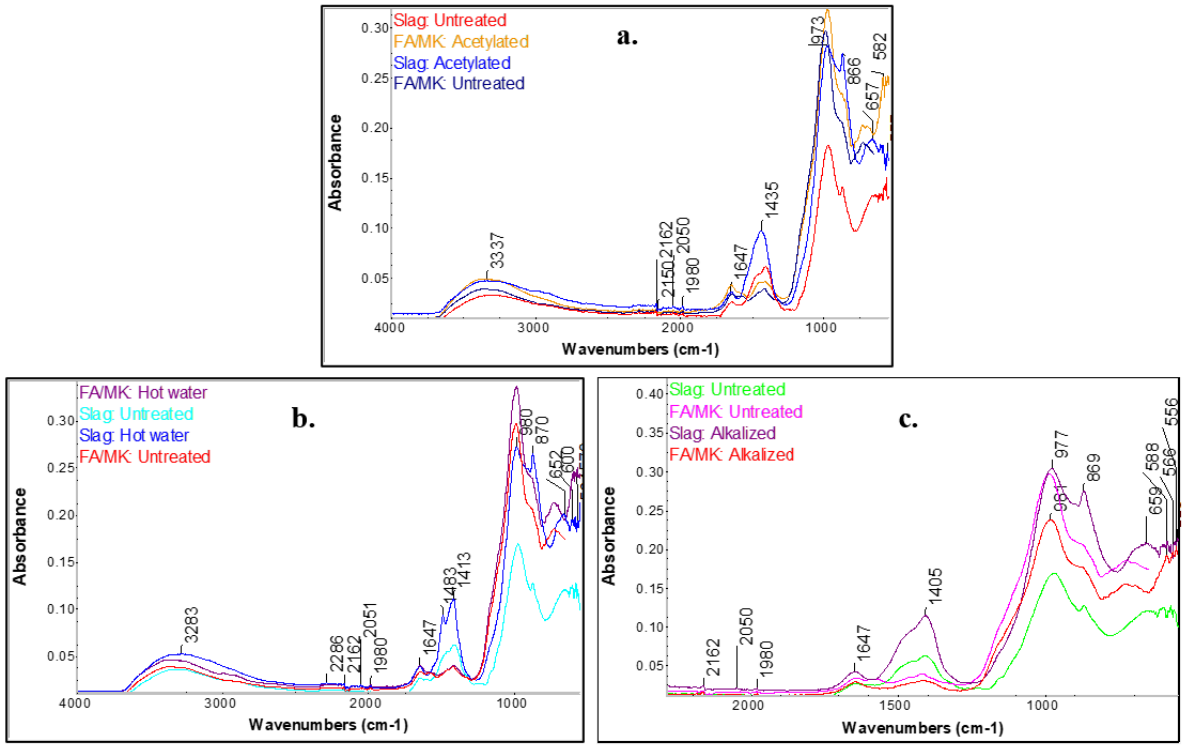


**Fig. 7-12** IR-spectra of treated and untreated AM boards in slag and FA/MK-based system (a) acetylated (b) hot water extracted (c) alkalized

### 7.3.2 *SEM*

The SEM images of untreated slag and FA/MK-based AM and SCB boards are shown in Figure 7-13, while Figure 7-14 shows the SEM images of the treated boards. The untreated FA/MK-based boards appeared to be less compact than the treated boards. The image of untreated AM board indicated evidence of fibre mineralization with the accumulation of the matrix components in the fibre bundles. These were not observed in the treated AM and SCB boards. Instead, the micrographs indicated formation of densely populated gel-like amorphous phases.

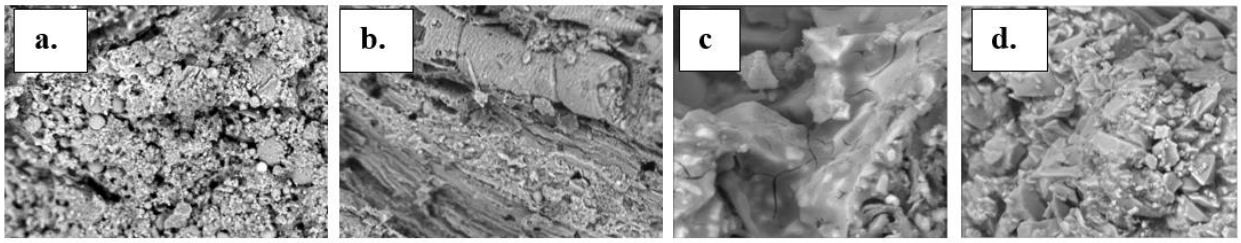


**Fig. 7-13** SEM images of boards (a) SCB in FA/MK matrix (b) AM in FA/MK matrix (c) AM in slag matrix (d) SCB in slag matrix

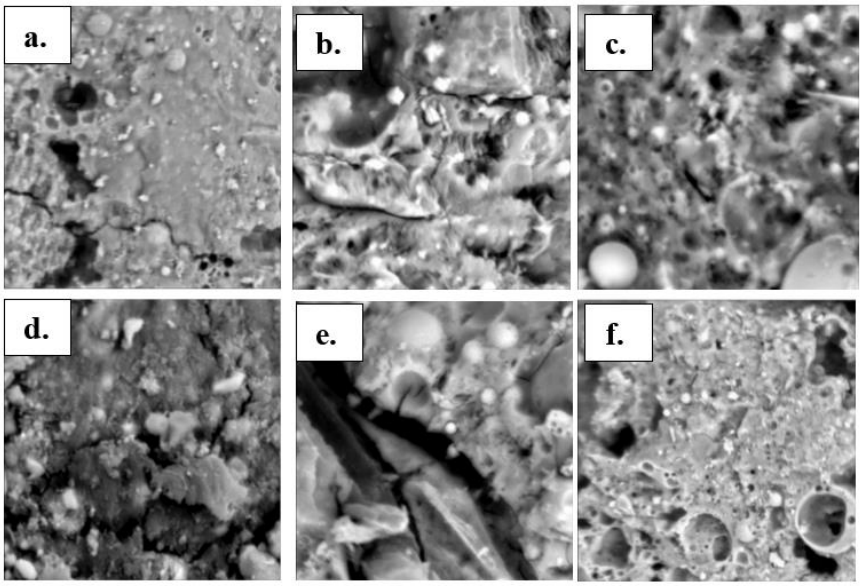


**Fig. 7-14** SEM images of treated FA/MK-based boards (a) hot water extracted AM (b) alkalized AM (c) acetylated AM (d) hot water extracted SCB (e) alkalized SCB (f) acetylated SCB

Since a Class F fly ash was used (low calcium content), the uniform compacted structures are believed to be sodium alumino-silicate hydrates (NASH) surrounded with partly reacted and unreacted fly ash

particles. The compacted microstructure and fewer unreacted particles support the FTIR results, which indicated increased geopolymerization reactions and formation of more geopolymeric products after fibre treatment. Images of the slag-based SCB and AM boards are shown in Figure 7-15. The images of alkalized boards depict better interface conditions than other treated boards for both AM and SCB. Formation of more hydrated grains, calcium silicate hydrates (CSH) and gel-like structure believed to be calcium alumino silicate hydrates (CASH) are more evident. There were no signs of efflorescence and the microstructure seem to contain less unreacted particles. The unreacted and partially reacted particles in the acetylated and hot water extracted boards appeared to be strongly fused in the compact microstructure. These are particles from the crystalline phase of the precursor material. They do not take part in geopolymer reaction, but they can contribute to improve product properties by serving as inactive fillers (Alomayri 2017).

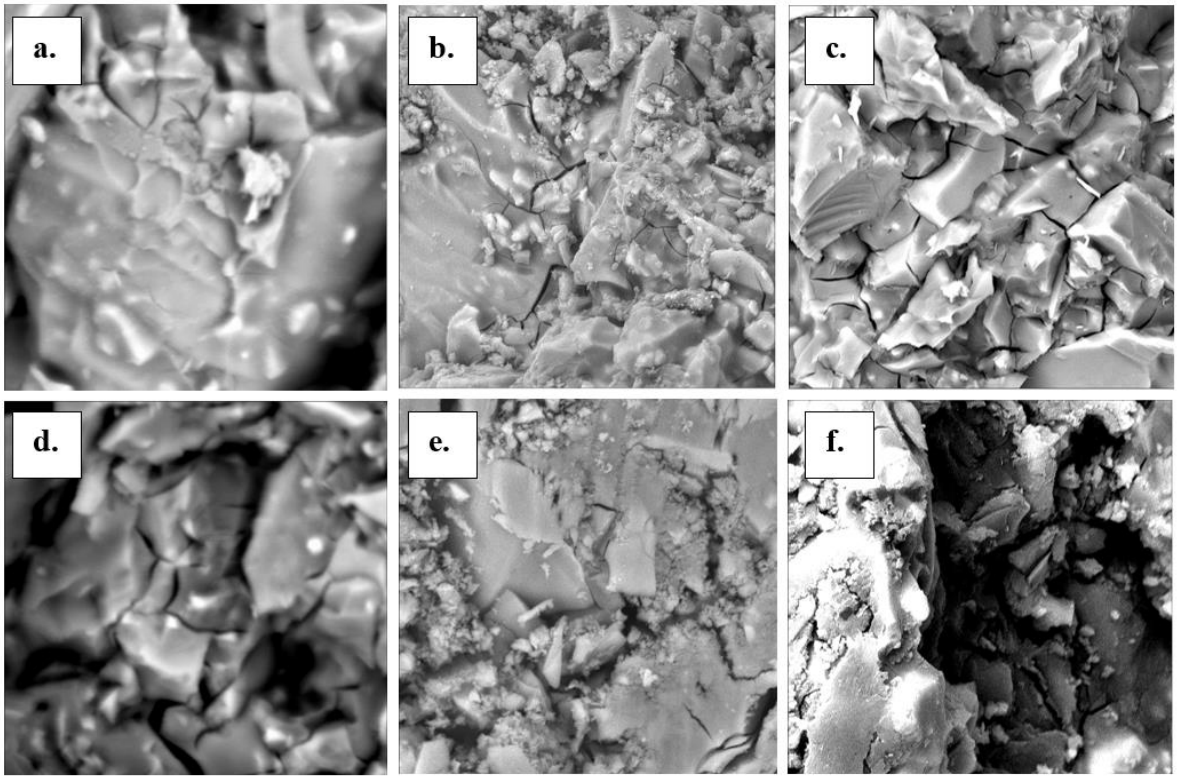


**Fig. 7-15** SEM images of treated slag-based boards (a) hot water extracted SCB (b) alkalized SCB (c) acetylated SCB (d) hot water extracted AM (e) alkalized AM (f) acetylated AM

## 7.4 Conclusions

This chapter investigated the effects of fibre modification on the properties of slag and FA/MK based geopolymer bonded wood composites, and degradation of fibres in the alkaline matrices. Based on the observations and findings discussed the following conclusions can be drawn:

1 The treatment improved the surface properties of the fibres, which resulted in better adhesion between fibre and geopolymer matrices.
2 Treatments had significant effects on all measured properties of SCB boards, apart from the density of slag-based boards. The influence of treatment varied for AM boards in both matrices. In slag-based matrix only the density was not significantly affected, while in FA/MK based matrix the effect was not significant for both density and MOE.
3 Acetylation had the best overall effect on the mechanical properties of FA/MK based boards, while hot water extraction had the best influence of the slag-based boards.
4 FTIR revealed increased concentration and formation of more geopolymer products in the treated boards. SEM images indicated densely populated pore structures with formation of new products, which confirmed the FTIR results. The images revealed no signs of fibre mineralization and efflorescence, which suggest that the fibres would be relatively stable in the matrices.
5 Despite the improvement, the bending strengths of bagasse and *A. mearnsii* boards were not adequate compared to the British Standard, but they compared well with the requirements for low density particleboards (Grade 1-L-1) bonded with synthetic resin (ANSI 1999).

# Chapter 8 : Conclusions and suggestions for future studies

## 8.1 Introduction

In the wake of finding alternative sustainable and environmentally friendly products to the conventional construction materials, geopolymer offers a wide range of potentials as a low carbon footprint product. The application of geopolymer in the construction industry is gaining unprecedented attention in recent years, but its utilization in wood composite manufacturing has not been extensively studied. Previous investigations have indicated possibility of incorporating lignocellulosic materials in geopolymer matrix, but there are knowledge gaps due to insufficient information on key parameters, which could derail its intended use. This study investigated the potentials of using unary and binary precursor based geopolymer bonded wood products in outdoor applications. In the first phase, the precursor materials were characterized to determine their compositions and inherent properties to ensure that they meet the requirements outlined in the literature for optimum geopolymer strength development. The physical and chemical composition of the lignocellulosic materials were also determined using the NREL procedures. This was particularly important so that we could understand how the variation in lignocellulose components affect the properties of the final products. In the second phase, the geopolymer matrix was formulated using a combination of fly ash and metakaolin at a weight ratio of 3:1, while in the third phase, the geopolymer was formulated using a 100% ground granulated blast slag. The precursors were activated using a combination of sodium silicate and sodium hydroxide at a weight ratio of 2.5:1. Lignocellulosic materials from the clearing of South African invasive wood species and sugarcane bagasse were incorporated into the geopolymer matrices to produce high-density boards targeted for use as replacements for cement-bonded particleboards in outdoor conditions. The properties of the geopolymer boards were tested to technical specifications of the British standard EN 634-2 (2007). The sections that follow discuss the conclusions from this study and recommend research areas for future works.

## 8.2 Conclusions

This study has demonstrated the possibility of producing high-density geopolymer boards reinforced with untreated wood particles from South African invasive species and sugarcane bagasse for outdoor applications. We have provided information about the development, the interactions of the lignocellulose components with the matrix, fibre modification to the improve properties and durability of the fibres in the geopolymer matrices. At every stage, the properties of the products were tested to technical specifications for cement bonded particleboards since a standard is not yet

available for geopolymer bonded products. To the best of our knowledge, this is the first time an attempt has been made to provide technical information about the performance of geopolymer boards against a standard specification for a targeted application.

Based on the objectives of this study, the following conclusions can be drawn:

- In the first phase, the precursor materials were characterized using XRF, PDF and XRD techniques. XRF revealed that the materials had less than 5% LOI, 10% $Fe_2O_3$ and about 40 – 50% $SiO_2$. PSD analysis indicated that about 80 – 90% of their particle sizes are less than or equal to 45µm. XRD confirmed that the materials are composed of a high quantity of amorphous content with few crystalline phases identified as quartz and mullite in fly ash and metakaolin. A few more crystalline phases, such as calcite, corundum, alumina, magnesite and magnoan in very low concentration were detected in the slag. The precursors meet the requirements for optimum bonding properties of geopolymer. NREL analysis revealed that the acacia species had similar compositions, which were different from sugarcane bagasse. The difference in composition affected the interaction with the geopolymer matrices.
- In the second phase, sugarcane bagasse and woody residues from the clearing of AIWS including long-leaved wattle (*A. longifolia*) and black wattle (*A. mearnsii*) were incorporated into a binary precursor geopolymer formulated using fly ash and metakaolin. The variables considered were curing pattern, precursor to activator ratio and the alkali concentration of the activator. Statistical analyses indicated that all variables had significant effects on the measured properties. For the acacia species, the same production conditions produced the best properties in their respective boards. These are the precursor-activator ratio of 2:1, curing temperature of 100°C for 6h and alkali concentration of 12M. For bagasse boards the conditions for the best-performed boards are curing temperature of 60°C (24h), alkali concentration of 10M and precursor-activator ratio of 2:1. All the boards had comparable sorption properties but only *A. longifolia* boards met the technical specifications (EN 634-2 2007) for cement bonded particleboards in outdoor applications.
- In the unary precursor system, Black wattle (*A. mearnsii*), Port Jackson (*A. saligna*) and sugarcane bagasse particles were encapsulated in geopolymer formulated using 100% slag material. Based on slag characterization and results from the first phase, the production conditions were a bit different. The precursor-activator ratio was fixed at 2:1, maximum curing temperature and alkali concentration set to 40°C and 8M, respectively. Similar to the binary precursor formulated geopolymer, all the production variables had significant effects

on the measured properties. The properties were tested against technical specification for cement bonded particleboards, only *A. saligna* boards produced with 6M alkali concentration and cured at 40°C met the technical requirements.

- Generally, increasing the curing temperature and alkali concentration increases the geopolymerization reaction, which enhances microstructural development. In the binary precursor system, this was observed in the acacia boards, but the internal structure of the SCB boards deteriorated at higher curing temperature leading to low strength development. Increasing the alkali concentration beyond 10M also affected the pore structure of *A.* mearnsii boards due to fibre mineralization revealed by SEM analysis. In the slag-based geopolymer, increasing the alkali concentration beyond 6M had a negative effect on the microstructure of the boards.
- FTIR and TGA analyses revealed partial degradation of lower molecular lignocellulose components in both formulated geopolymer matrices. The degraded components do not prevent geopolymer setting and FTIR analysis confirmed that geopolymerization had occurred. Concerns about durability of fibre in the matrices could derail the application of the products for the intended use. In order to enhance the durability and improve the final properties, the lignocellulosic materials were subjected to alkalization, hot water extraction and acetylation before being incorporated into geopolymer matrices. Bagasse and *A. mearnsii* were incorporated into geopolymer matrices developed using the best conditions from the previous investigations. The effects of the treatments on the fibre properties were evaluated using HPLC, SEM and FTIR, while the final composite products were characterized using SEM/EDS and FTIR.
- FTIR revealed that some peaks, which were attributed to the lower molecular components still disappeared in the spectra of treated boards, but the SEM images indicated densely populated pore structures with no sign of fibre mineralization. It was evident that the treatment improved the geopolymerization kinetics in both binders as FTIR and SEM analyses indicated high concentration and formation of new geopolymer products, which suggests that the fibres would be relatively stable in the matrices. The increased reaction kinetics influenced the physical and mechanical properties of the boards significantly. Despite the improvement, the bending strengths of bagasse and *A. mearnsii* boards were not adequate compared to the British Standard, but they compared well with the requirements for low density particleboards grade 1&2, bonded with synthetic resin (ANSI 1999). Hence, *A. longifolia* and *A. saligna*

boards can substitute cement bonded particleboards in outdoor conditions, while bagasse and *A. mearnsii* boards may be suitable for non-load bearing applications in outdoor conditions.

- All the boards are thermally stable, as the residue retained at the end of thermal analysis was above 70% for FA/MK boards and about 80% for slag formulated geopolymer boards.

## 8.3 Suggestion for future studies

The development of geopolymer bonded wood composite is still relatively new, such that concerns about its durability and production cost could affect its choice as a potential substitute to other inorganic bonded wood composites. This study has shown that geopolymer wood composites could substitute cement bonded particleboard in outside conditions, but further research is required to investigate the durability of the products over time.

The performance of geopolymer product is dependent on a number of factors related to the inherent properties of its precursor material and factors associated with the activating solutions. The bulk of materials for geopolymer wood composites could be derived from industrial residues and side streams, which could be assigned zero to low economic value. However, the production conditions, such as high temperature curing could affect its economic viability. Therefore, further study in the formulation of geopolymer binder, which requires low energy profile in production should be investigated.

## References

Abidoye, Luqman K., and R. A. Bello. 2010. “Restoration of Compressive Strength of Recycled Gypsum Board Powder .” *The Pacific Journal of Science and Technology* 11(2):42–50.

Ajayi, B., and S. O. .. Badejo. 2005. “Effects of Board Density on Bending Strenght and Internal Bond of Cement-Bonded Flakeboards.” *Journal of Tropical Forest Science* 17(2):228–34.

Albitar, M., M. M. Ali, P. Visintin, and M. Drechsler. 2015. “Effect of Granulated Lead Smelter Slag on Strength of Fly Ash-Based Geopolymer Concrete.” *Construction and Building Materials* 83:128–135.

Alomayri, T., F. U. A. Shaikh, and I. M. Low. 2013. “Characterisation of Cotton Fibre-Reinforced Geopolymer Composites.” *Composites Part B: Engineering* 50:1–6. doi: 10.1016/j.compositesb.2013.01.013.

Alomayri, Thamer. 2017. “Effect of Glass Microfibre Addition on the Mechanical Performances of Fly Ash-Based Geopolymer Composites.” *Journal of Asian Ceramic Societies* 5(3):334–40. doi: 10.1016/j.jascer.2017.06.007.

Alomayri, Thamer, Les Vickers, Faiz U. A. Shaikh, and It Meng Low. 2014. “Mechanical Properties of Cotton Fabric Reinforced Geopolymer Composites at 200-1000 C.” *Journal of Advanced Ceramics* 3(3):184–93. doi: 10.1007/s40145-014-0109-x.

Alonso, S., and A. Palomo. 2001. “Alkaline Activation of Metakaolin and Calcium Hydroxide Mixtures: Influence of Temperature, Activator Concentration and Solids Ratio.” *Materials Letters* 47(1–2):55–62. doi: 10.1016/S0167-577X(00)00212-3.

Amiandamhen, S. O., M. Meincken, and L. Tyhoda. 2016. “Magnesium Based Phosphate Cement Binder for Composite Panels: A Response Surface Methodology for Optimisation of Processing Variables in Boards Produced from Agricultural and Wood Processing Industrial Residues.” *Industrial Crops and Products* 94:746–54. doi: 10.1016/j.indcrop.2016.09.051.

Amiandamhen, S. O., M. Meincken, and L. Tyhoda. 2018. “The Effect of Chemical Treatments of Natural Fibres on the Properties of Phosphate-Bonded Composite Products.” *Wood Science and Technology* 52(3):653–75. doi: 10.1007/s00226-018-0999-9.

Amiandamhen, S. O., · Z Montecuccoli, · M Meincken, · M C Barbu, and · L Tyhoda. 2017. "Phosphate Bonded Wood Composite Products from Invasive Acacia Trees Occurring on the Cape Coastal Plains of South Africa." *European Journal of Wood and Wood Products* 0(0):0. doi: 10.1007/s00107-017-1191-x.

Andini, S., R. Cioffi, F. Colangelo, T. Grieco, F. Montagnaro, and L. Santoro. 2008. "Coal Fly Ash as Raw Material for the Manufacture of Geopolymer-Based Products." *Waste Management.* doi: 10.1016/j.wasman.2007.02.001.

ANSI, A208. .. 1999. *Particleboards*. Gaithersburg.

Araújo, Priscila C., Larissa M. Arruda, Cláudio H. S. Del Menezzi, Divino E. Teixeira, and Mário R. Souza. 2011. "Lignocellulosic Composites from Brazilian Giant Bamboo (Guadua Magna): Part 2: Properties of Cement and Gypsum Bonded Particleboards." *Maderas. Ciencia y Tecnología* 13(3):297–306. doi: 10.4067/S0718-221X2011000300005.

Archibald, S., A. Nickless, N. Govender, R. J. Scholes, and V. Lehsten. 2010. "Climate and the Inter-Annual Variability of Fire in Southern Africa: A Meta-Analysis Using Long-Term Field Data and Satellite-Derived Burnt Area Data." *Global Ecology and Biogeography* 19(6):794–809. doi: 10.1111/j.1466-8238.2010.00568.x.

Arioz, E., Ö. Arioz, and Ö. M. Koçkar. 2013. "The Effect of Curing Conditions on the Properties of Geopolymer Samples." *International Journal of Chemical Engineering and Applications* 4(6):423–26. doi: 10.7763/IJCEA.2013.V4.339.

Aro, Matthew. 2008. "Wood Strand Cement Board." *11th International Inorganic-Bonded Fiber Composites Conference* (Adair):169–79.

ASTM. 2013. *ASTM D1037-13 Standard Test Methods for Evaluating Properties of Wood-Base Fiber and Particle*.

ASTM. 2019. "ASTM C618-19, Standard Specification for Coal Fly Ash and Raw or Calcined Natural Pozzolan for Use in Concrete." *Annual Book of ASTM Standards* (C):5. doi: 10.1520/C0618-19.

Al Bakri Abdullah, Mohd Mustafa, Ahmad Mohd Izzat, M. T. Muhammad Faheem, H. Kamarudin,

I. Khairul Nizar, M. Bnhussain, A. R. Rafiza, Yahya Zarina, and J. Liyana. 2012. “Feasibility of Producing Wood Fibre-Reinforced Geopolymer Composites (WFRGC).” *Advanced Materials Research* 626:918–25. doi: 10.4028/www.scientific.net/AMR.626.918.

Barbosa, Valeria F. F., Kenneth J. D. Mackenzie, and Clelio Thaumaturgo. 2000. “Synthesis and Characterisation of Materials Based on Inorganic Polymers of Alumina and Silica : Sodium Polysialate Polymers.” 2:309–17.

Beaudoin, J. J., and V. S. Ramachandran. 1975. “Strength Development in Magnesium Oxychloride and Other Cements.” *Cement and Concrete Research* 5(6):617–30. doi: 10.1016/0008-8846(75)90062-9.

Bilim, Cahit, Okan Karahan, Cengiz Duran Atiş, and Serhan Ilkentapar. 2013. “Influence of Admixtures on the Properties of Alkali-Activated Slag Mortars Subjected to Different Curing Conditions.” *Materials and Design* 44:540–47. doi: 10.1016/j.matdes.2012.08.049.

Bilinski, H., B. Matkovic, C. Mazuravic, and T. .. Zunic. 1984. “The Formation of Magnesium Oxychloride Phases in the System MgO-MgCl2-H2O and NaOH-MgCl2-H2O.” *Journal of American Ceramic Society* 67(4):266–74.

Bitay, Enikő, Irén Kacsó, Szilamér Péter Pánczél, and Erzsébet Veress. 2019. “Comparative Study of Roman Iron Slags Discovered in the Roman Auxiliary Fort and Settlement of Călugăreni.” *Acta Materialia Transilvanica* 1(2):65–72. doi: 10.2478/amt-2018-0022.

Bledzki, A.K., Gassan, J. and Theis, S. 1998. “Wood-Filled Thermoplastic Composites.” *Mechanics of Composite Materials* 34(13):563–568.

Bledzki, A.K. and Gassan, J. 1999. “Composites Reinforced with Cellulose Based Fibers.” *Progress in Polymer Science* 24:221–274.

Bledzki, A. K., A. A. Mamun, M. Lucka-Gabor, and V. S. Gutowski. 2008. “The Effects of Acetylation on Properties of Flax Fibre and Its Polypropylene Composites.” *Express Polymer Letters* 2(6):413–22. doi: 10.3144/expresspolymlett.2008.50.

Chareerat, T., A. Lee-Anansaksiri, and P. Chindaprasirt. 2006. “Synthesis of High Calcium Fly Ash and Calcined Kaoline Geopolymer Mortar.” P. May 24-25 in *International Conference on*

*Pozzolan, Concrete and Geopolymer*. Khhon Kaen, Thailand.

Chen, Rui. 2014. "Bio Stabilization for Geopolymer Enhancement and Mine Tailings Dust Control." Dissertation. University of Arizona.

Chen, Rui, Saeed Ahmari, and Lianyang Zhang. 2014. "Utilization of Sweet Sorghum Fiber to Reinforce Fly Ash-Based Geopolymer." *Journal of Materials Science* 49(6):2548–58. doi: 10.1007/s10853-013-7950-0.

Chen, W., and H. J. H. Brouwers. 2007. "The Hydration of Slag, Part 1: Reaction Models for Alkali- Activated Slag." *J Mater Sci* 42:428–43.

Chimphango, Anderson. 2020. "The Valorisation of Paper Sludge for Green Composite Material." M.Sc. Dissertation. Stellenbosch University.

Chindaprasirt, P., and W. Chalee. 2014. "Effect of Sodium Hydroxide Concentration on Chloride Penetration and Steel Corrosion of Fly Ash-Based Geopolymer Concrete under Marine Site." *Construction and Building Materials* 63:303–10. doi: 10.1016/j.conbuildmat.2014.04.010.

Chindaprasirt, Prinya, Chai Jaturapitakkul, Wichian Chalee, and Ubolluk Rattanasak. 2009. "Comparative Study on the Characteristics of Fly Ash and Bottom Ash Geopolymers." *Waste Management* 29(2):539–43. doi: 10.1016/j.wasman.2008.06.023.

Christensen, R. M. (Richard M. .., A. Subsidiary, and H. Brace. 1982. *Theory of Viscoelasticity : An Introduction*. Academic Press.

Chuah, S., W. H. Duan, Z. Pan, E. Hunter, A. H. Korayem, X. L. Zhao, F. Collins, and J. G. Sanjayan. 2016. "The Properties of Fly Ash Based Geopolymer Mortars Made with Dune Sand." *Materials and Design* 92:571–78. doi: 10.1016/j.matdes.2015.12.070.

Cioffi, R., L. Maffucci, and L. Santoro. 2003. "Optimization of Geopolymer Synthesis by Calcination and Polycondensation of a Kaolinitic Residue." *Resources, Conservation and Recycling*. doi: 10.1016/S0921-3449(03)00023-5.

Criado, M., A. Palomo, and A. Fernández-Jiménez. 2005. "Alkali Activation of Fly Ashes. Part 1: Effect of Curing Conditions on the Carbonation of the Reaction Products." *Fuel* 84(16):2048–54. doi: 10.1016/j.fuel.2005.03.030.

Cristina, Roberta, Novaes Reis, Fabiana Magalhães, Teixeira Mendes, Clarissa Cruz Perrone, Celso Sant Anna, Wanderley De Souza, Yuri Abud, Elba Pinto, and Viridiana Ferreira-leitão. 2012. "Structural Evaluation of Sugar Cane Bagasse Steam Pretreated in the Presence of CO 2 and SO 2." ??? 5(1):1. doi: 10.1186/1754-6834-5-36.

Cui, Yue, Erman Guleryuz, Waltraud Kriven, Seid Koric, and Ange-Therese. Akono. 2017. "Molecular Dynamics Study on the Mechanical and Fracture Properties of Geopolymer Binders." in *8th Advances in Cement-Based Materials (Cements 2017)*. Atlanta.

Davidovits, J. 1988. "Geopolymers of the First Generation: SILIFACE-Process." in *Geopolymer '88, First European Conference on Soft Mineralurgy*. Compiegne, France.

Davidovits, J. 1994. "High-Alkali Cements for 21st Century Concretes." Pp. 383–97 in *Concrete Technology, Past, Present and Future. Proceedings of V. Mohan Malhotra Symposium*. ACI SP- 144.

Davidovits, J. 2008. *Geopolymer Chemistry and Applications*. 3rd ed. Institute Geopolymere, Saint-Quentin, France.

DEA. 2019. "Working for Water (WfW) Programme | Department of Environmental Affairs." *Department of Environmental Affairs*. Retrieved January 16, 2021 (https://www.environment.gov.za/projectsprogrammes/wfw).

Van Deventer, J. S. J., J. L. Provis, P. Duxson, and G. C. Lukey. 2007. "Reaction Mechanisms in the Geopolymeric Conversion of Inorganic Waste to Useful Products." *Journal of Hazardous Materials* 139(3):506–13. doi: 10.1016/j.jhazmat.2006.02.044.

Dimas, D., I. Giannopoulou, and D. Panias. 2009. "Polymerization in Sodium Silicate Solutions: A Fundamental Process in Geopolymerization Technology." *Journal of Materials Science* 44(14):3719–30. doi: 10.1007/s10853-009-3497-5.

Doan, Hung Tran, Petr Louda, Dora Kroisová, and Oleg Bortnovsky. 2010. "Thermal-Mechanical Behavior of Silica-Based Geopolymer – Carbon Composite." 1–8.

Duan, Ping, Chunjie Yan, Wei Zhou, and Wenjun Luo. 2016. "Fresh Properties, Mechanical Strength and Microstructure of Fly Ash Geopolymer Paste Reinforced with Sawdust."

*Construction and Building Materials* 111:600–610. doi: 10.1016/j.conbuildmat.2016.02.091.

Van Elten, E. J. 2006. "Cement Bonded Particle Board (Cbpb) and Wood Strand Cement Board (Eltoboard)." *Inorganic-Bonded FIber Composites Conference* 10th:1–10.

Van Elten, G. J. 1999. "Innovation in the Production of and Wood-Wool Cement Board." *Inorganic Bonded Wood and Fiber Composite Materials Conference* (May).

EN 634-2, BS. 2007. *Cement-Bonded Particleboards –Specifications- Part 2: Requirements for OPC Bonded Particleboards for Use in Dry, Humid and External Conditions.*

Evan, P. D. 2000. "Wood – Cement Composites in the Asia – Pacific Region." *ACIAR Proceeding* (December).

Fauzi, Amir, Muhd Fadhil, Ahmad B. Malkawi, Mohd Mustafa, and Al Bakri. 2016. "Study of Fly Ash Characterization as a Cementitious Material." *Procedia Engineering* 148:487–93. doi: 10.1016/j.proeng.2016.06.535.

Felton, C. C., and R. C. DeGroot. 1996. "The Recycling Potential of Preservative-Treated Wood." *Forest Products Journal* 46(7–8):37–46.

Feng, D., H. Tan, and J. S. J. Van Deventer. 2004. "Ultrasound Enhanced Geopolymerisation." *Journal of Materials Science* 39(2):571–80. doi: 10.1023/B:JMSC.0000011513.87316.5c.

Fernandez-Jimenez, A. Monzo, M., M. Vicent, A. Barba, and A. Palomo. 2008. "Alkaline Activation of Metakaolin-Fly Ash Mixtures: Obtain of Zeoceramics and Zeocements." *Microporous and Mesoporous Materials* 108:41–49.

Fernández-Jiménez, A., A. Palomo, and M. Criado. 2005. "Microstructure Development of Alkali-Activated Fly Ash Cement: A Descriptive Model." *Cement and Concrete Research* 35(6):1204–9. doi: 10.1016/j.cemconres.2004.08.021.

Fernández-Jiménez, A., and F. Puertas. 2002. "The Alkali-Silica Reaction in Alkali-Activated Granulated Slag Mortars with Reactive Aggregates." *Cement and Concrete Research* 32:1019–24.

FPASA. 2017. "FIRE STATS 2015 SA Fire Loss Statistics 2015 In Context : Direct Fire Loss

Figure Close to R3-Billion for 2015." (June).

Garrote, G., H. Domínguez, and J. C. Parajó. 1999. "Hydrothermal Processing of Lignocellulosic Materials." *Holz Als Roh - Und Werkstoff* 57(3):191–202. doi: 10.1007/s001070050039.

Glid, Maroua, Isabel Sobrados, Hafsia Ben Rhaiem, Jesús Sanz, and Abdeslem Ben Haj Amara. 2017. "Alkaline Activation of Metakaolinite-Silica Mixtures: Role of Dissolved Silica Concentration on the Formation of Geopolymers." *Ceramics International* (June). doi: 10.1016/j.ceramint.2017.06.144.

Görhan, Gökhan, Ridvan Aslaner, and Osman Şinik. 2016. "The Effect of Curing on the Properties of Metakaolin and Fly Ash-Based Geopolymer Paste." *Composites Part B: Engineering* 97:329–35. doi: 10.1016/j.compositesb.2016.05.019.

Gouny, F., F. Fouchal, O. Pop, P. Maillard, and S. Rossignol. 2013. "Mechanical Behavior of an Assembly of Wood-Geopolymer-Earth Bricks." *Construction and Building Materials* 38:110–18. doi: 10.1016/j.conbuildmat.2012.07.113.

Gouny, Fabrice, Fazia Fouchal, Pascal Maillard, and Sylvie Rossignol. 2012. "A Geopolymer Mortar for Wood and Earth Structures." *Construction and Building Materials* 36:188.

Guo, Xiaolu, and Xuejiao Pan. 2018. "Mechanical Properties and Mechanisms of Fiber Reinforced Fly Ash–Steel Slag Based Geopolymer Mortar." *Construction and Building Materials* 179:633–41. doi: 10.1016/j.conbuildmat.2018.05.198.

Habert, G., J. B. D'Espinose De Lacaillerie, and N. Roussel. 2011. "An Environmental Evaluation of Geopolymer Based Concrete Production: Reviewing Current Research Trends." *Journal of Cleaner Production* 19(11):1229–38. doi: 10.1016/j.jclepro.2011.03.012.

Habert, Guillaume, and Claudiane Ouellet-Plamondon. 2016. "Recent Update on the Environmental Impact of Geopolymers." *RILEM Technical Letters* 1(April):17–23. doi: 10.21809/rilemtechlett.2016.6.

Hajiha, Hamideh, Mohini Sain, and Lucia H. Mei. 2014. "Modification and Characterization of Hemp and Sisal Fibers Modification and Characterization of Hemp and Sisal Fibers." *Journal of Natural Fibers* 11(2):144–68. doi: 10.1080/15440478.2013.861779.

Hanzlíček, Tomáš, and Michaela Steinerová-Vondráková. 2002. “Investigation of Dissolution of Aluminosilicates in Aqueous Alkaline Solution under Laboratory Conditions.” *Ceramics - Silikaty* 46(3):97–103.

Hardjito, Djwantoro, and B. Vijaya Rangan. 2005. *Development and Properties of Low-Calcium Fly Ash-Based Geopolymer Concrete*. Research report GC1, Curtin University of Technology, Perth, Australia.

Hardjito, Djwantoro, and B. Vijaya Rangan. 2014. “Geopolymer Concrete for Environmental Protection.” *Research Report GC* (April):41–59. doi: 10.16953/deusbed.74839.

Herrmann, A. .., J. NIckel, and U. Riedel. 1998. “Construction Materials Based upon Biologically Renewable Resources— from Components to Finished Parts.” *Polym. Degrad. Stab* 59(1–3):251–61.

IARC. 2012. “Chemical Agents and Related Occupations.” *IARC Monographs on the Evaluation of Carcinogenic Risks to Humans / World Health Organization, International Agency for Research on Cancer* 100(Pt F):9–562. doi: now it’s officially a carcinogen...

Ibraheem, Sameer Adnan, Subramania Sarma Sreenivasan, Khalina Abdan, Shamsuddin A. Sulaiman, Aidy Ali, Dayang Laila, and Abang Abdul. 2016. “The Effects of Combined Chemical Treatments on the Mechanical Properties of Three Grades of Sisal.” *BioResources* 11(4):8968–80.

Indian Standards. 1985. *Specification for Wood Particleboard for General Purposes*. New Delhi.

Irle, Mark. 2010. *Wood-Based Panels An Introduction for Specialists*.

Jang, Yong Chul, and Timothy Townsend. 2001. “Sulfate Leaching from Recovered Construction and Demolition Debris Fines.” *Advances in Environmental Research* 5(3):203–17. doi: 10.1016/S1093-0191(00)00056-3.

Jorge, F. C., C. Pereira, and J. M. F. Ferreira. 2004. “Wood-Cement Composites: A Review.” *Holz Als Roh - Und Werkstoff* 62(5):370–77. doi: 10.1007/s00107-004-0501-2.

Khale, Divya, and Rubina Chaudhary. 2007. “Mechanism of Geopolymerization and Factors Influencing Its Development: A Review.” *Journal of Materials Science* 42(3):729–46. doi:

10.1007/s10853-006-0401-4.

Komnitsas, Konstantinos A. 2011. “Potential of Geopolymer Technology towards Green Buildings and Sustainable Cities.” *Procedia Engineering* 21:1023–32. doi: 10.1016/j.proeng.2011.11.2108.

Korniejenko, Kinga, Janusz Mikuła, and Michał Łach. 2015. “Fly Ash Based Fiber-Reinforced Geopolymer Composites as the Environmental Friendly Alternative to Cementitious Materials.” (Bmeet):164–71.

Li, Xue, Lope G. Tabil, and Satyanarayan Panigrahi. 2007. “Chemical Treatments of Natural Fiber for Use in Natural Fiber-Reinforced Composites: A Review.” *Journal of Polymers and the Environment* 15(1):25–33. doi: 10.1007/s10924-006-0042-3.

Lima, Adauto Jose Miranda de, Setsuo Iwakiri, and Maria Guadalupe Lomeli-Ramirez. 2015. “Study of the Interaction of Portland Cement and Pinus Wood for Composites Using Bragg Sensors in Optical.” 10(August 2015):6690–6704. doi: 10.15376/biores.10.4.6690-6704.

Liu, Wanjun, Amar K. Mohanty, Per Askeland, Lawrence T. Drzal, and Manjusri Misra. 2004. “Influence of Fiber Surface Treatment on Properties of Indian Grass Fiber Reinforced Soy Protein Based Biocomposites.” *Polymer* 45:7589–96. doi: 10.1016/j.polymer.2004.09.009.

Machado, Grazielle, Fernando Santos, Douglas Faria, Taiane Nunes De Queiroz, Flávia Zinani, José Humberto De Queiroz, and Fernando Gomes. 2018. “Characterization and Potential Evaluation of Residues from the Sugarcane Industry of Rio Grande Do Sul in Biorefinery Processes.” 175–87. doi: 10.4236/nr.2018.95011.

Le Maitre, D. C., D. B. Versfeld, and R. .. Chapman. 2000. “The Impact of Invading Alien Plants on Surface Water Resources in South Africa: A Preliminary Assessment.” *Water SA* 26:397–408.

Marvin, Emma. 2000. *Gypsum Wallboard Recycling and Reuse Opportunities in the State of Vermont*. Vol. 9. Vermont.

Mellado, A., C. Catalán, N. Bouzón, M. V. Borrachero, J. M. Monzó, J. Payá, and M. V. Borrachero. 2014. “Carbon Footprint of Geopolymeric Mortar: Study of the Contribution of

the Alkaline Activating Solution and Assessment of an Alternative Route." *RSC Adv.* 4(45):23846–52. doi: 10.1039/C4RA03375B.

Del Menezzi, Cláudio Henrique Soares, Vinicius Gomes De Castro, and Mario Henrique De Souza. 2007. "Wood-Cement Boards Produced With Oriented." *Maderas. Ciencia y Tecnologia* 9(2):105–15. doi: 10.4067/S0718-221X2007000200001.

Miranda, Isabel, Jorge Gominho, Inês Mirra, and Helena Pereira. 2012. "Chemical Characterization of Barks from Picea Abies and Pinus Sylvestris after Fractioning into Different Particle Sizes." *Industrial Crops & Products* 36:395–400. doi: 10.1016/j.indcrop.2011.10.035.

Misra, A. K., and Renu Mathur. 2007. "Magnesium Oxychloride Cement Concrete." *Bulletin of Materials Science* 30(3):239–46. doi: 10.1007/s12034-007-0043-4.

Mohassab, Yousef, and Hong Yong Sohn. 2015. "Analysis of Slag Chemistry by FTIR-RAS and Raman Spectroscopy: Effect of Water Vapor Content in H2-H2O-CO-CO2 Mixtures Relevant to a Novel Green Ironmaking Technology." *Steel Research International* 86(7):740–52. doi: 10.1002/srin.201400186.

Mortensen, A. (Andreas). 2007. *Concise Encyclopedia of Composite Materials*. Elsevier.

Moyo, HPM, and A. Fatunbi. 2010. "Utilitarian Perspective of the Invasion of Some South African Biomes by Acacia Mearnsii." *Glob J Environ Res* 4(1):6–17.

Mucina, L., BD Hoare, MC Lötter, PJ du Preez, MC Rutherford, RC Scott-Shaw, GJ Bredenkamp, LW Powrie, L. Scott, KGT Camp, SS Cilliers, H. Bezuidenhout, TH Mostert, SJ Siebert, PJD Winter, JE Burrows, L. Dobson, RA Ward, M. Stalmans, EGH Oliver, F. Siebert, Schim, and L. Kose. 2006. "The Grassland Biome." Pp. 348–437 in *The vegetation of South Africa, Lesotho and Swaziland*, edited by L. Mucina and M. Rutherford. Pretoria: South African National Biodiversity Institute.

Na, Bin, Zhipeng Wang, Zhiqiang Wang, Tao Ding, Rong Huang, and L. Xiaoling. 2014. "Study On Hydration Mechanism of Low Density Magnesia-Bonded Wood Wool Panel." *Wood Research* 59(1):137–47.

Najimi, Meysam, Nader Ghafoori, Brittany Radke, and Kimberly Sierra. 2016. "Properties of

Alkali-Activated Natural Pozzolan and Fly Ash Mortars : A Comparative Study."

Nasrazadani, S., and T. Springfield. 2014. "Application of Fourier Transform Infrared Spectroscopy in Cement Alkali Quantification." *Materials and Structures/Materiaux et Constructions* 47(10):1607–15. doi: 10.1617/s11527-013-0140-3.

Natali, A., S. Manzi, and M. C. Bignozzi. 2011. "Novel Fiber-Reinforced Composite Materials Based on Sustainable Geopolymer Matrix." *Procedia Engineering* 21:1124–31. doi: 10.1016/j.proeng.2011.11.2120.

Ndukwe, Ifeanyi, and Qiuyan Yuan. 2016. "Drywall (Gyproc Plasterboard) Recycling and Reuse as a Compost-Bulking Agent in Canada and North America: A Review." *Recycling* 1(3):311–20. doi: 10.3390/recycling1030311.

Nematollahi, Behzad, and Jay Sanjayan. 2014. "Effect of Different Superplasticizers and Activator Combinations on Workability and Strength of Fly Ash Based Geopolymer." *Materials and Design* 57:667–72. doi: 10.1016/j.matdes.2014.01.064.

Neupane, Kamal, Paul Kidd, Des Chalmers, Daksh Baweja, and Rijun Shrestha. 2016. "Investigation on Compressive Strength Development and Drying Shrinkage of Ambient Cured Powder-Activated Geopolymer Concretes." *Australian Journal of Civil Engineering* 14(1):72–83. doi: 10.1080/14488353.2016.1163765.

Nikolov, Alexander, Ivan Rostovsky, and Henk Nugteren. 2017. "Geopolymer Materials Based on Natural Zeolite." *Case Studies in Construction Materials* 6(August 2016):198–205. doi: 10.1016/j.cscm.2017.03.001.

Ogundiran, Mary B., and Sanjay Kumar. 2016. "Synthesis of Fly Ash-Calcined Clay Geopolymers: Reactivity, Mechanical Strength, Structural and Microstructural Characteristics." *Construction and Building Materials* 125:450–57. doi: 10.1016/j.conbuildmat.2016.08.076.

Oladele, Isiaka O., Jimmy L. Olajide, and Adekunle S. Ogunbadejo. 2015. "The Influence of Chemical Treatment on the Mechanical Behaviour of Animal Fibre-Reinforced High Density Polyethylene Composites." *American Journal of Engineering Research* (0402):2320–2847.

Omoniyi, T. E. &. Akinyemi B. A. 2012. "Durability Based Suitability of Bagasse-Cement

Composite for Roofing Sheets." *Civil Engineering and Construction Technology* 3(December):280–90. doi: 10.5897/JCECT12.041.

Onuaguluchi, Obinna, and Nemkumar Banthia. 2016. "Plant-Based Natural Fibre Reinforced Cement Composites: A Review." *Cement and Concrete Composites* 68:96–108. doi: 10.1016/j.cemconcomp.2016.02.014.

van Oss, Hendrik G., and Amy C. Padovani. 2003. "Cement Manufacture and the Environment-Part II: Environmental Challenges and Opportunities." *Journal of Industrial Ecology* 7(1):93–126. doi: 10.1162/108819802320971650.

Pacheco-Torgal, Fernando, João Castro-Gomes, and Said Jalali. 2008. "Alkali-Activated Binders: A Review. Part 2. About Materials and Binders Manufacture." *Construction and Building Materials* 22(7):1315–22. doi: 10.1016/j.conbuildmat.2007.03.019.

Pacheco-Torgal, Fernando, and Said Jalali. 2011. "Cementitious Building Materials Reinforced with Vegetable Fibres: A Review." *Construction and Building Materials* 25(2):575–81. doi: 10.1016/j.conbuildmat.2010.07.024.

Palomo, A., M. W. Grutzeck, and M. T. Blanco. 1999. "Alkali-Activated Fly Ashes: A Cement for the Future." *Cement and Concrete Research* 29(8):1323–29. doi: 10.1016/S0008-8846(98)00243-9.

Pelaez-Samaniego, Manuel Raul, Vikram Yadama, Tsai Garcia-Perez, Eini Lowell, and Thomas Amidon. 2014. "Effect of Hot Water Extracted Hardwood and Softwood Chips on Particleboard Properties." *Holzforschung* 68(7):807–15. doi: 10.1515/hf-2013-0150.

Pelaez-samaniego, Manuel Raul, Vikram Yadama, Eini Lowell, Thomas E. Amidon, and Timothy L. Chaffee. 2013. "Hot Water Extracted Wood Fiber for Production of Wood Plastic Composites ( WPCs )." 67(2):193–200. doi: 10.1515/hf-2012-0071.

Pereira Ferraz, Gabriela, Craig Frear, Manuel Raul Pelaez-Samaniego, Karl Englund, and Manuel Garcia-Perez. 2016. "Hot Water Extraction of Anaerobic Digested Dairy Fiber for Wood Plastic Composite Manufacturing." *BioResources* 11(4). doi: 10.15376/biores.11.4.8139-8154.

Petermann, Jeffrey C., and Athar Saeed. 2012. "Alkali-Activated Geopolymers: A Literature

Review." *Air Force Research Laboratory* (February):1–99.

Plekhanova, T. A., J. Keriene, A. Gailius, and G. I. Yakovlev. 2007. "Structural, Physical and Mechanical Properties of Modified Wood-Magnesia Composite." *Construction and Building Materials* 21(9):1833–38. doi: 10.1016/j.conbuildmat.2006.06.029.

Provis, J. .., and J. S. J. van Deventer. 2009. *Geopolymers - Structure, Processing, Properties and Industrial Applications*. Woodhed Publishing Limited and CRC Press LLC.

Provis, John L., and J. S. J. Van Deventer. 2014. *Alkali Activated Materials*.

Qin, Te Fu, and Luo Hua Huang. 2005. "Study on the Difference of Chemical Properties among Five Acacia Species." *Forest Research*.

Quiroga, A., V. Marzocchi, and I. Rintoul. 2016. "Influence of Wood Treatments on Mechanical Properties of Wood-Cement Composites and of Populus Euroamericana Wood Fibers." *Composites Part B: Engineering* 84:25–32. doi: 10.1016/j.compositesb.2015.08.069.

Raijiwala, D. B., H. S. Patil, and I. U. Kundan. 2012. "Effect of Alkaline Activator on the Strength and Durability of Geopolymer Concrete." *Journal of Engineering Research* III(I):18–21.

Rao, K. Venkateswara. 2015. "Study on Strength Properties of Low Calcium Based Geopolymer Concrete." 6(11):149–55.

Ridi, Francesca, Dipartimento Chimica, and Università Firenze. 2010. "Critical Reviews Hydration of Cement :" 110–17.

Ruiz, Raymond, and Tina Ehrman. 1996. "HPLC Analysis of Liquid Fractions of Process Samples for Monomeric Sugars and Cellobiose." *NREL* LAP 013.

Sales, Almir, Francis Rodrigues De Souza, and Fernando Do Couto Rosa Almeida. 2011. "Mechanical Properties of Concrete Produced with a Composite of Water Treatment Sludge and Sawdust." *Construction and Building Materials* 25(6):2793–98. doi: 10.1016/j.conbuildmat.2010.12.057.

Sarmin, Siti Noorbaini, and Johannes Welling. 2016. "Lightweight Geopolymer Wood Composite Synthesized from Alkali-Activated Fly Ash and Metakaolin." *Jurnal Teknologi* 78(11):49–55.

doi: 10.11113/.v78.8734.

Sarmin, Siti Noorbaini, Johannes Welling, Andreas Krause, and Ali Shalbafan. 2014. “Investigating the Possibility of Geopolymer to Produce Inorganic-Bonded Wood Composites for Multifunctional Construction Material - A Review.” *BioResources* 9(4):7941–50.

Sarmin, SN. 2016. “The Influence of Different Wood Aggregates on the Properties of Geopolymer Composites.” *Key Engineering Materials* 723(December 2016):74–79. doi: 10.4028/www.scientific.net/KEM.723.74.

Sarmin, SN, and J. Welling. 2015. “Study on Properties of Lightweight Cementitious Wood Composite Containing Fly Ash/Metakaolin.” *Pro Ligno* 11(4):116–21.

Sawpan, Moyeenuddin A., Kim L. Pickering, and Alan Fernyhough. 2011. “Effect of Fibre Treatments on Interfacial Shear Strength of Hemp Fibre Reinforced Polylactide and Unsaturated Polyester Composites.” *Composites Part A: Applied Science and Manufacturing* 42(9):1189–96. doi: 10.1016/j.compositesa.2011.05.003.

Sebio-pun, Teresa, and Jorge Lo. 2012. “Species Thermogravimetric Analysis of Wood , Holocellulose , and Lignin from Five Wood Species.” (October 2015). doi: 10.1007/s10973-011-2133-1.

Sedira, Naim, João Castro-Gomes, Gediminas Kastiukas, Xiangming Zhou, and Alexandre Vargas. 2017. “A Review on Mineral Waste for Alkali-Activated Binders Due to Their Chemical Characteristics.” *Mining Science* 24(May):29–58. doi: 10.5277/msc172402.

Semple, K. E., and P. D. Evans. 2004. “Wood-Cement Composites — Suitability of Western Australian Mallee Eucalypt, Blue Gum and Melaleucas: A Report for the RIRDC/Land & Water Australia/FWPRDC/MDBC Joint Venture Agroforestry Program.” (04):65.

Shackleton, Ross T., Charlie M. Shackleton, and Christian A. Kull. 2019. “The Role of Invasive Alien Species in Shaping Local Livelihoods and Human Well-Being: A Review.” *Journal of Environmental Management* 229(October 2017):145–57. doi: 10.1016/j.jenvman.2018.05.007.

Simatupang, Maruli H., and Robert L. Geimer. 1990. “Inorganic Binder for Wood Composites: Feasibility and Limitations.” *Proceeding of Wood Adhesive Symposium* 169–76.

Simatupang, Maruli H., Norbert Sedding, Christoph Habighorst, and Robert L. Geimer. 1991. "Technologies for Rapid Production of Mineral-Bondedwood Composite Boards." *Inorganic Bonded Wood and Fiber Composite Materials: Proceedings of the 2d International Inorganic Bonded Wood and Fiber Composite Materials Conference* 18–27.

Singh, Manjit, and Mridul Garg. 1994. "Gypsum-Based Fibre-Reinforced Composites: An Alternative to Timber." *Construction and Building Materials* 8(3):155–60. doi: 10.1016/S0950-0618(09)90028-9.

Škvára, František. 2007. "Alkali Activated Material–Geopolymer." *... Alkali Activated Materials–Research, Production and ...* 661–76.

Sluiter, A., B. Hames, D. Hyman, C. Payne, R. Ruiz, C. Scarlata, J. Sluiter, D. Templeton, and J. Wolfe Nrel. 2008. "Determination of Total Solids in Biomass and Total Dissolved Solids in Liquid Process Samples Biomass and Total Dissolved Solids in Liquid Process Samples." (March).

Somna, Kiatsuda, Chai Jaturapitakkul, Puangrat Kajitvichyanukul, and Prinya Chindaprasirt. 2011. "NaOH-Activated Ground Fly Ash Geopolymer Cured at Ambient Temperature." *Fuel* 90(6):2118–24. doi: 10.1016/j.fuel.2011.01.018.

Song, S., D. Sohn, H. M. Jennings, and T. O. Mason. 2000. "Hydration of Alkali-Activated Ground Granulated Blast Furnace Slag." *Journal of Materials Science* 35(1):249–57. doi: 10.1023/A:1004742027117.

Soutsos, Marios, Alan P. Boyle, Raffaele Vinai, Anastasis Hadjierakleous, and Stephanie J. Barnett. 2016. "Factors Influencing the Compressive Strength of Fly Ash Based Geopolymers." 110:355–68. doi: 10.1016/j.conbuildmat.2015.11.045.

Sudin, R., and N. Swamy. 2000. "Bamboo and Wood Fiber Cement Composite for Sustainable Infrastructure Regeneration." Pp. 21–26 in *Wood-Cement Composites in the Asia-Pacific Region: Proceedings of a Workshop held at Rydges Hotel, Canberra, Australia*. Canberra, Australia.

Sun, Ming Qing, Jun Li, Ying Jun Wang, and Xiao Yu Zhang. 2015. "Preparation of Carbon Fiber Reinforced Cement-Based Composites Using Self-Made Carbon Fiber Mat." *Construction and*

*Building Materials* 79:283–89. doi: 10.1016/j.conbuildmat.2015.01.060.

T204. 2007. “Solvent Extractives of Wood and Pulp.” *Tappi Standards* 7–10.

T211. 2012. “Ash in Wood , Pulp , Paper and Paperboard : Combustion at 525 ° C.” *Tappi Standards*.

T257. 2012. “Sampling and Preparing Wood for Analysis ( Proposed Revision of T 257 Cm-02 as a Standard Practice ).” *Tappi Standards*.

T264. 2007. “Preparation of Wood for Chemical Analysis.” *TAPPI* 1988:1–4.

Tan, Yanni, Yong Liu, and Liam Grover. 2014. “Effect of Phosphoric Acid on the Properties of Magnesium Oxychloride Cement as a Biomaterial.” *Cement and Concrete Research* 56:69–74. doi: 10.1016/j.cemconres.2013.11.001.

Tran, D. H., P. Louda, O. Bortnovsky, and P. Bezucha. 2009. “Effect of Curing Temperature on Flexural Properties of Silica-Based Geopolymer-Carbon Reinforced Composite.” *Manufacturing Engineering* 37(2):492–97.

Turley, W. 1998. “What’s Happening in Gypsum Recycling.” *Constr. Build. Mater* 5(8–12).

U.S Census Bureau, HUD. 2017. *Monthly New Residential Construction, September 2017*. accessed: Nov. 5, 2017.

Ved, E. .., E. .. Zharov, and H. .. Phong. 1976. “Mechanism of Magnesium Oxychlorides Formation during the Hardening of Magnesium Oxychloride Cements.” *Zh Prikl Khim* 49(10):2154–62.

Wallah, S. E., and B. V. Rangan. 2006. “Low-Calcium Fly Ash-Based Geopolymer Concrete: Long-Term Properties.” *Concrete* 107.

Walling, Sam A., and John L. Provis. 2016. “Magnesia-Based Cements: A Journey of 150 Years, and Cements for the Future?” *Chemical Reviews* 116(7):4170–4204. doi: 10.1021/acs.chemrev.5b00463.

Williams, P. Jason, Joseph J. Biernacki, Larry R. Walker, Harry M. Meyer, Claudia J. Rawn, and Jianming Bai. 2002. “Microanalysis of Alkali-Activated Fly Ash-CH Pastes.” *Cement and*

*Concrete Research* 32(6):963–72. doi: 10.1016/S0008-8846(02)00734-2.

Yang, Tsung-yin, Chia-ching Chou, and Chuan-chi Chien. 2012. "The Effects of Foaming Agents and Modifiers on a Foamed-Geopolymer."

Ye, Hanzhou, Yang Zhang, Zhiming Yu, and Jun Mu. 2018. "Effects of Cellulose, Hemicellulose, and Lignin on the Morphology and Mechanical Properties of Metakaolin-Based Geopolymer." *Construction and Building Materials* 173:10–16. doi: 10.1016/j.conbuildmat.2018.04.028.

Ylmén, Rikard, and Ulf Jäglid. 2013. "Carbonation of Portland Cement Studied by Diffuse Reflection Fourier Transform Infrared Spectroscopy." *International Journal of Concrete Structures and Materials* 7(2):119–25. doi: 10.1007/s40069-013-0039-y.

Youngquist, John A. 1999. "Wood-Base Composites and Panel Products." Pp. 1–31 in *Wood handbook—Wood as an engineering material*.

Yuan, Jingkun, Peigang He, Dechang Jia, Chao Yang, Yao zhang, Shu Yan, Zhihua Yang, Xiaoming Duan, Shengjin Wang, and Yu Zhou. 2016. "Effect of Curing Temperature and SiO2/K2O Molar Ratio on the Performance of Metakaolin-Based Geopolymers." *Ceramics International* 42(14):16184–90. doi: 10.1016/j.ceramint.2016.07.139.

Yunsheng, Zhang, Sun Wei, Li Zongjin, Zhou Xiangming, Eddie, and Chau Chungkong. 2008. "Impact Properties of Geopolymer Based Extrudates Incorporated with Fly Ash and PVA Short Fiber." *Construction and Building Materials* 22(3):370–83. doi: 10.1016/j.conbuildmat.2006.08.006.

Zhang, Hai Yan, Venkatesh Kodur, Liang Cao, and Shu Liang Qi. 2014. "Fiber Reinforced Geopolymers for Fire Resistance Applications." *Procedia Engineering* 71:153–58. doi: 10.1016/j.proeng.2014.04.022.

Zhang, Z., C. Dai, Q. Zhang, B. Guo, and W. Liu. 1991. "Study on the Formation of 5-Phase and 3-Phase Crystal." *China Sci.* 1:82–89.

Zhou, Xiangming, and Zongjin Li. 2012. "Light-Weight Wood-Magnesium Oxychloride Cement Composite Building Products Made by Extrusion." *Construction and Building Materials* 27(1):382–89. doi: 10.1016/j.conbuildmat.2011.07.033.

Zhuang, Xiao Yu, Liang Chen, Sridhar Komarneni, Chun Hui Zhou, Dong Shen Tong, Hui Min Yang, Wei Hua Yu, and Hao Wang. 2016. “Fly Ash-Based Geopolymer: Clean Production, Properties and Applications.” *Journal of Cleaner Production* 125(August):253–67. doi: 10.1016/j.jclepro.2016.03.019.